PHD

Insulin signalling and membrane fusion in adipose cells

Ribe, David Raymond

Award date:
2005

Awarding institution:
University of Bath

INSULIN SIGNALLING AND MEMBRANE FUSION IN ADIPOSE CELLS

submitted by David Raymond Ribé

for the degree of PhD

of the University of Bath

2005

ProQuest LLC
789 East Eisenhower Parkway
P.O. Box 1346
Ann Arbor, MI 48106-1346

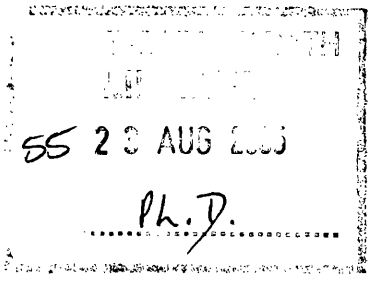
55 2 3 AUG 2005
Ph.D.

Acknowledgements

I would first like to express my gratitude to Professor Geoffrey Holman for his supervision and advice throughout this PhD. I would also like to thank all members of the Holman lab, who have helped with the work but more than that have made my spell in the lab a happy experience, namely Darren Harper, Makoto Hashimoto, Alois Hodel, Francoise Koumanov, Scott Lawrence, Judith Richardson, Paul Whitley and Jing Yang.

A very special thanks goes to Veronica, Madeleine and Jesper, who have supported me through this work in many ways. Support in a more material sense came from the Medical Research Council, and for that they have my gratitude also.

Abstract

Insulin regulates glucose uptake in responsive cells by trafficking GLUcose Transporter 4 (GLUT4) molecules to the plasma membranes of these cells. This thesis focuses on events at the plasma membrane, including membrane fusion and activation of GLUT4. Wortmannin inhibition experiments in rat adipocytes did not show the trafficking-independent inhibition of insulin-stimulated glucose transport activity at low wortmannin concentrations seen in other cell types. The p38 MAP kinase inhibitor SB203580 inhibited labelling of cell surface GLUT4 as well as glucose transport activity.

Purified recombinant protein standards were used to quantify SyNaptosome-Associated Protein (SNAP) REceptor (SNARE) proteins in rat adipocytes. There were approximately 2,500,000 copies of syntaxin4, 8,900,000 copies of SNAP23, 1,900,000 copies of VAMP2 and 1,000,000 copies of Munc18c in each adipose cell. Syntaxin4, SNAP23 and Munc18 were predominantly localised to the plasma membrane. SNAP23 was in large excess compared to the other proteins in plasma membranes, suggesting that its availability was tightly regulated. VAMP2 was distributed between the plasma membrane and intracellular membranes. Insulin caused a two-fold increase in VAMP2 at the plasma membrane.

The small amounts of syntaxin4 in intracellular membranes were in large excess over Munc18c in the same membranes. These results suggest that Munc18c is unlikely to play a major role in trafficking syntaxin4 to the plasma membrane as has been suggested. A number of approaches were applied to expressing and purifying recombinant SNAREs. The purified proteins were reconstituted into liposomes. This system is intended to be the future basis for experiments on SNARE function and their regulation by insulin.

List of Abbreviations

AMP	Adenosine monophosphate
AMPK	AMP-activated protein kinase
AP1	Adaptor protein 1
AS160	Akt Substrate of 160 kDa
ATP	Adenosine triphosphate
BoNT	Botulinum neurotoxin
BSA	Bovine serum albumin
CAP	Cbl-activating protein
CREB	C-response element binding protein
csp	Cysteine string protein
DAG	Diacylglycerol
DMSO	Dimethyl sulphoxide
DTT	Dithiothreitol
EDTA	Ethylenediamine tetraacetic acid
ER	Endoplasmic reticulum
GFP	Green fluorescent protein
GLUT	Glucose transporter
GST	Glutathione-S-transferase
GTP	Guanidine 5'-triphosphate
HA-tag	Hemagglutinin epitope tag
Hepes	4-(2-Hydroxyethyl)piperazine-1-ethanesulphonic acid
His-tag	Hexahistidine tag
HMIT	H^+-myo-inositol transporter
HRP	Horseradish peroxidase

IF	Immunofluorescence
IP3	Inositol triphosphate
IPTG	isopropyl-β-D-thiogalactopyranoside
IRAP	Insulin responsive aminopeptidase
IRS	Insulin receptor substrate
JNK	Jun N-terminal protein kinase
LB	Luria-Bertani
MAPKAPK-2	MAP kinase-activated protein kinase 2
MAP kinase	Mitogen activated protein kinase
Munc18	Mammalian unc-18 protein
NSF	N-ethylmaleimide sensitive factor
NucA	Nuclease A
N-WASP	Neural Wiskott-Aldrich syndrome protein
PCR	Polymerase chain reaction
PDK	3'-phosphoinositide-dependent protein kinase
PI 3-kinase	Phosphoinositide 3'-kinase
PI3P	Phosphatidylinositol-3-phosphate
PI(3,4,5)P3	Phosphatidylinositol-3,4,5-triphosphate
PI(4,5)P2	Phosphatidylinositol-4, 5-bisphosphate
PLC	Phospholipase C
PKC	Protein kinase C
RT-PCR	Reverse transcription - PCR
SAPK	Stress-activated protein kinase
SDS	Sodium-dodecyl sulphate
SDS-PAGE	SDS-polyacrylamide gel electrophoresis

SM	Sec1/Munc18 family
αSNAP	Soluble NSF attachment protein
SNAP23	Synaptosome-associated protein of 23 kDa
SNARE	Soluble NSF attachment protein receptor
TGN	Trans-Golgi network
Tris	Tris (hydroxymethyl) methylamine
t-SNARE	target SNARE
VAMP	Vesicle-associated membrane protein
VAP-33	VAMP/synaptobrevin-binding protein
Vps	Vacuolar protein sorting
v-SNARE	Vesicular SNARE

List of figures

List of tables

CONTENTS

Communication arising from this thesis

Refereed publication

Ribe, D., Yang, J., Patel, S., Koumanov, F., Cushman, S. W., and Holman, G. D. (2005). Endofacial competitive inhibition of GLUT4 intrinsic activity by the MAP kinase inhibitor SB203580. Endocrinology 146, 1713-1717.

Chapter 1 - Introduction and Review of the Literature

1.1. Glucose Homeostasis

Glucose is a major source of energy and an important source of carbon for the synthesis of organic molecules in eukaryotic cells. In vertebrates, glucose is transported throughout the body in the blood, and moves into and out of cells via a family of transporter proteins called GLUTs (GLUcose Transporters). Because GLUTs transport glucose down its concentration gradient, and cells require glucose as an energy source, it is vital that glucose homeostasis is maintained in the body. This is achieved by balancing the antagonistic effects of the hormones insulin and glucagon. Insulin is secreted by the pancreas in response to elevated blood glucose and promotes uptake and storage of glucose in responsive tissues. The pancreas secretes glucagon when blood glucose concentration is low. Glucagon stimulates the breaking down of glucose stored in responsive tissues and the release of this glucose into the blood.

1.1.1. Diabetes

A deficiency of insulin or a loss of response to insulin results in diabetes mellitus. The resulting elevated blood glucose causes the kidneys to excrete glucose and with it large volumes of water. Fat becomes the main source of energy for cellular respiration, and its breakdown causes the accumulation of acidic metabolites in the blood which can be life threatening as a result of the lowered pH. Type 1 diabetes is caused by an attack by the body's own immune system on the pancreas, resulting in a deficiency in insulin secretion. Type 2 diabetic patients show normal insulin secretion but display insulin resistance, an inability to respond normally to insulin. This condition is associated with obesity. There is a great heterogeneity in the genetic

defects that cause type 2 diabetes (Jenkins and Campbell, 2004). The end result however is the same regardless of the cause – elevated blood glucose.

The incidence of type 2 diabetes is growing rapidly in many populations (Diamond, 2003). This has led to an expansion of research into the biochemistry of glucose metabolism. The increase in type 2 diabetes is thought to be due to the tendency towards regular carbohydrate-rich meals in populations that are genetically adapted to periods of fluctuating food availability. The ability to rapidly convert dietary intake to fat at times of high food abundance would have been a selective advantage in populations where the food supply was intermittent. However, this ability could lead to obesity and type 2 diabetes when regular carbohydrate-rich meals and reduced exertion become the norm (Neel, 1962).

1.2. The glucose transporter family

The increase in the uptake of glucose from the blood in response to insulin by muscle, fat and liver cells is largely a result of the increase in the abundance of glucose transporter molecules on the surface of these cells that occurs in response to insulin. The glucose transporters, or GLUTs are members of the SLC2 family of glucose and polyol transporters. Thirteen members of this family have been identified in humans, either by purification or by sequence similarity. Twelve of the family members have been classified as GLUTs, and the remaining family member is the H^+-myo-inositol cotransporter (HMIT1). The family is split into four main classes based on their genetic similarity. Class I GLUTs are the best characterised, and comprise of GLUT1, GLUT2, GLUT3 and GLUT4. Class II is made up of GLUT5, GLUT7, GLUT9 and GLUT11. Class III includes GLUT6, GLUT8, GLUT10 and GLUT12, and HMIT1.

The different GLUTs differ in their substrate specificities and tissue distribution. GLUTs 1-4 are specific transporters of glucose. GLUT1 is ubiquitously expressed, and is the predominant GLUT in erythrocytes and in the brain (Mueckler *et al.*, 1985). GLUT2 is expressed in pancreatic β-cells, liver, kidney and the small intestine, and is able to transport fructose and glucosamine as well as glucose (Fukumoto *et al.*, 1988; Cheeseman, 1993; Uldry *et al.*, 2002). GLUT2 plays a role in the mechanism that senses blood glucose levels and thereby controls secretion of insulin and glucagon (Thorens, 2001; Thorens, 2003). GLUT3 is expressed in the brain and most other tissues (Kayano *et al.*, 1988), and GLUT4 is expressed only in the insulin-responsive tissues - heart, skeletal muscle and adipose tissue (Fukumoto *et al.*, 1989).

GLUT5 is a fructose transporter and is responsible for fructose uptake in the small intestine, testes and kidney (Kayano *et al.*, 1990). GLUT5 is also expressed in spermatozoa, where fructose is a major source of energy (Burant *et al.*, 1992). GLUT7 is able to transport both glucose and fructose, and is expressed in the small intestine, colon, testes and prostate (Li *et al.*, 2004). GLUT9 is a glucose transporter and is expressed predominantly in the small intestine, placenta, lung and leukocytes, and may be important in early preimplantation development (Phay *et al.*, 2000; Carayannopoulos *et al.*, 2004). GLUT11 is thought to be predominantly a fructose transporter, but also shows some glucose transport activity. It is expressed in the pancreas, placenta, kidney, heart and skeletal muscle (Doege *et al.*, 2001).

Class III GLUTs are the most closely related to glucose transporters in prokaryotes and lower eukaryotes (Joost and Thorens, 2001). Class I and II GLUTs are thought to have evolved from class III GLUTs as a result of the complex requirements for glucose homeostasis in mammals. GLUT6 is specific for glucose and

is expressed in brain, spleen and peripheral leukocytes (Doege *et al.*, 2000a). GLUT8 and GLUT12 are thought to transport galactose and fructose as well as glucose (Doege *et al.*, 2000b; Rogers *et al.*, 2003). GLUT8 is predominantly expressed in testes, but is found at lower levels in most tissues (Ibberson *et al.*, 2000; Carayannopoulos *et al.*, 2000). GLUT12 is expressed in heart and prostate (Macheda *et al.*, 2002). GLUT10, whose substrate specificity has not yet been characterised is predominantly expressed in the pancreas and liver (McVie-Wylie *et al.*, 2001). However, its substrate specificity. HMIT shows transport activity for myo-inositol and related molecules and is predominantly expressed in the brain (Uldry *et al.*, 2001).

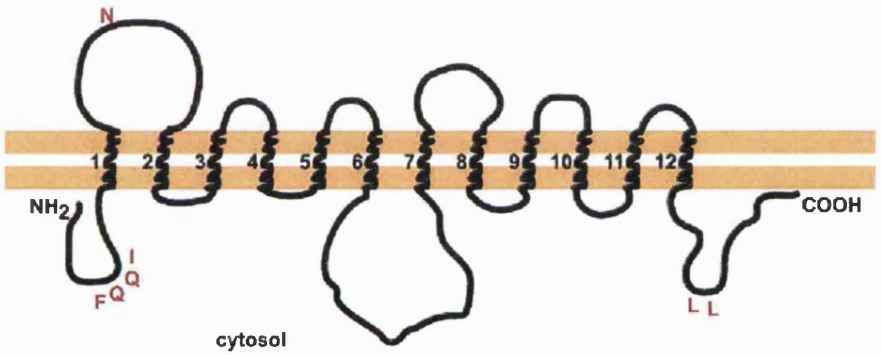

Figure 1.1. Important features of GLUT4 structure. The major features shown include : the 12 amphipathic transmembrane helices with cytosolic amino and carboxy termini; the N-glycosylation site (N) on the extracellular loop between helices 1 and 2; the FQQI motif (FQQI) in the amino terminal cytosolic domain, and the dileucine motif (LL) in the carboxy terminal domain, both important for intracellular sorting and recruitment of adaptor proteins.

The GLUTs are facilitative transporters of their substrates. That is, their transport activities are not coupled to any energy or cargo exchange other than the

movement of substrates down their concentration gradients (Baldwin *et al.*, 1981). All of these proteins share a characteristic topology with cytosolic amino and carboxy terminal ends flanking twelve transmembrane domains, with a glycosylation site on either the first (Class I and II) or the fifth (Class III) extracellular loop (Figure 1.1.). The seventh transmembrane domain is thought to be important in determining substrate specificities of the different family members (Arbuckle *et al.*, 1996). Overall sequence homology between the members of the GLUT family is less than 40%. There is however a much higher degree of sequence identity within the transmembrane domains.

Insulin results in a 20 to 40-fold increase in glucose uptake in responsive cells. GLUT1, which is only expressed at low levels in muscle and adipocytes is largely confined to the plasma membrane, and GLUT1 levels in the plasma membrane of adipocytes increase 2 to 3-fold in response to insulin. GLUT4, whose expression is confined to insulin-responsive tissues is expressed at far higher levels in muscle and adipocytes than GLUT1. In resting (or basal) cells, GLUT4 is largely confined to intracellular membranes. GLUT4 levels at the cell surface increase 20 fold in response to insulin stimulation. GLUT4 is therefore the dominant GLUT in the insulin response (Bryant *et al.*, 2002). Tissues from patients with type 2 diabetes show defects in the trafficking and translocation of GLUT4 (Garvey *et al.*, 1998). Therefore, understanding how GLUT4 trafficking is regulated should help in understanding and identifying the defects that underlie diabetes, and thereby aid the search for treatments directed towards specific molecular targets. The focus of this thesis is on the events at the plasma membrane that lead to the increased exposure of GLUT4 on the exterior surface of adipocytes in response to insulin.

1.3. Intracellular GLUT4 compartments

GLUT4 is found in numerous intracellular compartments including the trans-Golgi nertwork (TGN) and the endosomal system. GLUT4 colocalises with different classes of vesicles including AP1/clathrin coated vesicles that bud from the TGN or endosomes, AP2-coated vesicles that bud from the plasma membrane, and insulin-responsive vesicles that contain proteins such as the insulin-responsive aminopeptidase (IRAP) (Figure 1.2.) (James *et al.*, 1994; James and Piper, 1994; Keller *et al.*, 1995).

There is a general exocytic response to insulin, even in nonspecialised cells such as fibroblasts. However, the magnitude of the GLUT4 response is much larger than that of endosomal or trans-Golgi network (TGN) markers in insulin-sensitive cells (Hudson *et al.*, 1993; Ross *et al.*, 1998). This suggests that there is a separate insulin-sensitive compartment containing GLUT4 that is independent of the endosome and the TGN. The existence of the insulin-sensitive compartment is not dependent on the presence of GLUT4 itself, as IRAP trafficking responds normally to insulin in experiments where GLUT4 expression is downregulated or prior to GLUT4 expression in 3T3-L1 pre-adipocytes (Ross *et al.*, 1998; Zhou *et al.*, 2000).

Biochemically blocking the recycling endosome compartment using a transferrin-horseradish peroxidase conjugate only partially inhibits the GLUT4 response (Livingstone *et al.*, 1996), as does treatment with inhibitors of phospholipase D (Millar *et al.*, 2000). These data suggest that the insulin-sensitive compartment is not dependent on the recycling endosome.

Separation of vesicles by size or density and electron microscopy studies identified insulin-responsive vesicles that contained GLUT4 and IRAP but no TGN or

endosomal markers (Livingstone *et al.*, 1996; Wei *et al.*, 1998; Hashiramoto and James, 2000). The SNARE protein vesicle-associated membrane protein 2 (VAMP2) was also selectively localised to the insulin-responsive GLUT4 compartment (Sevilla *et al.*, 1997). Cellugyrin was associated with GLUT4 vesicles found in the recycling endosome system, but not with insulin-sensitive GLUT4 vesicles (Kupriyanova and Kandror, 2000). The insulin-sensitive GLUT4 compartment is therefore biochemically distinct from the other GLUT4 compartments.

Morphological studies using electron microscopy in 3T3-L1 adipocytes and rat adipocytes showed that intracellular GLUT4 was distributed between vesicular and reticular membrane structures. A proportion of the vesicular structures and some of the reticular structures also contained VAMP2. The VAMP2-positive GLUT4 vesicles were separate from GLUT4 vesicles that also contain GLUT1 and transferrin receptors.

Insulin stimulation is thought to result in a rapid exocytosis of GLUT4 originating from the vesicular VAMP2-containing pool, and a slower phase of exocytosis originating from stimulation of replenishment of this pool from the reticular VAMP2-positive GLUT4 compartment (Xu and Kandror, 2002). Disrupting VAMP2 function, or those of its SNARE partners syntaxin4 and SNAP23 selectively abolished insulin-stimulated GLUT4 traffic to the plasma membrane without affecting other GLUT4 trafficking events (Cheatham *et al.*, 1996; Tamori *et al.*, 1996; Tellam *et al.*, 1997; Rea *et al.*, 1998). Insulin also appeared to stimulate the budding of vesicles from the reticular pool (Xu and Kandror, 2002).

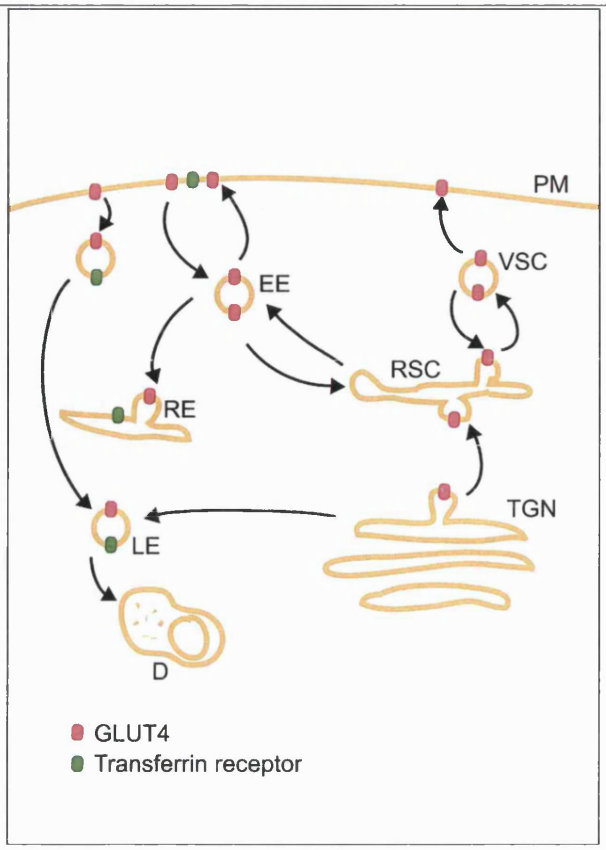

Figure 1.2. Insulin-responsive GLUT4 trafficking. GLUT4 is sorted through the trans-Golgi network (TGN) into a reticular storage compartment (RSC). GLUT4 cycles between the RSC and an insulin responsive vesicular storage compartment (VSC). Budding of vesicles from the RSC to the VSC may be increased on insulin stimulation. GLUT4 in the VSC is rapidly trafficked and fuses to the plasma membrane (PM) in response to insulin. The alternative route for GLUT4 from the RSC is to the endosomal system, comprising of the early endosome (EE), late endosome (LE), and recycling endosome (RE), which constitutively shuttle GLUT4 and other proteins like transferrin between the PM and the endosome. Exocytosed GLUT4 re-enters the cell via the endosomal system. Defective proteins are sorted to the degradative pathway (D) from the LE and the RSC. This figure is adapted from the review by (Holman and Sandoval, 2001).

1.3.1. GLUT4 sorting motifs

A number of sorting signals are present on GLUT4. These include a FQQI motif at the amino terminus, and an acidic cluster at the carboxy terminus, which also contains a dileucine motif (Figure 1.1). The dileucine motif and the FQQI motif are thought to act in recruitment of the adaptor proteins, but the function of the acidic cluster is not known. The FQQI motif is important in sorting GLUT4 away from the endosome (Sandoval *et al.*, 2000; Palacios *et al.*, 2001), and the dileucine motif has been shown to act in sorting GLUT4 between the TGN and GLUT4 storage vesicles (Jhun *et al.*, 1992; Marsh *et al.*, 1998; Holman and Sandoval, 2001).

1.3.2. IRAP

IRAP is completely colocalised with the insulin responsive GLUT4 compartment, and co-trafficked with GLUT4 in response to insulin (Ross *et al.*, 1996). It is a type II membrane protein with a 109 residue cytoplasmic tail and a large 894 amino acid lumenal domain. The lumenal domain is heavily glycosylated and contains an aminopeptidase catalytic domain (Keller *et al.*, 1995). The catalytic domain has been shown to catalyse the cleavage of a number of vasoactive peptide hormones *in vitro* (Tsujimoto *et al.*, 1992; Herbst *et al.*, 1997; Matsumoto *et al.*, 2001). This suggests that IRAP may function in regulating blood circulation in response to insulin stimulation. However the *in vivo* substrates of IRAP have not been identified. The cytosolic tail of IRAP contains a dileucine motif and an acidic cluster, which may regulate its intracellular trafficking in a similar manner to those of GLUT4 (Subtil *et al.*, 2000; Johnson *et al.*, 2001).

1.3.3. Regulation of GLUT4 trafficking

Kinetic studies indicate that insulin both increases the rate of appearance of GLUT4 at the cell surface, and to a lesser degree decreases the re-endocytosis rate of GLUT4 (Jhun *et al.*, 1992; Czech and Buxton, 1993; Satoh *et al.*, 1993; Yang and Holman, 1993). Four points at which insulin signals might regulate exocytosis of GLUT4 are: 1) the release of vesicles from the reticular storage pool to the insulin-sensitive vesicular storage pool, 2) trafficking of vesicles to the plasma membrane, 3) vesicle tethering or docking with the plasma membrane and 4) vesicle fusion with the plasma membrane. Insulin has been demonstrated to stimulate trafficking of GLUT4 to the plasma membrane and budding of vesicles from the reticular GLUT4 pool (Xu and Kandror, 2002). On insulin stimulation, vesicles containing GFP-tagged GLUT4 appeared to accumulate at a number of discrete points where they slowly fuse with the plasma membrane before GFP fluorescence rapidly disperses in the plane of the membrane (Fletcher *et al.*, 2000). The speed of this membrane fusion step appears to be enhanced in insulin-treated cells, suggesting that this step may also be regulated by insulin.

1.4. Insulin signalling

There is a great diversity of responses that follow when insulin binds its receptor. These include increased glucose transport, cell division, and regulation of metabolic enzymes. A brief overview of the events linking insulin signalling to insulin-stimulated glucose transport in adipocytes is included here.

1.4.1. The insulin receptor

The insulin receptor is a member of the receptor tyrosine kinase family. This family includes receptors for a number of other peptide hormones, and shares many downstream effectors with other members of the family (Patti and Kahn, 1998). The receptor consists of two α and two transmembrane β subunits joined together by disulphide bonds to make up a αβ heterodimer. Binding of insulin to the receptor causes a conformational change that activates the autocatalytic tyrosine kinase activity of one β subunit. This phosphorylates three tyrosine residues in the activation loop of the other β subunit, causing the activation loop to move away from the catalytic site so that ATP and substrates can bind.

1.4.2. Insulin receptor substrates

Members of the insulin receptor substrate (IRS) protein family bind the insulin receptor via phosphotyrosine binding domains, which recognise phosphorylated tyrosine residues on the receptor. IRS proteins are scaffolding proteins that do not have catalytic activity, but instead link downstream signaling molecules to the insulin receptor. Four IRS proteins have been characterised, of which IRS1 and IRS2 were ubiquitously expressed (Sun *et al.*, 1991; Sun *et al.*, 1995), IRS3 was restricted to adipose tissue (Lavan *et al.*, 1997), and IRS-4 was expressed in the thymus, brain, kidney and possibly β-cells (Uchida *et al.*, 2000).

IRS proteins contain a conserved series of protein interaction domains, including phosphotyrosine binding domains, through which they interact with the insulin receptor, and pleckstrin homology domains which are implicated in phosphoinositide binding and may also bind the insulin receptor. They also contain a number of tyrosine phosphorylation sites, which allow recruitment of downstream

signalling proteins such as Grb-2, Nck and PI 3-kinase via their phosphotyrosine-binding src homology-2 (SH2) domains (Giovannone *et al.*, 2000).

Studies of IRS proteins have been hampered by the partially redundant functions of the proteins. In experiments with IRS-1 knockout mice, downstream targets of insulin were activated nearly to the same extent as they were in wild type mice in cells that expressed IRS-2, whereas cells with low IRS-2 levels showed little downstream activation, suggesting that IRS-2 was able to compensate for lack of IRS-1 (Araki *et al.*, 1994). IRS-3 also appeared to compensate for lack of IRS-1 in adipocytes from these knockout mice (Smith-Hall *et al.*, 1997). Studies with IRS-1 and IRS-2 knockout mice indicated that IRS-1 was the major insulin receptor substrate involved in regulation of glucose uptake by insulin in target tissues (Araki *et al.*, 1994; Tamemoto *et al.*, 1994), whereas IRS-2 was more important in regulating insulin secretion in beta cells (Withers *et al.*, 1998; Higaki *et al.*, 1999).

Tyrosine phosphorylation of IRS proteins by the insulin receptor enables binding of downstream proteins containing SH2 domains. The most important of these for insulin stimulated glucose transport is the p85 subunit of the Class 1A PI 3-kinase.

1.4.3. PI 3-kinases

PI 3-kinases are a family of enzymes that catalyse the phosphorylation of the 3' hydroxyl on the inositol ring on membrane lipid head groups. The 3'-phosphorylated lipid products that are produced by these enzymes act as targets for the recruitment of signalling molecules to membranes via specific lipid-binding domains, such as pleckstrin homology (PH), FYVE and Phox domains. PI 3-kinases are found in all eukaryotic cells and regulate many processes, including cell growth,

division, differentiation, survival, motility and membrane trafficking (Katso *et al.*, 2001).

Although studies with inactive mutants of p85, microinjection of SH2 domains, and inactivating antibodies to the p110 subunit have implicated the class 1a PI 3-kinases in insulin stimulation of glucose uptake, the existence of multiple isoforms complicates the picture (Kotani *et al.*, 1995; Haruta *et al.*, 1995; Sharma *et al.*, 1998; Hausdorff *et al.*, 1999). It is not known which of the five p85 isoforms and the three p110 isoforms form complexes *in vivo*, nor the differences between the functions downstream of the different isoforms (Vanhaesebroeck *et al.*, 1997). The importance of the isoform specificity is illustrated by a study in which different p85 isoforms directed PI 3-kinase activities either to the plasma membrane or to GLUT4 vesicles in heart muscle (Kessler *et al.*, 2001).

IRS function appears to be important for the specificity of downstream effects of PI 3-kinase activity. Growth factors other than insulin stimulated PI 3-kinase activity without increasing glucose uptake (Isakoff *et al.*, 1995). This PI 3-kinase activity was recruited directly to the tyrosine kinase receptors and consequently 3' phosphoinositide production was restricted to the immediate vicinity of the receptor. Recruitment by IRS molecules however, is unique to the insulin signalling pathway, and may enable remote activation of PI 3-kinase activity in specialised domains of the plasma membrane or on intracellular membranes. This may facilitate the activation of the specific downstream substrates required for recruitment of GLUT4 to the plasma membrane (Figure 1.3.A.).

1.4.3.1. Downstream targets of PI 3-kinase

Atypical protein kinase C (PKCζ and PKCλ), a serine/threonine phosphatase, is recruited to sites of insulin signalling when its amino terminal domain interacts with the PI 3-kinase product PI(3,4,5)P3 (Standaert *et al.*, 2001). Transfection of inactive mutants of PKCζ/λ resulted in attenuation of insulin stimulated glucose transport (Bandyopadhyay *et al.*, 1997; Standaert *et al.*, 1997; Bandyopadhyay *et al.*, 1999a). However, siRNA depletion of PKCζ or PKCλ or of both isoforms did not have any effect on insulin stimulated glucose transport (Zhou *et al.*, 2004). Although the specific role played by PKCζ/λ in insulin stimulated glucose transport is still controversial, there is evidence that it mediates an interaction between Rab4 and the microtubule motor kinesin, which suggests that PKCζ/λ may have a role in stimulating GLUT4 vesicle translocation to the plasma membrane (Imamura *et al.*, 2003). PKCζ/λ also phosphorylates serine residues that occur in the cytoplasmic domain of IRAP and it has been suggested that these phosphorylated residues play a role in IRAP and GLUT4 trafficking, although there is no evidence for this as yet (Ryu *et al.*, 2002).

Akt, a serine/threonine kinase also known as protein kinase B (PKB) is recruited to sites of insulin signalling via interactions through its PH domain with PI(3,4,5)P3 on membrane lipid head groups. Akt represents a point of divergence on the insulin signalling cascade, as it mediates insulin regulation of glycogen synthesis and gene expression as well as glucose uptake (Cross *et al.*, 1995; Nave *et al.*, 1999; Nakae *et al.*, 1999). Expression of constitutively active forms of Akt stimulated glucose transport in 3T3-L1 adipocytes and rat adipocytes (Kohn *et al.*, 1996; Tanti *et al.*, 1997), and microinjection of antibodies against Akt inhibited insulin stimulated GLUT4 translocation (Hill *et al.*, 1999). Furthermore, glucose transport was

attenuated in Akt2 knockout mice, but not in Akt1 knockouts (Cho *et al.*, 2001a; Cho *et al.*, 2001b), and reduction of Akt levels by siRNA inhibited insulin stimulated glucose transport (Jiang *et al.*, 2003). However, there are also studies that argue against such a major role for Akt. Expression of inactive mutants of Akt1 and Akt2 did not inhibit insulin-stimulated glucose transport, but inhibited insulin stimulated protein synthesis in 3T3-L1 adipocytes (Kitamura *et al.*, 1998). Furthermore, expression of inactive Akt2 only slightly inhibited insulin-stimulated glucose transport in another study in rat adipocytes (Cong *et al.*, 1997).

Akt and PKCζ/λ are activated by phosphorylation of threonine residues in their regulatory domains by 3'-phosphoinositide-dependent protein kinase-1 (PDK-1) (Alessi *et al.*, 1997; Chou *et al.*, 1998; Le Good *et al.*, 1998; Bandyopadhyay *et al.*, 1999b; Alessi, 2001). SH2 domains on the adaptor protein Grb14, which exists in a complex with PDK-1 are recruited by phosphorylated tyrosine residues in the insulin receptor that are phosphorylated following insulin binding (King and Newton, 2004). This brings PDK-1 into contact with its substrates.

Full Akt activation also requires phosphorylation on Ser473 by a second PDK, which has not been identified (Hresko *et al.*, 2003). However, targeting Akt to GLUT4 vesicles resulted in basal levels of GLUT4 translocation similar to those seen with insulin in normal cells, indicating that the substrates of Akt may lie on or near GLUT4 vesicles (Ducluzeau *et al.*, 2002; Chen *et al.*, 2003). The Rab GTPase-activating protein AS160 was identified as an Akt substrate using an antibody directed against a consensus ATP substrate sequence. Mutation of the Akt phosphorylation site on AS160 blocked insulin stimulated GLUT4 exocytosis at a step prior to docking with the plasma membrane (Sano *et al.*, 2003; Zeigerer *et al.*, 2004). The postulated Rab protein downstream of AS160 has not been identified.

Synip, a protein that regulates the docking of GLUT4 vesicles with the plasma membrane is also a substrate of Akt2 (Min *et al.*, 1999; Yamada *et al.*, 2005). Phosphorylation of synip at its Akt substrate site appeared to regulate its binding to syntaxin4, a protein with an important role in the fusion of GLUT4 vesicles with the plasma membrane.

The effects of wortmannin inhibition of PI 3-kinase on insulin stimulated glucose uptake were alleviated by adding membrane permeable esters of PtdIns(3,4,5)P_3 in the presence of insulin. However, these lipid analogs by themselves were not sufficient to stimulate glucose transport in the absence of insulin (Jiang *et al.*, 1998). In addition, insulin-independent stimulation of IRS-1, PI 3-kinase and Akt via beta-integrin failed to elicit a glucose transport response (Guilherme and Czech, 1998). These results suggest that insulin activates another pathway in addition to PI 3-kinase that is required for the stimulation of glucose uptake. Two pathways whose activation has been suggested to complement PI 3-kinase are those containing phospholipase Cγ (PLCγ) and the GTPase TC10 (Chiang *et al.*, 2001; Lorenzo *et al.*, 2002).

1.4.4. Phospholipase C

Phospholipase C (PLC) catalyses the hydrolysis of PI(4,5)P2 to IP3 and DAG. PLC was implicated in insulin stimulated glucose transport when it was observed that lithium, a treatment for bipolar disorder and an inhibitor of enzymes that degrade inositol phosphates, enhanced insulin stimulated glucose transport when administered to animal and human subjects (Shah *et al.*, 1986; Rossetti, 1989). Chemical inhibition of PLC or disruption of PLCγ binding to the insulin receptor by microinjection of PLCγ SH2 domains inhibited insulin stimulated glucose transport (Epps-Fung *et al.*,

1997; Kayali *et al.*, 1998). This inhibition was rescued by a cell permeable DAG analogue. A recent study showed that inhibition of PLCγ abolished PKCζ activation by insulin, but also that the role of PLCγ in insulin stimulated glucose transport was

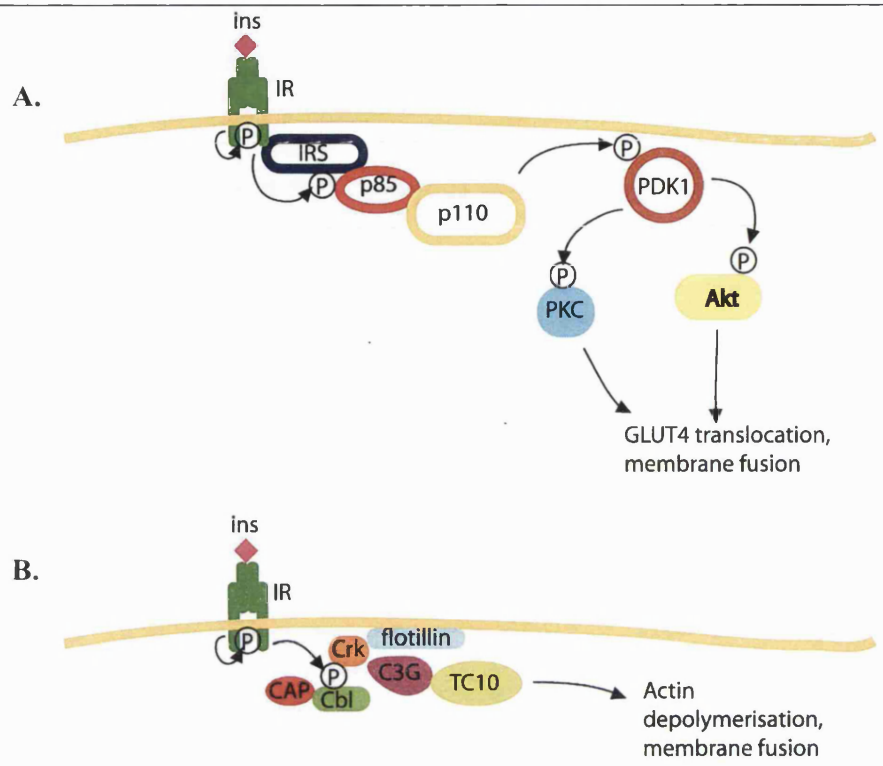

Figure 1.3. Insulin signalling leading to glucose uptake. A. The PI 3-kinase pathway. When insulin binds, the insulin receptor (IR) autophosphorylates, activating its tyrosine kinase activity, which phosphorylates IRS proteins, allowing recruitment and activation of p85 and p110 subunits of PI 3-kinase. The resulting increase in 3' phosphorylated lipids activates PDK1, which phosphorylates its substrates Akt and atypical PKC, leading to insulin-stimulated glucose uptake**. B.** The TC10 pathway. The IR phosphorylates Cbl, which recruits CAP. The complex then translocates to lipid rafts, where it associates with flotillin. TC10 is subsequently activated via the Crk/C3G complex, and promotes actin rearrangements and fusion of GLUT4 vesicles with the plasma membrane.

only partly mediated through PKCζ (Lorenzo *et al.*, 2002). This same study also showed that PLCγ activation by insulin was PI 3-kinase dependent. This suggests that PLCγ is part of the PI 3-kinase dependent pathway that is required for activation of PKCζ.

1.4.5. The TC10 pathway

The second proposed PI 3-kinase independent insulin signalling pathway is the TC10 pathway (Figure 1.3.B.). This pathway is activated through the tyrosine phosphorylation of c-Cbl by the insulin receptor, which is recruited to the insulin receptor through SH2 domains on the adaptor protein APS. Following phosphorylation of Cbl, a complex of Cbl with Cbl activating protein (CAP) is translocated to lipid rafts, where it binds flotillin, a raft associated protein. Cbl recruits a complex containing the adaptor protein CrkII and the GTPase exchange factor C3G. GTP exchange by this complex activates the TC10 GTPase (Watson *et al.*, 2001). Expression of a CAP mutant that is unable to bind Cbl resulted in partial inhibition of insulin stimulated glucose transport in 3T3-L1 adipocytes (Ribon *et al.*, 1998; Baumann *et al.*, 2000). Expression of a dominant negative TC10 also partially inhibited insulin stimulated glucose transport (Chiang *et al.*, 2001). Conversely, (Thirone *et al.*, 2004) and (JeBailey *et al.*, 2004) reported that there was no increase in Cbl phosphorylation in response to insulin in muscle tissue. Furthermore, wortmannin inhibited the proposed downstream effects of TC10 on actin remodelling without inhibiting TC10 activation and expression of a dominant negative mutant of TC10 did not inhibit insulin stimulated actin remodelling in myoblasts (JeBailey *et al.*, 2004). In addition, supression of c-Cbl, CrkII and CAP proteins by siRNA had no effect on insulin stimulated glucose transport (Mitra *et al.*, 2004). The conflicting data mean

that the role of this pathway in insulin stimulated glucose transport remains controversial.

As well as the role in actin remodelling, TC10 has also been implicated in the assembly of the exocyst complex. The exocyst is involved in membrane tethering. Disruption of the exocyst complex disrupts insulin stimulated fusion of GLUT4 vesicles with the plasma membrane (Inoue *et al.*, 2003). These data suggest that insulin stimulation of the TC10 pathway plays a role in stimulating membrane fusion. (Maffucci *et al.*, 2003) reported that PI3P was produced in response to insulin downstream of TC10 activation, and that this lipid head group stimulated GLUT4 translocation in a PI 3-kinase independent manner in response to insulin.

To summarise, there is good evidence for a major role in insulin stimulated glucose uptake for IRS and PI 3-kinase dependent pathways, and for the requirement of at least one additional pathway. The identities of the additional pathways are unknown, and there are conflicting data in the literature both supporting and apparently ruling out roles for the PLCγ and TC10 pathways. Although the relevance of these pathways is disputed, the insulin signalling field is approaching the point at which one can name an unbroken chain of molecules that connect the initial activation of the insulin receptor to the fusion of GLUT4 vesicles with the plasma membrane.

1.5. The role of the cytoskeleton in GLUT4 vesicle trafficking

Possible roles for the microtubule and actin cytoskeletons have already been mentioned in connection with the downstream targets of the PKCζ/λ and TC10 signalling pathways. Kinesin motors play important roles in transporting vesicles along microtubules in neurons and polarized epithelial cells (Fath *et al.*, 1994; Goldstein and Philp, 1999). The intermediate filament protein vimentin and the

microtubule protein α-tubulin were found in the perinuclear GLUT4 compartment in 3T3-L1 adipocytes (Guilherme *et al.*, 2000). Disruption of the motor proteins dynein and kinesin inhibited insulin stimulated GLUT4 translocation (Guilherme *et al.*, 2000; Emoto *et al.*, 2001). However, chemical depolymerisation of the microtubule cytoskeleton resulted in the accumulation of GLUT4 vesicles beneath the plasma membrane, possibly because the GLUT4 vesicles could not be retained in the perinuclear compartment or because GLUT4 recycling from the plasma membrane to the endosome was disrupted. These GLUT4 vesicles were able to fuse with the plasma membrane on insulin stimulation and were reinternalised following removal of insulin, but remained in the vicinity of the plasma membrane (Molero *et al.*, 2001; Shigematsu *et al.*, 2002). This implies that the intact microtubule cytoskeleton and kinesin and dynein activity are required for maintaining intracellular compartmentalization of GLUT4, but not for insulin stimulated GLUT4 externalization. It is possible that the geometry of adipose cells, with their relatively small cytosolic volume obviates the need for the long distance vesicle transport mediated by the microtubule cytoskeleton.

Insulin stimulates actin rearrangements in many cell types (Ridley and Hall, 1992; Tsakiridis *et al.*, 1994; Nobes *et al.*, 1995; Berfield *et al.*, 1996). Insulin stimulated GLUT4 exocytosis was blocked by the actin depolymerizing agents latrunculins A and B (Wang *et al.*, 1998; Omata *et al.*, 2000). Insulin treatment also caused recruitment of PI 3-kinase to GLUT4 vesicles, and this process was also dependent on actin depolymerisation and reassembly (Wang *et al.*, 1998). Insulin-induced actin polymerisation was mediated by the actin-regulatory neural Wiskott-Aldrich syndrome protein (N-WASP), which was localised to the plasma membrane in response to insulin. A dominant negative TC10 mutant inhibited plasma membrane

localisation of N-WASP and actin rearrangements in response to insulin (Jiang *et al.*, 2002). The actin motor Myo1c was also localised to GLUT4 vesicles in response to insulin and was required, along with an intact actin network for the accumulation of GLUT4 vesicles at the plasma membrane. This insulin-induced localisation of Myo1c to GLUT4 vesicles was insensitive to wortmannin, and appeared to promote fusion of GLUT4 vesicles with the plasma membrane by driving membrane remodelling (Bose *et al.*, 2002). Wortmannin-independent actin rearrangements are therefore required upstream of insulin-induced fusion of GLUT4 vesicles with the plasma membrane. The process of fusion itself was inhibited by inhibitors of PI 3-kinase (Bose *et al.*, 2004), and may be dependent on the recruitment of PI 3-kinase to GLUT4 vesicles (Wang *et al.*, 1998). However, this inhibition of GLUT4 vesicle fusion with the plasma membrane by PI 3-kinase inhibitors was overcome by overexpression of Myo1c (Bose *et al.*, 2004). This suggests that the various insulin signalling pathways, as well as interacting with each other, may have overlapping functions. This may be a reason for the conflicting experimental data on the various pathways.

Cortical actin rearrangements therefore occur in response to insulin signalling and are required for fusion of GLUT4 vesicles with the plasma membrane, whereas the microtubule cytoskeleton appears to be involved in intracellular GLUT4 retention, but not in the exocytic response.

1.6. Regulation of GLUT4 transporter activity

As well as regulating GLUT4 vesicle trafficking and fusion with the plasma membrane, there is evidence that insulin also directly regulates the glucose transport activity of GLUT4. There is a delay following insulin stimulated GLUT4 exocytosis before glucose uptake is detected, suggesting that the transporters are inactive when

first inserted into the plasma membrane (Karnieli *et al.*, 1981; Yang *et al.*, 1992; Satoh *et al.*, 1993). Treatments of 3T3-L1 adipocytes with cell permeable analogues of the lipid products of PI 3-kinase activity were able to mimic insulin-induced GLUT4 exocytosis, but not glucose transport in the presence of wortmannin. Cells treated with wortmannin regained full glucose transport activity when both insulin and the lipid products of the PI 3-kinase reaction were added to them (Jiang *et al.*, 1998; Sweeney *et al.*, 2004). These data suggest the existence of a further PI 3-kinase independent insulin signal that regulates the transporter activity of GLUT4 following insertion into the plasma membrane. Results from the Klip laboratory have implicated the p38 MAP kinase pathway in this process (Somwar *et al.*, 2001b; Somwar *et al.*, 2002), and are discussed in detail in Section 3.1.

1.7. Membrane fusion

Insulin signalling results in the movement of GLUT4 vesicles towards the plasma membrane. Glucose uptake through GLUT4 requires the simultaneous exposure of the GLUT4 molecule to the outside and inside of the cell. This is achieved by fusion of GLUT4 containing vesicles with the plasma membrane. The cellular machinery involved in eukaryotic membrane fusion has been intensively studied in many endocytic and secretory pathways. These pathways have many features in common that have prompted unifying hypotheses regarding the conserved mechanism of membrane fusion.

Fusion of membranes requires that opposing membranes be brought together. The transition from long range transport to docking of membranes is termed tethering, and is mediated by the Rab family of GTPase proteins. The identities of the tethering factors involved in GLUT4 exocytosis are not known, though Rab4 and Rab11 have

been found on insulin responsive GLUT4 vesicles (Kessler *et al.*, 2000). The interaction of Rab4 with the motor protein KIF3 was stimulated by insulin via the PI 3-kinase and PKCλ signalling pathways, and disruption of this interaction inhibited insulin stimulated glucose transport (Imamura *et al.*, 2003). Rab4 was also found to interact with the SNARE protein syntaxin4 in an insulin dependent manner (Li *et al.*, 2000). Syntaxin4 is involved in the later stages of GLUT4 vesicle fusion with the plasma membrane. This suggests that Rab4 may link long and short range transport of GLUT4 vesicles in the exocytic pathway, although Rab-mediated tethering typically occurs via an intermediate tethering complex, rather than directly to SNARE proteins (Zerial and McBride, 2001).

1.7.1. Docking and SNARE proteins

The SNARE proteins are thought to act following the tethering of transport vesicle and target membrane. SNAREs were originally identified in synaptic vesicles (Sollner *et al.*, 1993), and are a large family with 24 known members in yeast, and at least 35 in mammals (Bock *et al.*, 2001). They can be functionally classified as vesicular (v-SNARE) and target (t-SNARE) SNAREs according to the membrane on which they are present. The best characterised SNARE proteins are those involved in synaptic transmission. They are syntaxin1 and SNAP25, which reside on the plasma membrane and act as the t-SNARE, and VAMP, which is present on synaptic vesicles and is the v-SNARE. SNARE proteins vary greatly in structure, but share a common SNARE motif. This is a stretch of 60-70 amino acids that include eight heptad repeats, typical of coiled coil motifs. Most SNAREs include a membrane anchor at their carboxy terminus adjacent to the SNARE motif, although some are soluble and

others, like SNAP25 contain post-translational lipid additions that act as the membrane anchor.

SNARE motifs are relatively unstructured in solution. However, SNARE motifs from cognate SNARE proteins spontaneously assemble into four-helical bundles in a parallel configuration, called the core complex (Hanson *et al.*, 1997; Lin and Scheller, 1997). Syntaxin1 and VAMP2 each contribute one SNARE motif to the core complex, and SNAP25 contributes two SNARE motifs. The core complex is an extremely stable structure, able to withstand denaturation by SDS and temperatures of up to 95°C (Fasshauer *et al.*, 2002).

1.7.2. The role of SNARE proteins in membrane fusion

SNARE-specific clostridial neurotoxins have been useful tools in studying SNARE function. VAMP is cleaved by tetanus toxin and botulinum toxins (BoNT) B, D, F and G. SNAP-25 is cleaved by BoNT A, C and E. Syntaxin is cleaved by BoNT C (Pellizzari *et al.*, 1999). SNARE proteins on opposing membranes form the core complex prior to membrane fusion *in vivo*. Prevention of the formation of this complex by cleaving SNAREs with clostridial neurotoxins blocked neurotransmitter release and led to an accumulation of docked synaptic vesicles (Hunt *et al.*, 1994).

The assembly of the trans-SNARE complex brings the opposing membranes into close proximity, and the energy released by the assembly of this stable complex is thought to provide sufficient energy to overcome the repulsion between membranes, and thereby catalyse fusion (Hanson *et al.*, 1997; Skehel and Wiley, 1998). Following fusion, all three proteins in the SNARE complex reside in the target membrane as a cis-complex (Figure 1.4.). Recycling of the SNAREs for further rounds of fusion requires ATP-dependent disassembly of the cis-complex by NSF and

αSNAP (Whiteheart and Matveeva, 2004). The case for SNARE proteins as the machinery for membrane fusion was strengthened further by experiments in which purified SNARE proteins were able to catalyse fusion between artificial lipid bilayers (Weber *et al.*, 1998).

In vitro interactions between SNAREs are relatively unspecific, meaning t-SNAREs bind v-SNAREs promiscuously (Fasshauer *et al.*, 1999). However, according to the SNARE hypothesis, interactions between cognate SNAREs are responsible for maintaining the specificity of fusion events between membrane compartments (Sollner *et al.*, 1993). This is supported by results from *in vitro* fusion experiments with combinations of yeast SNAREs. With just one exception out of 147 combinations, only combinations of SNAREs that had been shown to function together *in vivo* were able to catalyse *in vitro* membrane fusion, despite the ability of their cytosolic domains to bind promiscuously (Parlati *et al.*, 2002). This specificity adds support to the suggestion that SNAREs catalyse fusion *in vivo*. However, studies of complex formation *in vivo* have so far failed to provide a direct demonstration that SNAREs provide the machinery that catalyses fusion. Studies on both sea urchin cortical granules and yeast vacuoles showed that SNARE complex formation preceded membrane fusion, but that subsequent disassembly of the complexes did not prevent completion of the fusion reaction (Coorssen *et al.*, 1998; Tahara *et al.*, 1998; Ungermann *et al.*, 1998). Furthermore, synaptic transmission still occured in VAMP knockout mice, albeit at reduced frequency compared to wild types (Schoch *et al.*, 2001).

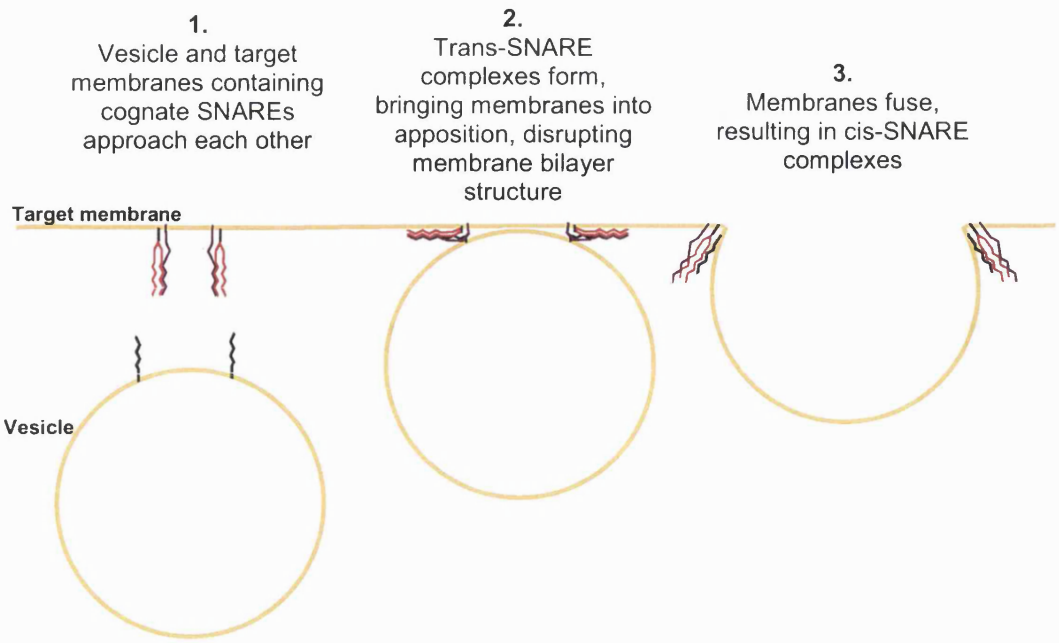

Figure 1.4. The SNARE hypothesis and SNARE-mediated membrane fusion. Specific v- and t-SNAREs in opposing membranes form trans-SNARE complexes that bridge the vesicle and target membranes, bringing them into close proximity. The SNARE complex may cause dehydration of the membranes, bringing them closer together, and exerts a force on membrane lipids, causing deformation of the lipid bilayer. These actions lower the energy barrier to full fusion. Following fusion, the SNAREs are bound in a cis-complex that is disassembled by NSF and αSNAP, after which they can partake in further rounds of fusion.

One alternative mechanism for membrane fusion involves the v-type ATPases. In the yeast vacuole system, SNAREs act upstream of the v-ATPase by bringing opposing membranes together. v-ATPase complexes (whose previously characterised function was in active pumping of protons into the vacuole) form a bridge between the membranes, and may drive membrane fusion by forming a proteinaceous discontinuity in the lipid bilayer, which opens up to form an aqueous pore, thereby

achieving membrane fusion (Peters *et al.*, 2001). This type of fusion has only been observed in the yeast vacuole system, although v-ATPases are present in many types of vesicle, including GLUT4 vesicles (Malikova *et al.*, 2004).

Apart from catalyzing membrane fusion, it has been suggested that SNAREs may act as a link between membrane fusion and other events in the cell, such as signalling. For example, SNARE proteins may be involved in regulating membrane fusion sensitivity to calcium ion concentration (Stewart *et al.*, 2000). SNAP25 and SNAP23 have been shown to differentially regulate fusion with respect to calcium ion concentration by interacting with diverse members of the synaptotagmin family (Chieregatti *et al.*, 2004). SNAREs have also been shown to interact directly with and regulate the activities of calcium channels (Jarvis *et al.*, 2002; Ji *et al.*, 2003; Merz and Wickner, 2004; Verderio *et al.*, 2004). SNARE proteins may thus regulate both the availability of calcium ions and the sensitivity of the fusion apparatus to calcium. GLUT4 vesicle fusion with the plasma membrane is one of many membrane fusion events that have been shown to require increased calcium ion concentration (Whitehead *et al.*, 2001). Other proteins that interact with SNAREs, such as proteins of the Sec1/Munc18 (SM) family may link membrane fusion to regulation by signalling pathways (Barclay *et al.*, 2003).

The SNARE proteins therefore have a function in bringing lipid membranes together upstream of the fusion reaction, and may themselves catalyse the fusion reaction. There is a lack of direct evidence for SNARE-catalysed membrane fusion *in vivo,* and the exact role played by SNAREs is still controversial.

1.7.3. SNAREs in GLUT4 exocytosis

The adipocyte homologs of syntaxin1, SNAP25 and VAMP that are involved in GLUT4 exoytosis are syntaxin4, SNAP23, and VAMP2. They are thought to be structurally analogous in the SNARE complex, that is syntaxin4 and VAMP2 are both single transmembrane domain proteins that contribute one SNARE domain each to the SNARE complex, and SNAP23 is attached to the membrane via palmitoylated cysteine residues and contributes two SNARE domains to the core complex (Thurmond and Pessin, 2001).

Interference with syntaxin4 function by introduction of anti-syntaxin4 antibodies, or soluble domains of syntaxin4 into cells inhibited insulin stimulated GLUT4 exocytosis and glucose uptake (Cheatham *et al.*, 1996; Volchuk *et al.*, 1996). Insulin stimulation also increased co-immunoprecipitation of GLUT4 vesicles with syntaxin4 (Olson *et al.*, 1997), suggesting that insulin signalling regulates interactions of GLUT4 vesicles with syntaxin4.

Treatment of 3T3-L1 adipocytes with BoNT B or BoNT D inihibited insulin stimulated glucose uptake (Tamori *et al.*, 1996), suggesting a role for VAMP2 or VAMP3 (cellubrevin) in this process. Inhibition of insulin stimulated glucose uptake by cleavage of VAMP2 and VAMP3 with tetanus toxin could be reversed by addition of toxin resistant VAMP2 in muscle cells (Randhawa *et al.*, 2004). Several studies have also indicated that VAMP2 is associated with the insulin responsive GLUT4 compartment, whereas VAMP3 colocalises with GLUT4 in non insulin responsive compartments (Martin *et al.*, 1996; Sevilla *et al.*, 1997; Millar *et al.*, 1999).

Proteolytic cleavage by BoNT A of SNAP25, which is present in adipocytes did not affect insulin stimulated glucose transport (Chen *et al.*, 1997; Macaulay *et al.*, 1997). However, addition of the toxin insensitive homolog SNAP23 to permeabilised

3T3-L1 adipocytes inhibited insulin stimulated GLUT4 translocation (Rea *et al.*, 1998). SNAP23 participated in complexes with syntaxin4 and VAMP2 both in adipocytes and *in vitro* (Tamori *et al.*, 1998; St Denis *et al.*, 1999). These data implicate syntaxin4, SNAP23 and VAMP2 as the SNAREs involved in insulin-stimulated GLUT4 exocytosis (Figure 1.5.).

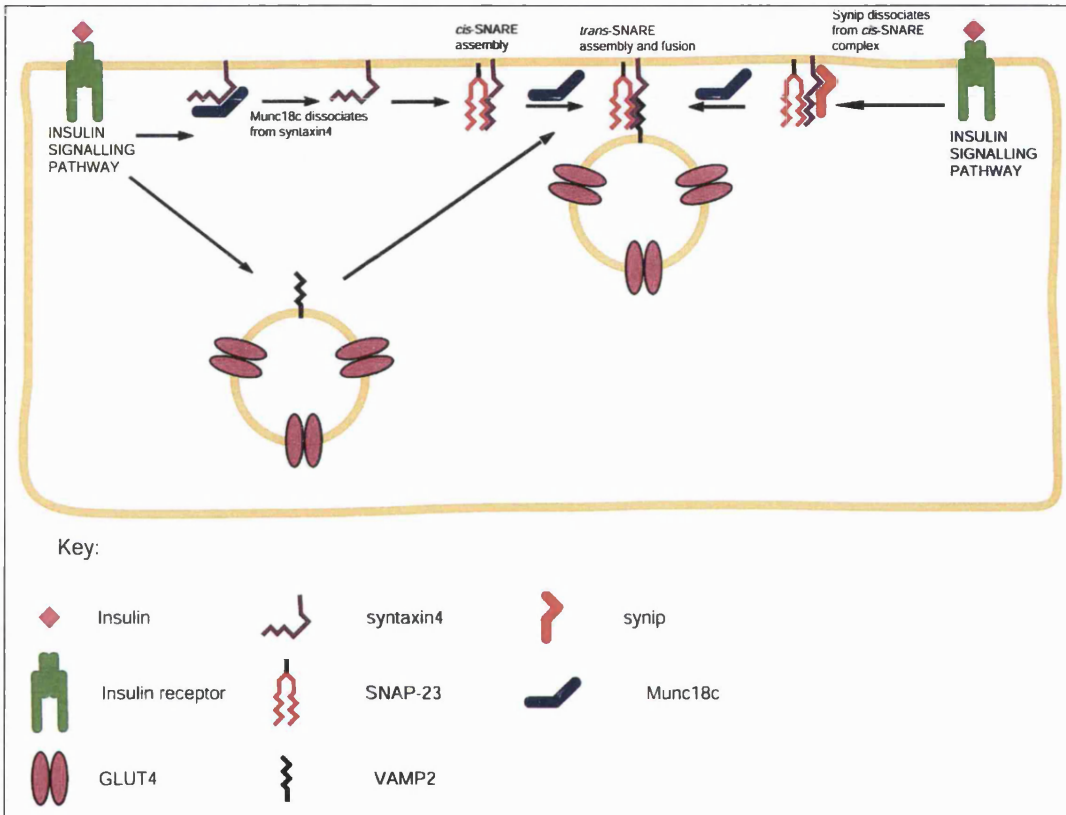

Figure 1.5. Membrane fusion in insulin stimulated glucose uptake. Insulin signalling stimulates translocation of GLUT4 vesicles to the plasma membrane, and induces dissociation of Munc18c from syntaxin4. This allows a t-SNARE complex to form, which then form a ternary SNARE complex, perhaps with the help of Munc18c, leading to fusion with the plasma membrane. Similarly, insulin signalling dissociates the syntaxin4/synip complex, allowing SNARE complex assembly and subsequent fusion.

1.7.4. SNARE-interacting proteins in GLUT4 exocytosis

1.7.4.1. Synip and Munc18c

Synip and the Sec1/Munc18c family (SM family) protein Munc18c are associated with syntaxin4 in the basal state, but dissociate from syntaxin4 on insulin stimulation (Araki *et al.*, 1997; Tamori *et al.*, 1998; Min *et al.*, 1999). Synip has also been identified as a substrate of Akt2, and phosphorylation on a serine residue by Akt2 appears to regulate its interaction with syntaxin4 in response to insulin (Yamada *et al.*, 2005). This was the first interaction to be identified that directly linked insulin signalling to the vesicle fusion machinery.

Both synip and Munc18c appear to block SNARE complex formation when associated with syntaxin4, so are thought to be possible negative regulators of SNARE complex assembly. PI 3-kinase inhibition did not block insulin stimulated GLUT4 exocytosis in adipocytes derived from Munc18c -/- mouse embryos, implying that Munc18c also plays a critical role in the PI 3-kinase mediated regulation of the vesicle fusion machinery (Kanda *et al.*, 2005). Disruption of the Munc18c/syntaxin4 complex by injection of complex inhibiting peptides caused accumulation of unfused GLUT4 vesicles at the plasma membrane, suggesting that Munc18c may also have a positive role to play in the fusion reaction (Thurmond *et al.*, 2000).

This apparent dual inhibitory and stimulatory role of Munc18c is not uncommon in SM family proteins. The SM family proteins are unusual in that although they show a high degree of sequence homology and they all bind to syntaxins, they also show great diversity in their modes of binding to syntaxins. For example, neuronal Munc18a binds to a closed conformation of syntaxin that is incompatible with SNARE complex formation (Dulubova *et al.*, 1999). The yeast SM protein, Sec1p binds to an assembled ternary SNARE core complex (Carr *et al.*,

1999). SM proteins present in the ER, the Golgi apparatus, and the TGN bind to a conserved amino-terminal domain in their syntaxin partners (Dulubova *et al.*, 2002; Yamaguchi *et al.*, 2002). Finally, the yeast SM protein Vps33p interacts with the syntaxin Vam3p indirectly via a multi-protein complex (Sato *et al.*, 2000). SM proteins have been associated with either negative or positive regulation of SNARE complex assembly in these systems, or both negative and positive regulation in the case of Munc18a (Pevsner *et al.*, 1994; Voets *et al.*, 2001).

Munc18c is thought to bind to syntaxin4 in the closed conformation, as it prevents SNARE complex formation when in this binary complex (Araki *et al.*, 1997; Tamori *et al.*, 1998). However, it can also bind a ternary syntaxin4/SNAP23/VAMP2 complex *in vitro* (Widberg *et al.*, 2003). These multiple modes of binding may indicate that Munc18c/SNARE interactions have more than one function upstream of membrane fusion.

1.7.4.2. Tomosyn

Tomosyn is a ubiquitously expressed protein that has been shown to bind to syntaxin4, the syntaxin4/SNAP23 dimer and the syntaxin4/Munc18c dimer *in vitro* via a VAMP2-like domain. Overexpression of tomosyn in 3T3-L1 adipocytes inhibited insulin stimulated GLUT4 vesicle translocation to the plasma membrane. Because of these interactions, and the similarity of the domain structure of tomosyn to that of the Golgi tethering factor p115, it has been suggested that tomosyn may function as a tethering factor for GLUT4 vesicles with the plasma membrane (Widberg *et al.*, 2003).

1.7.4.3. VAP-33

VAMP-associated protein of 33 kDa (VAP-33) binds to VAMP2 *in vitro*, and was found to colocalise with VAMP2 and GLUT4 in L6 myoblasts and 3T3-L1 adipocytes. Overexpression of VAP-33 or introduction of anti-VAP-33 antibodies into cells inhibited insulin-stimulated GLUT4 translocation (Weir *et al.*, 1998; Foster *et al.*, 2000). VAP-33 may therefore regulate VAMP2 availability and thereby GLUT4 vesicle fusion in insulin responsive tissues.

1.7.4.4. Cysteine string protein

Cysteine string protein (csp) is associated with synaptic vesicles and chaperone proteins and is thought to be involved in targeting chaperone proteins to the exocytic machinery where they can regulate assembly of protein complexes (Evans *et al.*, 2003). Csp was also detected in plasma membranes from 3T3-L1 adipocytes. Csp interacted with syntaxin4 in these cells, and may play a role in the assembly of complexes with syntaxin4 (Chamberlain *et al.*, 2001).

1.7.4.5. Pantophysin

Synaptophysin is a VAMP2-interacting protein that is expressed in neuroendocrine cells, and may have a role in regulating interactions with other SNARE proteins (Edelmann *et al.*, 1995). The related protein pantophysin was detected in 3T3-L1 adipocytes and in mouse adipose tissue. Pantophysin co-immunoprecipitated with VAMP2 and was postulated to regulate SNARE assembly in insulin-responsive cells, although there was no evidence of any insulin-induced changes to the protein (Brooks *et al.*, 2000).

Of these SNARE-interacting proteins, synip and Munc18c appear to be the best candidates for potential targets for insulin regulation of GLUT4 vesicle fusion with the plasma membrane. Both appear to negatively regulate trans-SNARE complex assembly in the basal state, and Munc18c may also be required at a late stage of insulin-stimulated membrane fusion. The distribution and quantitation of Munc18c and SNAREs is examined in this thesis.

1.8. Aims of the work described in this thesis

The work described in this thesis was undertaken with the overall aim of clarifying the relationships between insulin signalling pathways and docking and fusion of GLUT4 vesicles with the plasma membrane in the adipocyte. Chapter 3 addresses the question of whether insulin stimulates the transport activity of GLUT4 in addition to the fusion of GLUT4 vesicles with the plasma membrane, and examines the potential involvement of a p38 MAP kinase dependent pathway in this process. In Chapter 4, proteins involved in the membrane fusion reaction in adipocytes are quantified, with the aim of providing an improved basis for the interpretation of results of experiments involving these proteins. Chapter 5 describes the development of an *in vitro* assay for membrane fusion mediated by syntaxin4, SNAP23 and VAMP2. The rationale for devising this assay was that it would facilitate the interpretation of molecular and cellular events underlying *in vivo* responses to insulin.

Chapter 2 - Materials and Methods

2.1. Chemical reagents

All laboratory chemicals and reagents were of analytical grade and were purchased from Sigma-Aldrich unless otherwise stated.

Enhanced chemiluminescent reagent (ECL), 3-O-[^{14}C]methyl-D-glucose, glutathione-sepharose 4B, NHS-sepharose-FF were obtained from Amersham Pharmacia Biotech.

Monocomponent porcine insulin was a generous gift of Dr. G. Daniellson (Novo Nordisk).

BioWest extended duration chemiluminescent substrate was obtained from UVP.

Optiphase Safe scintillation fluid was obtained from LKB.

Collagenase Type I was obtained from Worthington Biochemical.

Bovine Serum Albumin (BSA) (Bovine Cohn Fraction V) was from Intergen Company.

Protein molecular weight markers were obtained from Sigma and NEB.

Lipids were obtained from Avanti Polar Lipids.

Kanamycin sulphate and n-octylglucoside was obtained from Melford Laboratories.

Ni-NTA agarose was obtained from Novagen.

Acrylamide stock (30% acrylamide, 0.8% bis-acrylamide) was obtained from Flowgen.

Molecular biology grade agarose and DNA molecular weight markers were obtained from Invitrogen.

The plasmids pGEX-SNAP23 and pGEX-Munc18c were generous gifts from Dr. H. Tamori (Kobe University, Japan) and Prof. J. Pessin (University of Iowa, USA).

pSNiR3 was a generous gift from Prof. Dr. D. Langosch, Technische Universität München, Germany.

2.1.1. Oligonucleotide primers

DNA primers were made to order through EasyOligo (Helena Biosciences). Primer sequences are shown below:

Primer name	**Sequence**
stx4nt	atgcgcgacaggacccatgagttgaggc
stx4ct	tccaacggttatggtgatgccaatgatg
NcoIstx4	ccgccgccatgggccgacaggacccatgagt
stx4XhoI	cggcctcgagtgctccaacggttatggtga
EcoRI-stx4-5P	cgccgaattcatgcgcgacaggacccatga
Stx4-STOP-XhoI-3P	cgctcgagttatccaacggttatggtgatg
T7 promoter primer	taatacgactcactataggg
pSNiR3-HA	cgatcggaattcgccaccacgcggaaccag
pET-AvaI-rbs	tccctcgaggaccctctagaaataattttg
T7 terminator primer	gctagttattgctcagcgg
vamp2nt	atgtcggctaccgctgccaccgtcccga
vamp23p	ggcccttcttaggcagggcagactcctcag
NcoI-VAMP2	ggccagccatggcggctaccgctgccaccg
VAMP2-XhoI	cggtcgctcgagagtgctgaagtaacgat
EcoRI-VAMP2	gtataggaattcatgtcggctaccgctgcc
VAMP2-STOP-BamHI	cggcggatccttaagtgctgaagtaaacg

2.1.2. Buffers

Generally used buffers were made up as shown below and stored for up to one month at 4°C.

Electrophoresis Running buffer	0.025 M Tris-HCL, pH 6.3, 0.1% (w/v) SDS and 0.2 M glycine
HES buffer (Hepes/EDTA)	10 mM Hepes, pH 7.2, 1 mM EDTA and 250 mM Sucrose
Krebs-Ringer-Hepes, (KRH)	10 mM Hepes, pH 7.4, 140 mM NaCl, 4.7 mM KCl, 2.5 mM $CaCl_2$, 1.25 mM $MgSO_4$ and 2.5 mM NaH_2PO_4
Phosphate-buffered Saline, (PBS)	154 mM NaCl, 12.5 mM $Na_2HPO_4.12H_2O$, pH 7.2
Stacking Gel buffer (4x)	0.5 M Tris-HCL, pH 6.8 and 0.4% (w/v) SDS
Resolving Gel buffer (4x)	1.5 M Tris-HCL, pH 8.8 and 0.4% (w/v) SDS

The following solutions were stored at room temperature.

Ponceau stain	0.1% Ponceau S (w/v) in 3% trichloroacetic acid (v/v)
SDS Sample buffer	10% SDS (w/v), 0.5M Tris-HCl, pH 6.8, 0.05% (w/v) bromophenol blue and 10% (v/v) glycerol
Low-SDS Sample buffer	1% SDS (w/v), 0.5M Tris-HCl, pH 6.8, 0.05% (w/v) bromophenol blue and 10% (v/v) glycerol
Tris-buffered Saline (TBS)	10 mM Tris, pH 7.4, and 154 mM NaCl

TBS-Tween	10 mM Tris, pH 7.4, 154 mM NaCl and 0.1% (v/v) Tween-20
Transfer buffer	39 mM glycine, 48 mM Tris, pH 8.8, 0.0375% (w/v) SDS and 20% (v/v) methanol
Tris-acetate EDTA buffer	40 mM Tris-acetate, 1 mM EDTA, pH 8.

Protease inhibitor cocktail was made up as two separate 1000x stocks, the first containing 1 mg/ml leupeptin, 1 mg/ml aprotonin, 1 mg/ml pepstatin A, 1 mg/ml antipain. The second stock consisted of 100 mM 4-(2-aminoethyl) benzenesulphonyl fluoride (AEBSF).

LB media was made up with 10 g of Bacto-tryptone, 5 g of yeast extract and 10 g of NaCl per litre in water, pH was adjusted to 7.5 with NaOH, and the LB was sterilized by autoclaving.

2.1.3. Bovine Serum Albumin for adipocyte cultures

10 g of BSA (Fraction V) was dissolved in double distilled water overnight at 4°C. The solution was filtered through a Millipore type A 0.8 μm membrane filter under vacuum and the pH was adjusted to 7.6 with 10 M NaOH. Final BSA concentration was adjusted to 10% with double distilled water, and stored at -20°C.

2.1.4. Insulin

1 mg of porcine insulin was dissolved in 1 ml of 30 mM HCl and made up to 3 ml with double distilled water. 1 ml of this solution was diluted to 50 ml with 10 mM

Hepes buffer pH 7.6, 1% BSA. This solution, containing 1 μM insulin was stored in small aliquots at -20°C, and was not refrozen once thawed.

2.1.5. Antibodies

Primary antibodies used in this report are listed below. Working dilutions are of 1 mg/ml stocks and are given for western blotting and immunofluorescence (IF).

Antibody	Type	Source	Working dilution
Insulin receptor β-subunit	Purified rabbit polyclonal	Upstate Biotechnology	1:1000
p38 MAP kinase	Purified rabbit polyclonal	Cell Signaling Technology	1:1000
Phospho-p38 MAP kinase	Purified rabbit polyclonal	Cell Signaling Technology	1:1000
Phospho-p44/42 Erk MAP kinase	Purified rabbit polyclonal	Cell Signaling Technology	1:1000
Phospho-SAPK/JNK MAP kinase	Purified rabbit polyclonal	Cell Signaling Technology	1:1000
Phospho-CREB	Purified rabbit polyclonal	Upstate Biotechnology	1:1000

Phospho-Akt (Thr308)	Purified rabbit polyclonal	Cell Signaling Technology	1:1000
Phospho-Akt (Ser473)	Purified rabbit polyclonal	Cell Signaling Technology	1:1000
SNAP23	Purified rabbit polyclonal	Synaptic Systems	1:1000
SNAP23	Purified rabbit polyclonal	As described in Section 2.6.	1:1000
Syntaxin4	Purified rabbit polyclonal	G. D. Holman University of Bath	1:4000
VAMP2	Mouse monoclonal	Synaptic Systems	1:1000 1:100 (IF)
VAMP2	Purified rabbit polyclonal	As described in Section 2.6.	1:1000
Munc18c	Purified rabbit polyclonal	As described in Section 2.6.	1:1000
GLUT4	Purified rabbit polyclonal	G. D. Holman University of Bath	1:4000 1:200 (IF)

Secondary antibodies used are listed below. Working dilutions are given for western blotting (wb) and immunofluorescence (IF).

Antibody	**Source**	**Working dilution**
Goat anti-rabbit IgG peroxidase conjugate	Sigma Immunochemicals	1:4000 (wb)

Goat anti-mouse IgG peroxidase conjugate	Sigma Immunochemicals	1:1000 (wb)
AlexaFluor488-conjugated goat anti-rabbit IgG	Molecular Probes	1:200 (IF)
AlexaFluor568-conjugated goat anti-mouse IgG	Molecular Probes	1:200 (IF)

2.2. Protein Biochemistry Techniques

2.2.1. SDS-Polyacrylamide gel electrophoresis

Proteins were analysed by electrophoresis using a modification of the method of Kato, using the discontinuous buffer system of Laemmli (Laemmli, 1970; Kato *et al.*, 1983). Stacking gels were made from stock stacking gel buffer, acrylamide and double distilled water to give final concentrations of 125 mM Tris-HCl, pH 6.8 and 0.1% (w/v) SDS, 6% acrylamide and polymerised with addition of 0.005% (w/v) ammonium persulphate (APS) and 0.05% (w/v) N,N,N,N'-tetramethylethylenediamine (TEMED). Resolving gels were made at acrylamide concentrations of 10%, 12% and 14%, depending on the experiment in a buffered solution of 0.375 M Tris-HCl, pH 8.8 and 0.1% (w/v) SDS and polymerised by adding 0.005% (w/v) ammonium persulphate (APS) and 0.05% (w/v) N,N,N,N'-tetramethylethylenediamine (TEMED). Unless otherwise stated, protein samples were solubilised in SDS sample buffer and heated for 5 min at 95°C in SDS sample buffer containing 100 mM dithiothreitol (DTT). Samples were loaded onto gels and run in either the Protean II, Mini Protean II, or Mini Protean III gel systems (BioRad). Gels were run in 25 mM Tris-HCl, pH 8.3, 192 mM glycine, 0.1% (w/v) SDS at a constant

current of 25 mA per gel in the Protean II system, and at constant voltage of 180 V in the Mini Protean systems until the blue dye front had run out of the gel. Samples were run alongside Broad Range Molecular Weight Markers (NewEnglandBiolabs) or High Molecular Weight Markers (Sigma).

2.2.2. Coomassie Blue Staining

Gels were stained with coomassie brilliant blue reagent (0.2% (w/v) Coomassie blue R-250 in 30% (v/v) methanol, 10% (v/v) glacial acetic acid, 60% (v/v) water) overnight at room temperature, followed by destaining in 30% (v/v) methanol, 10% (v/v) glacial acetic acid, 60% (v/v) water.

2.2.3. Copper Staining

For quick visualisation of proteins, gel strips were stained for 5 min with 300 mM $CuCl_2$ and washed with water (Lee *et al.*, 1987).

2.2.4. Electrophoretic Transfer of Proteins to Nitrocellulose

Proteins were transferred by the semi-dry transfer method (Towbin *et al.*, 1979) using a Multiphor II NovaBlot electrophoretic transfer unit (Amersham Pharmacia Biotech). Nine pieces of Whatman 3 mm paper, cut to the size of the resolving gel were soaked in transfer buffer (39 mM glycine, 48 mM Tris base, 0.0375% (w/v) SDS and 20% (v/v) methanol, pH 8.8) and placed on the anode. A sheet of nitrocellulose (45 μM pore size, Gelman Sciences) was soaked in transfer buffer and placed on the paper. The resolving gel was soaked in transfer buffer and placed on the nitrocellulose sheet, followed by another nine pieces of Whatman paper that had been soaked in transfer buffer. The cathode was replaced on top of this and

the system was run at a fixed current of 0.8 mA per cm^2 of gel surface for 1 h 50 min. At the end of the run, the nitrocellulose sheet was rinsed in water and proteins were visualised with Ponceau stain. Positions of molecular weight markers were marked with a soft pencil, and stain was washed off with TBS-Tween.

2.2.5. Western blotting

Nonspecific protein binding sites were blocked by incubating the nitrocellulose membrane in 5% (w/v) Marvel dried skimmed milk in TBS-Tween for 30 min with gentle rocking. Excess milk was rinsed off with TBS-Tween and the membrane was incubated with the required dilution of primary antibody in TBS-Tween, 1% BSA for 1 h. The membrane was washed five times with TBS-Tween with vigorous rocking, with each wash lasting 10 min. The membrane was then incubated with the appropriate secondary antibody diluted in TBS-Tween, 5% (w/v) Marvel dried skimmed milk for 1 h with gentle rocking, and washed extensively as before.

Specific protein bands were visualised using ECL reagent or BioWest extended duration chemiluminescent substrate according to the respective manufacturers' instructions. Bands were detected using an EpiChemiII darkroom and digital camera system (UVP). Bands were quantified using Labworks software (UVP).

2.2.6. Competition western blot assay

2μg of purified Munc18c serum was incubated for 1 h at room temperature in 200μl of TBS with or without 0.2 mg of recombinant GST-Munc18c. Solutions were centrifuged at 10000g for 10 minutes at 4°C, made up to 2 ml with TBS-T and were

used to carry out western blots on adipocyte lysates by the usual method (Section 2.2.5).

2.3. Molecular Biology

2.3.1. DNA analysis

PCR products and digested plasmid DNA fragments were run on 1% agarose Tris-acetate EDTA gels run at a constant 160 V for 20 – 40 min and visualised by ethidium bromide staining under uv transillumination. Where required bands were excised from gels and purified using the GenElute agarose gel slice purification kit (Sigma). DNA sequencing was carried out using a PE Biosystems ABI 377 DNA Sequencer.

2.3.2. Polymerase chain reaction

DNA was amplified by PCR with 2 U of PfuTurbo DNA polymerase (Stratagene) in 50 µl reactions using the following program in MiniCycler (MJ Research): 94°C for 50 s, 55°C for 1 min, 72°C for 1 min. This cycle was repeated 34 times, followed by a final extension at 72°C for 6 min.

2.3.3. Plasmid manipulations

Plasmid DNA was purified from cultures of transformed XL1Blue strain *E. coli* in 5 ml of LB media using the Wizard Plus SV minipreps DNA purification system (Promega) according to the protocol provided by the manufacturer. Restriction enzymes were purchased from Promega or Sigma-Aldrich. Digests were carried out at 37°C according to the instructions of the manufacturer. Ligations were done using the LigaFast Rapid DNA Ligation System (Promega).

2.4. DNA cloning

2.4.1. Syntaxin4

2.4.1.1. Cloning of syntaxin4 from rat adipocytes

Total RNA was extracted from epididymal fat pads of male Wistar rats using Trizol (Invitrogen, UK) according to the manufacturer's instructions. Messenger RNA was isolated from the total RNA population using the PolyATtract IV system (Promega), and was reverse transcribed to produce a single stranded adipocyte cDNA library using Superscript II reverse transcriptase (GibcoBRL). The coding region of syntaxin4 was amplified by PCR using the first strand cDNA mixture as a template, with the primers stx4nt and stx4ct. The PCR product was blunt cloned directly into pT7Blue to yield the plasmid pT7Blue-stx4. This was repeated with the product from a second identical RT-PCR reaction, and the syntaxin4 inserts from both RT-PCR reactions were sequenced.

2.4.1.2. Construction of pET28a-stx4, a syntaxin4-his expression vector

The syntaxin4 coding region from pT7Blue-stx4 was amplified by PCR with the primers NcoIstx4 and stx4XhoI. The product, containing the syntaxin4 coding region flanked by NcoI and XhoI restriction sites, was blunt cloned into pT7Blue to produce pT7Blue-NcoIstx4XhoI. The syntaxin4 coding region was excised from this plasmid with the restriction enzymes NcoI and XhoI and ligated into pET28a that had been cut with the same enzymes.

The resulting plasmid, pET28a-stx4 therefore contained an insert coding for syntaxin4 with a carboxy-terminal his-tag under transcriptional control of the T7 promoter.

2.4.1.3. Construction of pDRSN1-stx4, a NucA-syntaxin4 expression vector

The NucA-syntaxin4 expressing plasmid was derived from pSNiR3. pSNiR3 is a pET21 derived plasmid designed to express a his-tagged NucA moiety at the amino terminus of the fusion protein, with a thrombin cleavage site between the NucA moiety and the multiple cloning site. There is also a hemaglutinin epitope tag (HA-tag) that remains on the target protein following thrombin cleavage. Following insertion of the syntaxin4 sequence, the plasmid was modified to remove the HA-tag from the target protein and to reduce the six-glycine residue spacer that remains on the fusion protein following thrombin digestion to two glycine residues.

EcoRI and XhoI sites were added to syntaxin4 coding DNA by PCR of pT7Blue-stx4 with the adaptor primers EcoRI-stx4-5P and Stx4-STOP-XhoI-3P. The PCR product was blunt cloned into pT7Blue to yield pT7Blue-EcoRIstx4-STOP-XhoI. The syntaxin4 coding fragment was excised from this plasmid using the restriction enzymes EcoRI and XhoI and ligated into the corresponding sites on pSNiR3 to produce pSNiR3-stx4. In order to modify this plasmid as described above, the NucA encoding region of pSNiR3 was amplified by PCR with the T7 promoter primer and pSNiR3-HA and the product was blunt cloned into pT7Blue to yield pT7Blue-NucA1. The NucA coding region was cut out from this plasmid with the enzymes XbaI and EcoRI and ligated into the corresponding sites on pSNiR3-stx4 to yield the modified NucA-syntaxin4 expressing plasmid pDRSN1-stx4.

2.4.1.4. Construction of pGEX-tSNAREs and pGEX-tSNAREs(NucA), t-SNARE co-expression vectors

The syntaxin coding region from pT7Blue-stx4-STOP was cut out with EcoRI and XhoI and ligated into pET28a cut with the same enzymes, making pET28a-stx4-STOP. The syntaxin coding sequence, together with the ribosome binding site was amplified from pET28a-stx4-STOP by PCR with the primers pET-AvaI-rbs and the T7 terminator primer. The purified PCR product was blunt cloned into pT7Blue. The insert was then cut out of this plasmid with XhoI, and was ligated into the XhoI site in pGEX-SNAP23, resulting in the plasmid pGEX-tSNAREs. This plasmid codes for bacterial expression of GST-SNAP23 and unmodified syntaxin4, both under control of the same *tac* promoter.

pGEX-tSNAREs(NucA) was made by amplifying the NucA-syntaxin4 coding region from pDRSN1-stx4 by PCR with the primers pET-AvaI-rbs and the T7 terminator primer. The PCR product was cloned into pT7Blue then cut out with XhoI and ligated into the XhoI site in pGEX-SNAP23. The resulting plasmid codes for bacterial expression of GST-SNAP23 and NucA-syntaxin4 under the control of a single *tac* promoter.

2.4.2. VAMP2

2.4.2.1. Cloning of VAMP2 from rat adipocyte cDNA

The coding sequence of VAMP2 was cloned from a Marathon (Clontech) rat adipocyte cDNA library, constructed according to the manufacturer's instructions by Dr. Paul Whitley (Whitley *et al.*, 2003). The coding region of VAMP2 was amplified from this library by PCR using the primers vamp2nt and vamp23p. The purified product was reamplified by PCR with the primers NcoI-VAMP2 and VAMP2-XhoI

to produce a PCR product containing the VAMP2 cloning region flanked by NcoI and XhoI restriction sites. This product was blunt cloned into pT7Blue to yield the plasmid pT7Blue-NcoIVAMPXhoI.

2.4.2.2. Construction of a pET28a-VAMP2, a VAMP2-his expression vector

The VAMP2 coding region was cut out from pT7Blue- NcoIVAMPXhoI with NcoI and XhoI and ligated into the NcoI and XhoI sites of pET28a. The resulting plasmid encoded the expression of full length VAMP2 with a carboxy-terminal his-tag.

2.4.2.3. Construction of pDRSN1-VAMP2, a NucA-VAMP2 expression vector

The VAMP2 coding region was amplified from pET28a-VAMP2 by PCR with the primers EcoRI-VAMP2 and VAMP2-STOP-BamHI. This fragment was blunt cloned into pT7Blue and cut out with EcoRI and BamHI, and ligated into pSNiR3 cut with the same enzymes to produce pSNiR3-VAMP2. The NucA coding region from pT7Blue-NucA1 was cut out with XbaI and EcoRI and ligated into PSNiR3-VAMP that had been cut with the same enzymes, resulting in pDRSN1-VAMP2.

2.4.2.4. Construction of pDRSN1-VAMP$_{cyt}$, a NucA-VAMP$_{cyt}$ expression plasmid

NucA-VAMP$_{cyt}$, a Nuclease A fusion protein with the cytosolic domain of VAMP2, was expressed from the plasmid pDRSN1-VAMP$_{cyt}$. This plasmid was constructed by restriction digest of pDRSN1-VAMP2 with BclI and BamHI, and re-ligating the remainder of the plasmid to itself. These enzymes cut VAMP2 either side of the transmembrane domain coding sequence and leave compatible sticky ends,

which when ligated together, leave a plasmid that codes for a Nuclease A fusion protein with the cytosolic domain of VAMP2.

2.4.3. SNAP23

2.4.3.1. Construction of pDRSN1-SNAP23, a NucA-SNAP23 expression vector

The SNAP23 coding region of pGEX-SNAP23 was cut out by restriction digest with EcoRI and XhoI and ligated into the EcoRI and XhoI sites in pSNiR3, producing pSNiR3-SNAP23. The NucA coding region from pT7Blue-NucA1 was cut out with XbaI and EcoRI and ligated into pSNiR3-SNAP that had been cut with the same enzymes, resulting in pDRSN1-SNAP23. This plasmid codes for the expression of SNAP23 with an amino terminal NucA tag.

2.5. Recombinant protein expression

In general, for a 1 l expression culture, a single colony of Rosetta(DE3)pLysS transformed with the appropriate expression plasmid was incubated for 16 h in 5 ml of LB supplemented with the appropriate antibiotics at 37°C with shaking at 200 rpm. The entire culture was then transferred to 1 l or 2 l of sterile LB which were incubated with shaking at 37°C until the optical density of the culture at 600 nm had reached 0.5. Expression was induced at this point by adding 0.5 mM IPTG for pGEX-based plasmids and 1 mM IPTG for pET-based plasmids. The culture was incubated for a further three hours, after which cells were harvested by centrifugation at 5000 g for 5 min. Cell pellets were stored at -70°C until required.

2.5.1. Expression and purification of syntaxin4-his

pET28a-stx4 was transformed into the Rosetta(DE3)pLysS strain and the cells were propagated in 2 l of LB supplemented with 50 mg/l kanamycin and 34 mg/l chloramphenicol. Following harvesting and freezing, the bacterial pellet was thawed and resuspended in 40 ml 25 mM sodium phosphate buffer pH 8, 1 M NaCl containing protease inhibitors and sonicated on ice with four pulses of 30 s with 30 s pauses between pulses. Triton X-100 was then added to a final concentration of 4% v/v. Following solubilisation for 1 hour at 4°C, the lysate was cleared by centrifugation at 20000g for 30 min at 4°C. Cleared lysate was bound to 0.5 ml Ni-NTA agarose for 2 h at 4°C under slow rotation. The Ni-NTA resin was then loaded onto a 2 ml gravity column and washed five times with 10 ml 25 mM phosphate buffer pH 7, 0.5 M NaCl, 1 % TritonX-100. Proteins were eluted from the resin with imidazole or on a pH gradient.

2.5.2. Expression and purification of NucA-syntaxin4

Rosetta(DE3)pLysS cells containing pDRSN1-stx4 were grown in 2 l of LB supplemented with 200 mg/l ampicillin and 34 mg/l chloramphenicol. Following harvesting and freezing, the cell pellet was allowed to thaw on ice and resuspended in 50 ml of 50 mM sodium phosphate buffer pH 8, 10 mM $CaCl_2$ containing protease inhibitors, then incubated on ice for 15 min to allow digestion of genomic DNA by NucleaseA. Crude inclusion bodies were pelleted by centrifugation at 10000g for 10 min at 4°C. At this point inclusion bodies were either solubilised in 50 ml of IB buffer (25 mM sodium phosphate buffer pH 8, 1.5 M NaCl, 1% (w/v) n-octylglucoside) for 1 hour at 4°C for binding to Ni-NTA, or washed three times with 50 ml of 50 mM

sodium phosphate buffer pH 7.5, 1 mM EDTA, 1% n-octylglucoside and then solubilised in 5 ml of IB buffer for 1 hour at 4°C.

Solubilised inclusion bodies from a 2 l culture were incubated with 0.75 ml of Ni-NTA agarose for 2 h at 4°C. The resin was loaded onto a gravity column and washed with 20 ml 25 mM sodium phosphate buffer pH 7, 1.5 M NaCl, 1% n-octylglucoside. Proteins were eluted in this same buffer containing an additional 500 mM imidazole. Alternatively, thrombin was used to digest the syntaxin4 moiety away from the resin. 2 units of thrombin (Novagen) were added to the Ni-NTA resin with bound syntaxin4 in a volume of 1.5 ml of IB buffer and digested for 16 h at 4°C. Cleaved syntaxin4 was recovered by loading the resin onto a gravity column and eluting the protein with 25 mM sodium phosphate buffer pH 7, 250 mM NaCl, 1% n-octylglucoside with additional varying concentrations of KCl.

2.5.3. Expression and purification of GST-SNAP23

Rosetta(DE3)pLysS cells transformed with pGEX-SNAP23 were grown in 2 l of LB media supplemented with 200 mg/l Ampicillin and 34 mg/l chloramphenicol. Following harvesting and freezing, the cell pellet was thawed on ice and resuspended in 50 ml of 50 mM Tris buffer pH 8 containing 500 mM NaCl, 10 mM DTT and protease inhibitors. The suspension was sonicated on ice at the maximum intensity that did not cause frothing for four 30 s pulses with pauses of 30 s. Insoluble material was pelleted by centrifugation at 20000g for 30 min. The supernatant was incubated with 1.5 ml of glutathione-sepharose for 2 hours with rotation at 4°C. The resin was washed in a 2 ml gravity column and bound proteins were eluted in the same buffer containing 20 mM glutathione.

2.5.4. Expression and purification of coexpressed t-SNAREs

Rosetta(DE3)pLysS cells transformed with pGEX-tSNAREs were grown in 2 l of LB media supplemented with 200 mg/l Ampicillin and 34 mg/l chloramphenicol. Following harvesting and freezing, the cell pellet was thawed on ice and resuspended in 50 ml of ice cold 50 mM Tris buffer pH 7.5, 1 mM EDTA, 1% n-octylglucoside containing protease inhibitors. DNA was sheared by sonication at the maximum intensity that did not produce frothing, with two 45 s pulses with a 45 s pause between pulses. The suspension was centrifuged at 16000g for 10 minutes. The pellet was washed three times with 50 ml of ice cold 50 mM Tris buffer pH 7.5, 1 mM EDTA, 1% n-octylglucoside.

Inclusion bodies were isolated from Rosetta(DE3)pLysS cells transformed with pGEX-tSNAREs and pGEX-tSNAREs(NucA) and washed in the same way as described for NucA-syntaxin4 purification (Section 2.5.2.). Both sets of washed inclusion bodies were solubilised in 5 ml of 6 M guanidine HCl, 10 mM DTT, 1% n-octylglucoside for 20 min at room temperature. Insoluble material was removed by centrifugation at 20000g for 30 min at 4°C.

2.5.5. Expression and purification of VAMP2-his

Rosetta(DE3)pLysS containing pET28a-VAMP2 were grown up in 2 l of LB media containing 50 mg/l kanamycin and 34 mg/l chloramphenicol. Following harvesting and freezing, cells were harvested and the cell pellet was stored at -70°C overnight.

The cell pellet was resuspended in 40 ml of 50 mM sodium phosphate buffer containing 500 mM NaCl and protease inhibitors. The cell suspension was sonicated on ice at the highest possible intensity that did not produce frothing for four 30 s

pulses with 30 s pauses in between. Triton X-100 was added to a final concentration of 4% (w/v) and the lysate was solubilised with rotation for 1 hour at 4°C. The lysate was cleared by centrifugation at 20000g for 30 min. 500 µl of Ni-NTA resin was added to the cleared lysates and incubated with slow rotation for 1 h at 4 °C. Following binding, the resin was loaded onto a 2 ml gravity column and washed with 20 ml 25 mM sodium phosphate buffer pH 7 containing 500 mM NaCl and 1% Triton X-100 (w/v), followed by washing with 20 ml of 25 mM sodium phosphate buffer pH 7, 500 mM NaCl, 1% n-octylglucoside. Proteins were eluted either by washing the column with a gradient of imidazole in the final wash buffer, or by a pH gradient of 50 mM phosphate and 50 mM phosphate-citrate buffers containing 300 mM KCl and 1% n-octylglucoside.

2.5.6. Expression and purification of NucA-VAMP2

Rosetta(DE3)pLysS cells containing pDRSN1-VAMP2 were grown in 1 l of LB supplemented with 200 mg/l ampicillin and 34 mg/l chloramphenicol. Crude inclusion bodies containing NucA-VAMP2 were prepared from these cells as described for NucA-syntaxin4, solubilised in 50 ml IB buffer and bound to 1.5 ml Ni-NTA agarose for 2 h at 4°C. The resin was washed with 20 ml IB buffer in a 2 ml gravity column. Proteins were eluted from the resin by a gradient of imidazole or by digestion with 10 u of thrombin in 2.5 ml IB buffer for 16 h at room temperature.

2.5.7. Expression and purification of NucA-VAMP$_{cyt}$

NucA-VAMP$_{cyt}$ was expressed and purified by binding to Ni-NTA agarose and eluted with imidazole as described for NucA-VAMP2 in Section 2.5.6.

2.5.8. Expression and purification of NucA-SNAP23

NucA-SNAP23 was expressed and purified by binding to Ni-NTA agarose and eluted with imidazole, as described for NucA-VAMP2 Section 2.5.6.

2.5.9. Expression and purification of GST-Munc18c

GST-Munc18c for quantitation experiments was purified from Rosetta(DE3)pLysS cells containing pGEX-Munc18c (a kind gift from Professor Jeffrey Pessin, University Of Iowa, USA) that were grown in 2 l of LB supplemented with 200 mg/l ampicillin and 34 mg/l chloramphenicol. Protein was purified from the harvested and frozen cell pellet as described for the coexpressed t-SNAREs (Section 2.5.4).

2.6. Preparation of novel rabbit antibodies against SNAP23, Munc18c and VAMP2

2.6.1. Immunisations

One rabbit was immunised per antigen. GST-SNAP23 and GST-Munc18c were purified by binding lysates of bacteria transformed with pGEX-SNAP23 or pGEX-Munc18c to glutathione sepharose and eluting with glutathione solution, as described for GST-SNAP23 in Section 2.5.3. VAMP2 was purified by thrombin digestion of NucA-VAMP2 as described in Section 2.5.6. Six 200 μg aliquots of each protein were desiccated in a rotary evaporator. Animal work was carried out by Harlan Sera-Lab (Leicestershire, UK). For each immunisation, one aliquot was resuspended in equal volumes of sterile PBS and adjuvant (Freund's complete adjuvant for initial immunisations, and incomplete Freund's adjuvant for subsequent booster immunisations) and injected subcutaneously into the rabbit. Five booster

immunisations were carried out at fortnightly intervals. Terminal bleeds were carried out one week after the final immunisation.

2.6.2. Affinity purification of antibodies

NucA-SNAP23 and NucA-$VAMP_{cyt}$ were extensively dialysed against PBS and concentrated with a Centricon Plus-20 centrifugal filter unit to around 0.5 ml containing ~10 mg/ml of protein as measured by absorbance at 280 nm, and bound to 0.5 ml of NHS-conjugated sepharose (Amersham Pharmacia Biotech) for 2 h at room temperature with rotation. The resin was loaded onto a 2 ml gravity column and was washed extensively with 50 mM Tris pH 7.5, followed by washes with 10 ml of 0.2 M glycine, pH 2.8, and 10 ml of 0.1 M $NaHCO_3$, pH 8.5, 0.5 M NaCl. These two washes were repeated twice and the column was equilibrated with TBS-Tween containing 0.5 M NaCl. 1.25 ml of 10x TBS-Tween and 1.25 ml of 5 M NaCl were added to 10 ml of immunised rabbit serum, and the buffered rabbit serum was adsorbed by slowly passing through the column three times batchwise using a peristaltic pump. The column was then washed with 20 ml TBS-Tween containing 0.5 M NaCl, and then with 20 ml TBS containing 0.5 M NaCl. Antibodies were eluted using 0.2 M glycine, pH 2.8 and collected in 1 ml fractions in tubes containing 50 ml 1 M Tris pH 8.5. Absorbance of eluted fractions was measured at 280 nm, and protein-containing fractions were pooled, dialysed against PBS containing 0.02% (w/v) NaN_3 overnight and concentrated in a Centricon Plus-20 centrifugal concentrator. Protein concentration was adjusted to 1 mg/ml and the purified sera were stored in 1% BSA at –20°C. Columns were washed extensively with 0.2 M glycine, pH 2.8 and stored in TBS-Tween containing 0.02% (w/v) NaN_3.

Because of the difficulty in obtaining sufficient amounts of soluble protein, serum against GST-Munc18c was affinity purified by binding to GST-Munc18c on a nitrocellulose membrane. 2 ml of solubilised inclusion bodies containing GST-Munc18c (Section 2.5.9.) were separated by SDS-PAGE in the ProteanII gel system, and electrophoretically transferred to nitrocellulose. The nitrocellulose was stained with Ponceau stain and the band at ~97 kDa, corresponding to the migration of GST-Munc18c was cut out. A 4 cm length of the nitrocellulose membrane was rinsed briefly in TBS-Tween and blocked for 1 h with 5% dried milk in TBS-Tween with gentle rocking. The membrane was washed three times for five min each with TBS-Tween. 0.1 ml of 10x TBS-Tween was added to 1 ml of serum and this was incubated together with the strip of membrane for 1 hour at room temperature in a 1.5 ml tube. The membrane was washed five times for five min each with TBS-Tween. Specific antibodies were eluted by incubating the membrane strip with 1 ml of 0.1M glycine-HCl pH 2.8 for 3 min. The supernatant was neutralised immediately following elution by transferring it to a 1.5 ml tube containing 0.1 ml 2M Tris pH 8 on ice. The eluate was then dialysed overnight against PBS containing 0.02% (w/v) NaN_3. Dialysate was concentrated, and protein concentration was adjusted to 1 mg/ml. The purified serum was stored in 1% (w/v) BSA at -20°C.

2.7. Isolation of rat adipocytes

Isolated adipocytes were prepared from the whole epididymal fat pads of male Wistar rats weighing 175-190 g as described (Taylor and Holman, 1981). Rats were killed by cervical dislocation. Immediately afterwards, epididymal fat pads were removed to KRH buffer, 1% BSA at 37°C for transportation. The washed tissue was placed in KRH buffer, 3.5% BSA, 5 mM glucose, 0.7 mg/ml collagenase (4 pads for

every 5 ml of buffer) and chopped finely with scissors. The tissue was then digested in a 37°C water bath with continuous agitation at ~140 rpm until most of the clumps of cells had dispersed. The cell suspension was then filtered through a 250 μm nylon mesh (Lockertex), returned to a still water bath, and cells were allowed to float. Buffer below the cells was removed using a blunt needle and syringe, and the cells were washed four to five times in 20 ml KRH buffer, 1% BSA to remove collagenase, allowing the cells to float and removing buffer with the needle and syringe each time. The cell suspension was adjusted to 40% packed cell volume. Cell density was estimated by resuspending the cells and taking up a sample into a capillary tube. The tube was then sealed at one end with plasticine and centrifuged briefly at 1000g. Packed cell volume was the fraction of the length of packed cells to total suspension in the tube.

2.8. 3-O-Methyl-D-Glucose Uptake Assay

3-O-methyl-D-glucose (3-OMG) uptake was measured by the method described by (Whitesell and Gliemann, 1979). Adipocytes were prepared by the standard method and made up to 40% packed volume in KRH buffer containing 1% (w/v) BSA and treated as required. 50 μl of this cell suspension were added to 10 μl of 200 μM 3-O-methyl-D-glucose in BSA-free KRH buffer also containing 0.15 μCi of 3-O-[^{14}C]methyl-D-glucose in a 4 ml polypropylene tube (Nunc). Uptake was terminated by addition of phloretin. Phloretin was dissolved to 60 mM in ethanol before adding BSA-free KRH to give a final concentration of 0.3 mM. 3 ml of this phloretin solution was added to the cells to terminate the experiment. Uptake (cpm_t) was measured over 3 seconds in insulin treated cells, timed with a metronome set to 120 beats per min. Uptake in basal cells was measured over a 2 min period, and the

equilibrium distribution of radioactivity (cpm_a) was determined by measuring the uptake by insulin treated cells over a 15 minute period. The background value (b), which measures extracellular trapped radioactivity, was determined by adding the cell suspension to the reaction after addition of phloretin. Following termination, 1 ml of 200/100 cs silicon oil (BDH) was overlaid onto the buffer containing the terminated uptake experiment, and the tubes were centrifuged at 2500 rpm in the swing-out rotor of a MSE benchtop centrifuge for 45 s. Following centrifugation, the cells appeared in aggregates in the oil layer. These cells were collected by adsorption to a short length of pipe-cleaner, with care being taken not to penetrate into the aqueous layer. The pipe-cleaner with adhered cells was then placed into a scintillation vial, to which was added 8 ml of scintillation fluid (Optiphase Safe™). ^{14}C activity was measured in a Packard 1500 TRI-CARB or 1600 TR liquid scintillation counter. The rate constant of sugar uptake (V/S) was calculated from the fractional filling (F) using the following equatiors, which assume that the rate of filling (approaching equilibrium) is a single exponential function of time:

$$F = \frac{cpm_t - b}{cpm_a - b}$$

$$\frac{V}{S} = \frac{(-\ln[1-F])}{t}$$

2.9. Photolabelling experiments

2.9.1. Labelling of cell surface GLUT4

Cells were labeled as described by (Holman *et al.*, 1990; Ryder *et al.*, 2000). 1 ml of treated adipocytes at 40% packed volume in KRH buffer containing 0.1% BSA were transferred to 35 mm polystyrene dishes at 18°C. 300 μM Bio-LC-ATB-BGPA photolabel was added to the cells, which were irradiated for 1 min in a Rayonet RPR-100 photochemical reactor with 300 and 350 nm lamps. Cells were then transferred to polystyrene tubes and washed three times with 25 ml KRH buffer containing 1% (w/v) BSA at 18°C, and once with PBS containing protease inhibitors.

2.9.2. Precipitation of labelled GLUT4

Cells were lysed in PBS containing 2% (w/v) Thesit (Roche) and protease inhibitors, and centrifuged at 20000g for 20 min at 4°C. Biotinylated transporters in the supernatant were precipitated with 40 μl of a 50% slurry of streptavidin-agarose beads (Pierce) overnight at 4°C with rotation. The beads were then washed four times with 1 ml PBS containing 1% (w/v) Thesit, four time with 1 ml PBS containing 0.1% (w/v) Thesit, and four times with 1 ml PBS. Bound proteins were eluted in 30 μl SDS-PAGE sample buffer at 95°C for 30 min. The eluate was collected, and the elution was repeated. Eluates pooled from these two elutions were analysed by SDS-PAGE and western blotting.

2.9.3. Measurement of exocytosis

Exocytosis was measured as described by (Yang *et al.*, 2002). 5 ml of adipocytes at 40% packed volume were treated with 5 nM insulin for 20 min at 37 °C and were labeled as described above, except that the GP15 photolabel was used

instead of Bio-LC-ATB-BGPA. Cells were transferred to polypropylene tubes and washed twice with 50 ml KRH buffer pH 6.0 and twice with 50 ml KRH buffer containing 1% (w/v) BSA and 2 mM D-glucose. Cells were incubated for 40 min at 37°C so that GLUT4 trafficking returned to the basal condition.

0.5 ml aliquots of cells were treated with 20 nM insulin and wortmannin as required. 40 μg/ml neutravidin was added at the same time as insulin, and exocytosis was allowed to proceed for 20 min. Reactions were terminated by adding 1 ml of 2 mM KCN in KRH buffer containing 0.1% BSA (w/v) at 18°C, and the cells were washed a further three times in the same buffer. The cells were lysed and unquenched labelled GLUT4 was precipitated on streptavidin-agarose beads as described above.

2.10. Plasma Membrane Lawn Assay

2.10.1. Coverslip preparation

22 mm square glass coverslips were cleaned by immersion in 70% (v/v) ethanol for 5 min, followed by brief immersion in absolute ethanol. They were allowed to dry on Whatman 3 mm paper in a drying cabinet set to 37°C. 1 mg/ml poly-L-lysine in water was diluted to a final concentration of 0.1 mg/ml in 100 mM sodium phosphate buffer pH 7.2. The poly-L-lysine solution was pipetted onto one surface of the coverslip, ensuring that the whole of the desired adhesive surface was covered, and was incubated at room temperature for 10 min. Coverslips were rinsed five times with 1 ml water and dried in the drying cabinet.

2.10.2. Lawn preparation

Treated cells were washed with KHME buffer in order to remove BSA. Cells were allowed to settle to the top of the tube and excess buffer was removed, leaving

densely packed cells. 100 µl of the cell suspension was pipetted onto a strip of parafilm. A poly-L-lysine coated coverslip was held with the adhesive side down in contact with the drop of cell suspension for 5 seconds. Unattached cells were washed off by gently pipetting 1 ml of KHME buffer over the coverslip. Attached cells were lysed by gently pipetting 1 ml of 1/3x KHME buffer over the coverslip. This was repeated a further three times. The coverslip was then placed with the adhesive side up in a 3 cm Petri dish containing 3 ml of KHME buffer. Loose material was washed off by up and down pipetting of the buffer over the cells on the coverslip. The buffer in each dish was replaced twice more to remove unattached material. The coverslip at this stage has a coating of plasma membranes with the cytosolic face up.

The coverslip was washed briefly with 3 ml PBS, and lawns were then fixed with 3 ml of 2% (w/v) paraformaldehyde in PBS for 30 min at room temperature.

2.10.3. Lawn labelling

Lawns were washed three times with PBS and blocked with 0.1% (w/v) saponin in PBS containing 1% (w/v) BSA and 3% (w/v) goat serum for 45 min at room temperature. Lawns were labeled by incubation with 5 µg/ml affinity purified rabbit anti-GLUT4 serum and 10 µg/ml monoclonal anti-VAMP2 antibody (Synaptic Systems) in the same buffer for 1 h at room temperature. Lawns were washed three times, each for 20 min in PBS containing 0.1% (w/v) saponin, and then incubated with AlexaFluor488-conjugated goat anti-rabbit IgG antibody and AlexaFluor568-conjugated goat anti-mouse IgG antibody, both diluted at 1:200 in PBS containing 1% (w/v) BSA for 1 h at room temperature. Lawns were washed three times with PBS for 20 min each at room temperature, embedded in Vectashield mounting medium (Vector Laboratories, Burlingame, CA), and mounted onto glass slides.

2.10.4. Fluorescence microscopy

Lawns were analysed using a Zeiss LSM-510 inverted laser-scanning confocal microscope with a 63x/NA1.4 plan-apochromatic oil-immersion objective. Fluorophores were excited at 488 nm and 568 nm with an argon and a helium-neon laser respectively. Fluorescence data was collected at a resolution of 1024 x 1024 pixels using the 505-550 nm band pass filter and the 560 nm high pass filter in multitrack mode and was analysed using the Zeiss LSM Software Version 2.5. Mean pixel fluorescence intensity was measured in a circle of area 298.56 μm^2 in three membrane patches per frame. Four frames were sampled per slide.

2.11. Detection of signalling proteins

1 ml of adipocytes at 40% packed volume in KRH containing 1% (w/v) BSA were treated with insulin as described in the figure legends with or without 20 min pre-treatment with 10 μM SB203580. For inhibition experiments SB203580 was dissolved to 10 mM in DMSO. SB203580 was replaced with 0.1% (v/v) DMSO in control cells.

Following insulin treatment, cells were washed briefly in 20 ml of KRH buffer containing 20 nM insulin where appropriate, but without BSA. Excess buffer was removed and cells were transferred to a 1.5 ml microfuge tube. Cells were allowed to float for ~15s, and 200 μl of packed cells from the top of the tube were removed with a pipette and lysed directly in 200 μl of 2 x SDS sample buffer containing 1 mM DTT, 1 mM Na_3VO_4, 20 mM NaF, 2 mM sodium molybdate, 100 nM okadaic acid, 7.5% (v/v) β-mercaptoethanol and protease inhibitors and heated for 15 min at 65 °C. Lysates were centrifuged at 1000g for 1 min and supernatants were analysed by SDS-

PAGE and transferred to nitrocellulose for western blotting. The amounts loaded on the gels were checked by blotting with antibodies against either p38 MAP kinase or the β-subunit of the insulin receptor.

2.12. Quantitation of membrane fusion proteins in rat adipocytes

2.12.1. Generation of protein standards for quantitative experiments

GST-syntaxin4, NucA-SNAP23, NucA-$VAMP_{cyt}$ and GST-Munc18c were expressed and purified according as described in Section 2.5. The proteins were further purified by preparatory SDS-PAGE in large format ProteanII format gels. When the dye front had run out of each gel, a thin strip was cut out parallel to the direction of the running of the gel and copper-stained to locate the protein band. A strip corresponding to the position of the protein band was cut out from the remaining gel and electroeluted in a model 422 electroeluter (BioRad) according to the manufacturer's instructions. Concentrations of recovered proteins were estimated by measuring absorbance at 280 nm against a blank consisting of the electroeluate from a gel strip of equivalent size from a gel run with only SDS sample buffer loaded. Molar extinction coefficients were calculated from the amino acid sequence (Gill and von Hippel, 1989).

The accuracy of routine estimation of protein purity is limited by the detection range of coomassie blue or silver staining on SDS-PAGE gels. The amount of protein required for detection of trace contaminants often saturates the standard protein bands, and when the standard protein band lies in the linear range the contaminant bands are often below the linear detection threshold. The method described below was used in a study by (Coorssen *et al.*, 2003) to eliminate this problem. The estimation of NucA-$VAMP_{cyt}$ purity is shown below as an example (Figure 2.1.). Following SDS-PAGE

of a series of increasing total concentrations of NucA-$VAMP_{cyt}$ protein standards, the gel was stained with coomassie blue. A digital image was taken of the backlit gel using the EpiChemiII darkroom and digital camera system (UVP) and analysed using Labworks software (UVP). From this image, measurements were taken in each lane of the integrated staining intensity (OD) of the specific NucA-$VAMP_{cyt}$ band and of the total staining intensity in the entire length and width of the lane above the background intensity.

The OD of specific bands and the OD of total staining in each lane were plotted against the loaded protein concentrations (Figure 2.1.). The linear range of the OD of the specific NucA-$VAMP_{cyt}$ bands was determined from this curve and extrapolated to the maximum protein loaded value for the purity calculation. The difference between the total lane OD the uncorrected NucA-$VAMP_{cyt}$ band OD at the maximum protein loaded value was taken as a measure of the contaminating proteins. This allowed estimation of low-abundance contaminating proteins even though the NucA-SNAP23 band was saturating. The purity was then calculated as a ratio of the extrapolated linear specific band OD to the sum of this value and the contaminating protein OD.

Concentration of specific proteins was calculated from the total protein concentration and the purity estimation. For quantification experiments, serial dilutions of the proteins were made with electrophoresis running buffer down to 10^{-12} molecules of specific protein/µl. These serial dilutions were stored at -80°C for later use.

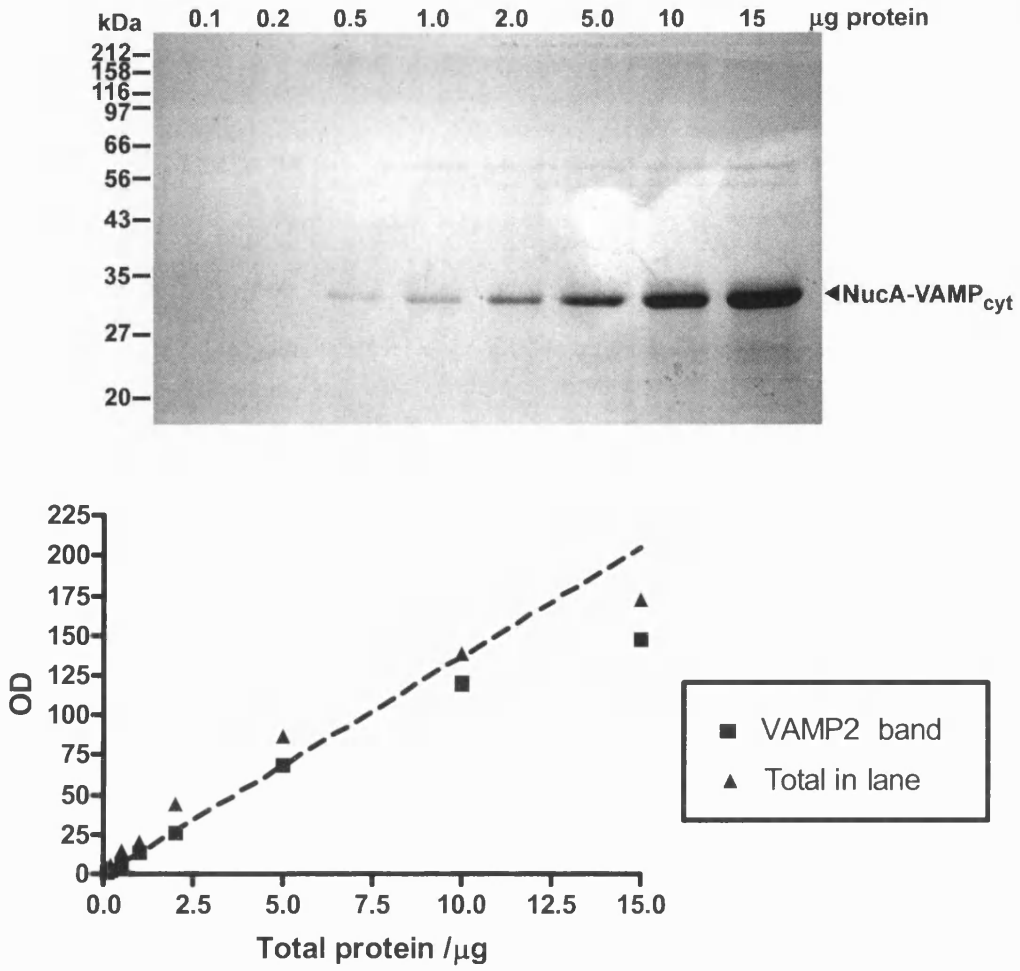

Figure 2.1. Estimation of NucA-VAMP$_{cyt}$ purity for quantification experiments. **A.** Purified recombinant NucA-VAMP$_{cyt}$ was analysed by SDS-PAGE and stained with coomnassie blue. **B.** Staining intensities (OD) were quantified from **a** digital image of the gel in **A** and specific band OD and total lane OD were plotted against the total protein loaded. Contaminating proteins were estimated by subtraction of the uncorrected specific protein band OD from the total staining in the 15 µg lane. Purity was calculated as the proportion of the extrapolated nonsaturating VAMP2 band density (VAMP2 linear, dashed line) over the sum of this value and the estimated contaminants. The estimated purity of NucA-VAMP$_{cyt}$ by this method was 88%.

2.12.2. Quantitation of SNAP23, syntaxin4, VAMP2 and Munc18c in rat adipocytes

Isolated adipocytes were washed twice in KRH buffer to remove BSA. Cell density was estimated by counting the average number of cells in 16 squares of a Neubauer Haemocytometer in triplicate. 0.5 ml of the cell suspension was lysed by adding an equal volume of 2 x SDS sample buffer containing 100 mM DTT and protease inhibitors. Lysates were heated at 95 °C for 10 minutes and allowed to cool to room temperature. The lysate below the fat layer was collected and the volume was made up to 1 ml with SDS sample buffer. Lysates were then standardised by adding SDS sample buffer so that each microlitre of lysate contained the equivalent of 10^3 cells, determined from the cell density counts.

For quantitation, 10 µl aliquots of standardised lysate were heated to 95°C for 10 minutes and were run in triplicate on SDS-PAGE alongside a dilution series of recombinant protein standards.

2.12.3. Distribution of SNAREs and Munc18c in rat adipocyte fractions

Following treatment, cells were washed three times with HES buffer containing protease inhibitors at 18°C. The subfractionation protocol was based on that described by (Weber, 1988). For subfractionation, adipocytes were homogenised by 10 strokes in a 55 ml Potter Elvehjem homogeniser, and the homogenate was centrifuged for 2 min at 1000g at room temperature. The homogenate was incubated on ice for five minutes, and the infranatant below the solidified fat layer was collected and centrifuged at 18000 rpm for 20 minutes in a Beckman TLA100.3 rotor at 4°C. The pellet, which contained crude plasma membranes, mitochondria and nuclei was retained for further purification. The supernatant containing the cytosol and

microsomal fractions was centrifuged at 30000 rpm in the TLA100.3 rotor for 9 minutes at 4°C. The pellet from this spin, which contained the high density microsomal fraction was resuspended in 200 µl of HES buffer containing protease inhibitors. The supernatant was centrifuged at 100000 rpm in the TLA100.3 rotor for 17 minutes at 4°C to pellet the low density microsomal fraction. This was resuspended in 400 µl HES buffer containing protease inhibitors. The supernatant from this spin was the cytosol. The crude plasma membrane pellet was resuspended in 300 µl of HES buffer containing protease inhibitors and carefully overlaid onto a 600 µl cushion of 1.12 M sucrose in 20 mM HEPES buffer pH 7.2, 1 mM EDTA. The sucrose cushion was centrifuged in a Beckman TLS55 rotor at 35000 rpm for 20 minutes at 4°C. The pellet from this spin, which contained mitochondria and nuclei was carefully washed with HES buffer and resuspended in 400 µl of HES buffer containing protease inhibitors. The sucrose cushion containing the plasma membranes was made up to 3 ml with HES buffer and centrifuged at 37000 rpm in the TLA100.3 rotor for 9 min at 4°C. The pellet containing the plasma membrane fraction was resuspended in 3 ml of HES buffer and the spin was repeated. The pellet was then resuspended in 400 µl HES buffer containing protease inhibitors. Protein content in each fraction was estimated using the BCA protein assay kit (Pierce) according to the manufacturer's instructions.

2.12.4. Detection of SDS-resistant complexes

In order to detect SNAREs in SDS-resistant complexes, freshly purified plasma membranes from basal or insulin-treated adipocytes were diluted to 0.2 mg/ml of protein in HES buffer. 50 µl of 3 x low-SDS sample buffer were added to 100 µl aliquots of the purified plasma membranes and mixed thoroughly. Two identical 45 µl

aliquots were taken from each of these samples, and one was heated at 95°C for 5 minutes, while the other was maintained at room temperature. Tubes were spun briefly at 1000 rpm to collect condensation and the entire contents of each tube were analysed by SDS-PAGE, transferred to nitrocellulose and western blotted with rabbit SNAP23 antibody, VAMP2 monoclonal antibody (both from Synaptic Systems, Gottingen, Germany) and anti-syntaxin4 rabbit serum.

2.13. Liposome reconstitution experiments

2.13.1. Reconstitution of t-SNAREs into liposomes

Lipids were purchased from Avanti Lipids. Reconstitution of syntaxin4 followed the method described by Weber et al. (1998). Specifically, 100 µl of a 15 mM mixture of POPC (1-palmitoyl, 2-oleoyl phosphatidylcholine):DOPS (1, 2-dioleoyl phosphatidylserine) at a ratio of 85:15 in chloroform was evaporated under a gentle stream of nitrogen and remaining chloroform was removed by exposure to vacuum for 30 min. The lipids were then resuspended in 500 µl of inclusion body preparation containing 3.6 mg/ml of NucA-syntaxin4 (Section 2.5.2.) and incubated at room temperature for 30 min on a slowly rocking platform.

The vial containing the solubilised lipids and protein was vortexed vigorously while 1 ml of IB buffer was rapidly added to it. The vial was vortexed for a further 30 s and dialysed overnight at 4°C against 2 litres of 25 mM sodium phosphate buffer pH 7.4, 250 mM NaCl, 2 mM DTT (reconstitution buffer) containing 4 g Biobeads SM2 beads (BioRad) to remove traces of detergent.

Liposomes were recovered by flotation in an Optiprep density gradient. This was set up by mixing 500 µl of dialysate with 1 ml of 60% (w/v) Optiprep density

gradient medium and loading this into a 2.2 ml centrifuge tube (Beckman). This was overlaid with 300 µl of 30% (w/v) Optiprep in reconstitution buffer followed by 200 µl of 20% (w/v) Optiprep in reconstitution buffer and 100 µl of reconstitution buffer. The sample was centrifuged in a TLS-55 rotor (Beckman) at 55000 rpm for 3 h 50 min at 4°C.

In order to form the t-SNARE complex on syntaxin4-containing liposomes, 1.5 ml of 2 mg/ml GST-SNAP23 equilibrated against 25 mM sodium phosphate buffer, 1.5 M NaCl, 5 mM DTT was added to the liposome preparation immediately following dilution of detergent and vortexing. This was then dialysed against 2 l of reconstitution buffer overnight at 4°C. Liposomes were recovered on an Optiprep gradient as described for NucA-syntaxin4.

2.13.2. Formation of t-SNARE complex on glutathione-sepharose

4 mg of GST-SNAP23 bound to 0.5 ml glutathione-sepharose was incubated with 3.6 mg of NucA-syntaxin4 inclusion body preparation in a total volume of 2 ml of IB buffer. The proteins were incubated with rotation for 2 h at 4°C, loaded onto a gravity column, and washed with 10 ml 50 mM borate buffer pH 8.5, 500 mM NaCl, 10 mM DTT, 1% n-octylglucoside, then eluted with the same buffer containing 20 mM glutathione.

2.13.3. Reconstitution of coexpressed t-SNAREs into liposomes

For reconstitution into liposomes, 500 µl of the solubilised inclusion body preparation expressed from cells containing the plasmid pGEX-tSNAREs was used (Section 2.5.4.). The buffer was exchanged for 25 mM sodium phosphate buffer pH 7.4, 750 mM NaCl, 1 mM DTT, 1% n-octylglucoside using a Bio-Spin 6 buffer

exchange column (Bio-Rad). There was noticeable precipitation of protein at this step. The protein solution was centrifuged at 20000g for 10 min to remove insoluble material and the supernatant was incubated at room temperature for 1 h to allow complexes to form and then reconstituted into liposomes exactly as described for NucA-syntaxin4 (Section 2.13.1).

2.13.4. Reconstitution of VAMP2 into liposomes

All lipids were from Avanti Polar Lipids. A 100µl mixture of 3 mM POPC:DOPS:NBD-DPPE:rhodamine-DPPE (82:15:1.5:1.5) in chloroform was dried under a gentle stream of nitrogen, followed by 30 min under vacuum. The lipids were resuspended in 100 µl of 4 mg/ml VAMP2 (purified as described in section 2.5.6.) and incubated for 30 minutes at room temperature on a rocking platform. Protein-free liposomes were made by substituting the protein solution with IB buffer. The vial containing the lipid-protein mixture was vortexed vigorously and 200 µl of reconstitution buffer were added to the vial while vortexing for a further 30 seconds. Liposomes were dialysed against 2 litres of reconstitution buffer containing 4 g of Biobeads SM2 beads (Bio-Rad).

Liposomes were recovered by flotation in a step gradient of Optiprep, set up in a 2.2 ml tube as follows: 300 µl of liposome dialysate was mixed with 600µl of 60% (w/v) Optiprep. This was overlaid with 600 µl of 30% Optiprep in reconstitution buffer followed by 200 µl of 20% Optiprep in reconstitution buffer, and 200 µl reconstitution buffer. The gradient was centrifuged at 55000 rpm for 3 h 50 min at 4°C in the TLS-55 rotor. Liposomes collected as a single bright pink band near the top of the gradient following centrifugation. Layers on the gradient were collected and analysed by SDS-PAGE.

2.13.4. Fusion assays

Nonfluorescent liposomes made with coexpressed t-SNAREs and fluorescent liposomes containing VAMP2 were used in the subsequent fusion assays. Assays were carried out in 96-well white FluoroNunc plates (Nunc). Relative concentrations of VAMP2 liposomes and protein-free fluorescent liposomes were measured by NBD fluorescence with the excitation filter set to 485 nm and emission measured at 535 nm in a FarCyte fluorescent plate reader (Amersham Biosciences).

For the fusion experiments, duplicate wells were loaded with 45 µl of t-SNARE liposome preparation, and VAMP2 liposomes were added so that syntaxin4 and VAMP2 were present at equimolar levels, in order to maximise the signal to noise ratio. Each well therefore contained approximately 30 pmoles of syntaxin4 and VAMP2. These were about $^{1}/_{10}$ the amounts used in the original assay on which this one is based, but still higher than the density in synaptic vesicle membranes (Walch-Solimena *et al.*, 1995b; Weber *et al.*, 1998). The final volume in each well was made up to 50 µl with reconstitution buffer. An equivalent amount of protein-free fluorescent liposomes was substituted for VAMP2 liposomes in some wells to act as a negative control. Liposome mixtures were incubated for 16 h at 4°C to allow liposomes to dock prior to measurements being taken. Fluorescence was measured in the FarCyte set to 37°C with the excitation filter set to 485 nm and emission measured at 535 nm, with 10 flashes and the integration time set to 40 µs. Measurements were taken at two minute intervals. After three hours of measurements, 10 µl of 2.5 % (w/v) TritonX-100 was added to dissolve lipids and therefore maximally disperse fluorescent and quenching head groups to set maximum fluorescence values for each well.

2.14. Data analysis

Numerical data were plotted using GraphPad Prism version 4.0 (GraphPad Software, Inc.). Prism 4.0 was also used for all statistical analyses. Inhibition profiles in Chapter 2 were fitted to the Hill equation, from which IC50 values were calculated. Other quantitative data were analysed by two tailed paired or unpaired t tests.

Chapter 3 - The role of p38 MAP kinase in the regulation of glucose uptake by insulin

3.1. Introduction

Insulin increases the number of GLUT4 molecules at the surface of responsive cells by both increasing the rate of translocation of GLUT4 vesicles to the plasma membrane and decreasing the rate of GLUT4 internalisation (Jhun *et al.*, 1992; Czech and Buxton, 1993; Satoh *et al.*, 1993; Yang and Holman, 1993). It is thought that the net increase in GLUT4 at the plasma membrane underlies the increase in glucose uptake following insulin stimulation. There is some evidence, introduced in Section 1.6., that as well as regulating the availability of GLUT4 at the cell surface, insulin also regulates the catalytic activity of GLUT4.

Time course studies have shown that the appearance of GLUT4 at the plasma membrane of adipocytes precedes insulin stimulated glucose uptake, suggesting that the transporters are inactive when first inserted into the plasma membrane (Karnieli *et al.*, 1981; Yang *et al.*, 1992; Satoh *et al.*, 1993). This effect was magnified when the temperature was reduced to 22°C (Somwar *et al.*, 2001a), though this may be because fusion of GLUT4 vesicles with the plasma membrane was slower at temperatures below 23°C (Elmendorf *et al.*, 1999).

It is important to define the sequence of the events leading to insulin stimulated glucose transport. These are GLUT4 vesicle translocation, where GLUT4 vesicles are translocated to the vicinity of the plasma membrane, followed by GLUT4 exocytosis, which results in exposure of GLUT4 to the outside of the cell and finally GLUT4-mediated glucose transport. Insulin stimulated glucose uptake and GLUT4 translocation are sensitive to the PI 3-kinase inhibitors wortmannin and LY294002

(Clarke *et al.*, 1994; Sanchez-Margalet *et al.*, 1994; Okada *et al.*, 1994; Cheatham *et al.*, 1994). Furthermore, transfections of inactivating truncated mutants of p85, the regulatory subunit of class 1A PI 3-kinase, or of one of its SH2 domains also blocked insulin stimulated GLUT4 translocation (Kotani *et al.*, 1995; Haruta *et al.*, 1995; Sharma *et al.*, 1998). Insulin stimulated glucose uptake and GLUT4 translocation were also inhibited by microinjection of antibody specific to the p110 catalytic subunit of the class 1A PI 3-kinase (Hausdorff *et al.*, 1999). This evidence indicates that the class 1A PI 3-kinase function upstream of GLUT4 translocation in insulin stimulated glucose transport (Section 1.4.).

Wortmannin irreversibly inhibits the catalytic activity of class 1 and class 3 PI 3-kinases with IC50s in the range 1 to 10 nM (Fruman *et al.*, 1998). Two recent studies on 3T3-L1 adipocytes and L6 myotubes suggested that there is a higher affinity target for wortmannin that can lead to reversible inhibition of glucose transport activity without affecting the insulin stimulated exposure of GLUT4 at the cell surface (Hausdorff *et al.,* 1999; Somwar *et al.,* 2001b). Wortmannin has been reported to inhibit glucose uptake and GLUT4 exocytosis with IC50s of 6 nM and 80 nM, respectively, in 3T3-L1 adipocytes. Expression of a constitutively active Akt abolished the sensitivity of glucose uptake of these cells to low concentrations of wortmannin, indicating that wortmannin did not inhibit glucose transport activity by direct interaction with GLUT4. This result also suggests that Akt interacts with the high affinity wortmannin pathway downstream of the low affinity target (Hausdorff *et al.*, 1999). Wortmannin inhibited insulin stimulated glucose uptake with an IC50 of 3 nM and GLUT4 exocytosis with an IC50 of 43 nM in L6 myotubes. In addition, the increase in p38 MAP kinase activity in response to insulin in L6 myotubes was inhibited at low wortmannin concentrations similar to those that inhibited glucose

transport but not GLUT4 exocytosis (Somwar *et al.*, 2001b). The authors suggested that there was a link between the effects of wortmannin on the p38 MAP kinase pathway and the inhibition of insulin stimulated glucose uptake, as previous studies had indicated that p38 MAP kinase played a role in the stimulation of glucose uptake by insulin.

There is also evidence that a PI 3-kinase independent insulin signalling pathway is required to stimulate GLUT4 transporter activity at the cell surface. Addition of cell-permeable analogs of the lipid products of PI 3-kinase activity mimic the action of insulin in translocating GLUT4 to the surface of responsive cells (Jiang *et al.*, 1998; Maffucci *et al.*, 2003; Sweeney *et al.*, 2004). However, these lipids do not increase glucose uptake above the basal rate, despite the increased presence of transporters on the cell surface. These lipids do however restore insulin-like glucose transport rates to wortmannin or LY294002-treated cells in combination with insulin, but have no effect on the transport rate in the absence of insulin (Jiang *et al.*, 1998; Maffucci *et al.*, 2003; Sweeney *et al.*, 2004). This indicates that there is an insulin signalling pathway that regulates glucose transporter activity at the cell surface independently of the lipid products of PI 3-kinase activity.

The pyridinyl imidazole p38 MAP kinase inhibitors SB203580 and SB202190 and the unrelated azaazulene p38 MAP kinase inhibitors A291077 and A304000 inhibit insulin stimulated glucose uptake (Sweeney *et al.*, 1999; Somwar *et al.*, 2002). The dual phosphorylation of p38α MAP kinase and p38β MAP kinase at their regulatory sites and their activities increased following insulin treatment in L6 myotubes and 3T3-L1 adipocytes. Both phosphorylation and the activity of p38 MAP kinase were inhibited by wortmannin in a manner consistent with this pathway being the high affinity target for wortmannin. Also, expression of a dominant negative p38

MAP kinase inhibited insulin stimulated glucose uptake without inhibiting GLUT4 exocytosis (Somwar *et al.*, 2001b; Somwar *et al.*, 2002). These results have led to a model, represented in Figure 3.1, in which the catalytic activity of GLUT4 is regulated by insulin in a p38 MAP kinase dependent pathway, independently of class 1A PI 3-kinase and GLUT4 exocytosis.

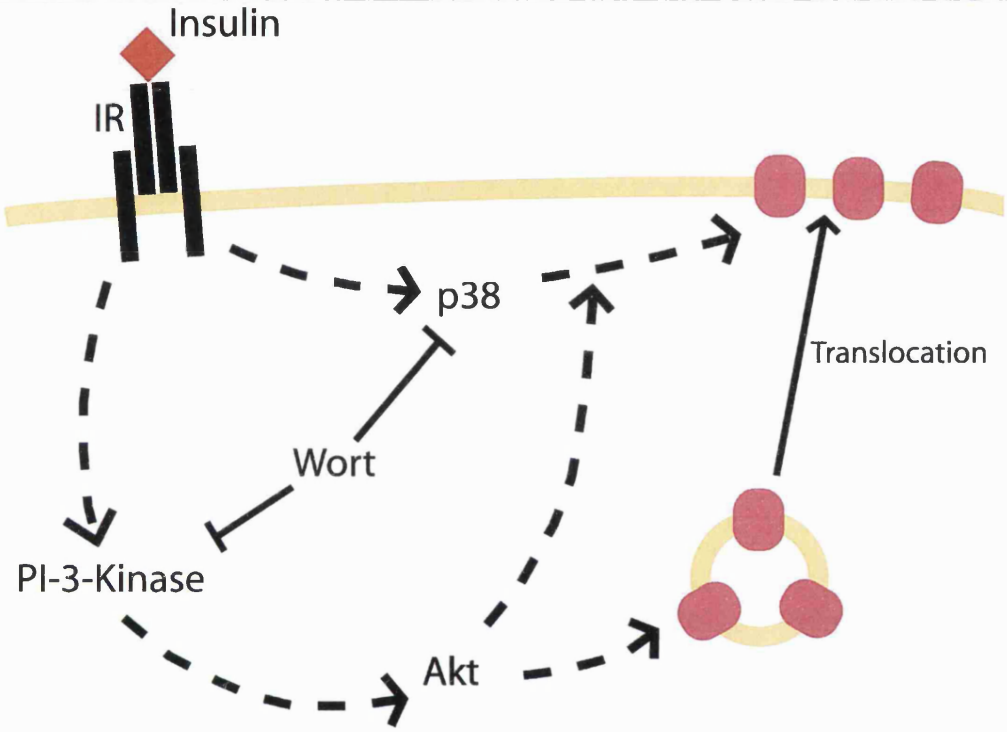

Figure 3.1. The model for p38 MAP kinase regulation of GLUT4 activity. Insulin, via the insulin receptor (IR), activates the class 1A PI 3-kinase pathway which stimulates translocation of GLUT4 vesicles to the plasma membrane. Insulin stimulates GLUT4 activity following insertion in the plasma membrane via a p38 MAP kinase (p38) dependent pathway. Both pathways are inhibited by wortmannin and can be bypassed by expressing a constitutively active Akt (Hausdorff *et al.*, 1999; Somwar *et al.*, 2001a; Somwar *et al.*, 2001b; Somwar *et al.*, 2002).

The conclusions drawn from this series of studies on p38 MAP kinase have been disputed by a number of other groups. Expression of dominant negative mutants of either p38 MAP kinase or of the p38 MAP kinase activator MKK6 in 3T3-L1 adipocytes did not inhibit insulin stimulated glucose transport, whereas a constitutively active MKK6 construct increased glucose transport independently of insulin in a wortmannin independent manner. This appeared to be a long term effect, mediated by increased expression of GLUT1, rather than increased exocytosis of GLUT4 (Fujishiro *et al.*, 2001). Furthermore, Kayali *et al.* (2000) reported that activity of dual phosphorylated p38 MAP kinase in 3T3-L1 adipocytes was not stimulated by insulin, and that insulin stimulated glucose transport was not significantly inhibited by the p38 MAP kinase inhibitors SB203580, SB202190, and PD169316 at concentrations that blocked p38 MAP kinase activity. Moreover, Carlson *et al.* (2003) did not detect any increase in p38 MAP kinase activity in isolated human adipocytes following insulin treatment.

The experiments described in this chapter examined the extent to which wortmannin was able to uncouple insulin-stimulated glucose transport from GLUT4 exocytosis. The effects of insulin and the p38 MAP kinase inhibitor SB203580 on the activation of the Akt and MAP kinase pathways were also examined. These results were linked to the effects of SB203580 on insulin-stimulated glucose uptake and GLUT4 translocation.

3.2. Results

3.2.1. Wortmannin inhibition of insulin stimulated GLUT4 translocation to the plasma membrane

The plasma membrane lawn assay described in Section 2.10 was used to determine the effect of wortmannin on insulin stimulated GLUT4 vesicle translocation. Lawn preparation was rapid, around 20 seconds from cell lysis to fixation, increasing the chances of capturing a representative snapshot of events on the intracellular face of the plasma membrane. Vesicles on the plasma membrane remain attached in this assay, meaning that it cannot distinguish between translocation and exocytosis (Robinson *et al.*, 1992; Avery *et al.*, 2000; Yang *et al.*, 2002). Unlike many other cell types, the small volume of cytosol in adipocytes relative to the fat droplet makes it difficult to distinguish between events inside the cell and those at or near the plasma membrane in intact cells under the microscope. The plasma membrane lawn assay increases the ability to resolve events at the plasma membrane.

In the following series of experiments, cells were treated with wortmannin for 20 min, followed by a further 20 min with insulin before being immobilised for the assay. In order to quantify GLUT4 vesicle translocation, the plasma membrane lawns were subjected to immunofluorescence analysis with antibodies to GLUT4 and VAMP2. VAMP2 is a component of GLUT4 vesicles (Cain *et al.*, 1992), and provided an additional measure of GLUT4 vesicle translocation.

The immunofluorescence (IF) (shown in Figure 3.2) was quantified on three membrane patches in each of four viewing fields per condition. The mean IF value for basal cells was subtracted from the IF value for each treatment. These were then

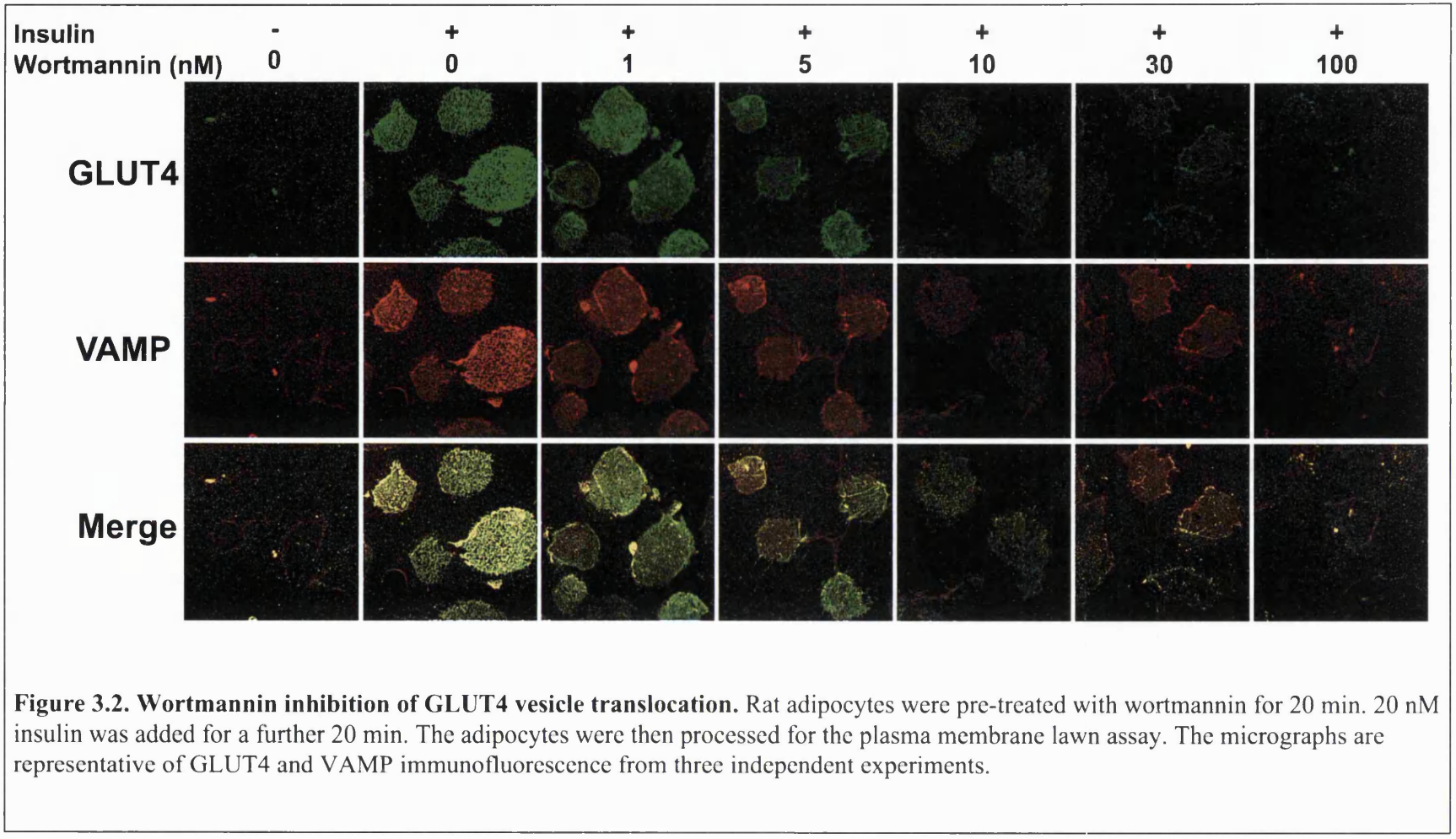

Figure 3.2. Wortmannin inhibition of GLUT4 vesicle translocation. Rat adipocytes were pre-treated with wortmannin for 20 min. 20 nM insulin was added for a further 20 min. The adipocytes were then processed for the plasma membrane lawn assay. The micrographs are representative of GLUT4 and VAMP immunofluorescence from three independent experiments.

expressed as a percentage of the difference in IF between non-wortmannin treated insulin stimulated and basal cells. This gave a measure of the inhibition of insulin stimulation by wortmannin. Wortmannin inhibited the insulin stimulated appearance of GLUT4 and on the plasma membrane with an IC50 of 14.1 nM (95% confidence interval (C.I.) 9.5 to 20.8 nM). VAMP2 appearance on the plasma membrane was inhibited with an IC50 of 12.5 nM (95% C.I. 9.0 to 17.4 nM) (Figure 3.4).

3.2.2. Wortmannin inhibition of insulin stimulated GLUT4 exocytosis

GLUT4 exocytosis in rat adipocytes was quantified by labelling molecules exposed to the exterior surface of the cell with GP15, a trifunctional photolabel. A hexose moiety on GP15 allows it to bind to the glucose binding site on the GLUT4 molecule. A photoactivateable diazirine group covalently links the label to any adjacent proteins when subjected to ultraviolet illumination. Thirdly, a biotin affinity tag allows the experimenter to purify labelled molecules. Labelled molecules can then be analysed by SDS-PAGE and Western blotting. GLUT4 that is exposed to the outside of the cell can be labelled in this way. However, direct labelling may exclude GLUT4 molecules whose glucose binding sites are altered, by allosteric regulation for example. This prompted a refinement in the technique, whereby cells were first stimulated with insulin and exocytosed GLUT4 was labelled as described above, insulin was then removed and cells were allowed to recover and re-internalise GLUT4 (Yang *et al.,* 2002). In order to measure exocytosed GLUT4, cells were treated in the presence of avidin in order to quench the biotin moiety photolabelled GLUT4 molecules on the cell surface. Unbound avidin was then washed away, and the cells were lysed. Any GLUT4 molecules that had unquenched label on them retained the

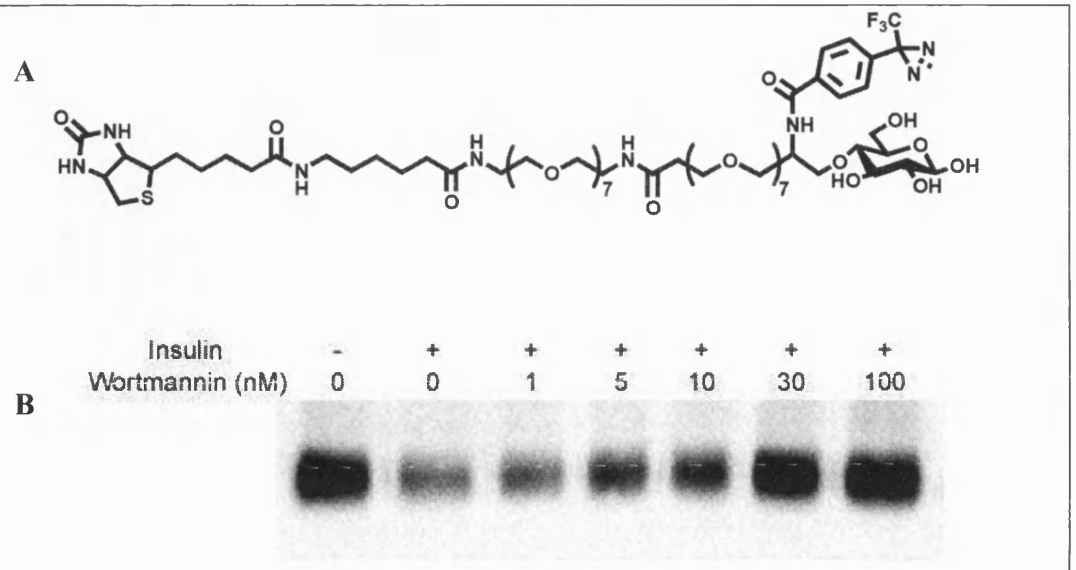

Figure 3.3. Wortmannin inhibition of GLUT4 exocytosis. Glucose transporters on the cell surface of rat adipocytes were labelled with GP15 photolabel (A) in the presence of 20 nM insulin for 40 min. Insulin and unbound photolabel were removed by extensive washing. For the inhibition experiments the cells were treated with wortmannin for 20 min, avidin and 20 nM insulin were added for a further 20 min. Cells were then solubilised, and biotinylated GLUT4 was precipitated with strepatividin-agarose and analysed by SDS-PAGE and Western blotting with GLUT4 antiserum. The blot shown in (B) is representative of three experiments carried out with Dr Jing Yang.

ability to be isolated by streptavidin precipitation, and must therefore have been inside the cell during treatment. When analysed by Western blot, this method provided a direct measure of translocation and exposure of the exofacial binding site at the cell surface. The assay was not dependent on any changes in the affinity of GLUT4 for glucose.

This indirect exocytosis assay was used as described in Section 2.9.3. to determine the effect of wortmannin on insulin-stimulated GLUT4 exocytosis in

adipocytes. The mean amount of exocytosed GLUT4 for basal cells was subtracted from the value for the other treatments. These values were then expressed as a percentage of the difference between non-wortmannin treated insulin stimulated and basal cells. This gave a measure of the inhibition of insulin stimulation of GLUT4 exocytosis by wortmannin. The results, shown in Figure 3.3 and plotted in Figure 3.4 show that insulin stimulated GLUT4 exocytosis was inhibited by wortmannin with an IC50 of 8.2 nM (95% C.I. 4.6 to 14.8 nM).

3.2.3. Wortmannin inhibition of insulin stimulated 3-O-Methyl-D-glucose uptake

Glucose transport activity was measured by the 3-O-methyl glucose uptake assay (Section 2.8.). The results were normalised with basal and insulin values in the absence of wortmannin set at 0% and 100% respectively. The normalised results were plotted together with those for GLUT4 vesicle translocation and GLUT4 exocytosis on the same axes (Figure 3.4). Wortmannin was found to inhibit insulin stimulated glucose uptake with an IC50 of 8.5 nM (95% C.I. 6.4 to 11.3 nM). This value was the same as the value obtained by measuring the rate of exposure of biotinylated GLUT4 and both these values were slightly smaller than those obtained for GLUT4 vesicle translocation, although the differences were not found to be statistically significant. However, the curves for inhibition of exocytosis and uptake were less sigmoidal in character than the translocation curves. The difference between the curves is most pronounced in the 5 nM wortmannin treatments, where there is a significantly smaller degree of inhibition of GLUT4 translocation than of glucose uptake ($p=0.012$, unpaired, two-tailed t-test).

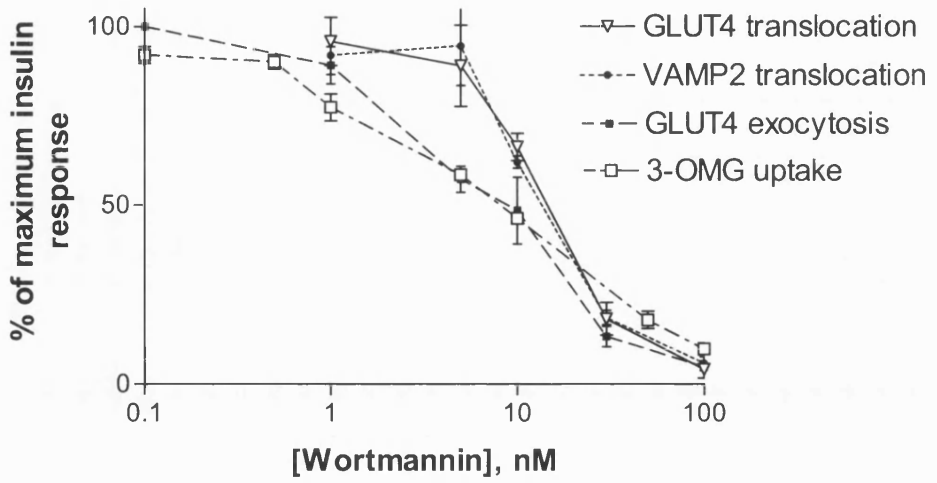

Figure 3.4. Wortmannin inhibition of insulin-stimulated glucose transport. Glucose transport activity was estimated in rat adipocytes that had been treated with wortmannin for 40 min in the presence of 20 nM insulin for the last 20 min, using the 3-OMG uptake assay. 3-OMG uptake measurements from five independent experiments are plotted in black alongside GLUT4 exocytosis, GLUT4 vesicle translocation and VAMP2 translocation. All data points are normalised against basal and insulin values in the absence of wortmannin.

3.2.4. Effect of insulin on activation of MAP kinase pathways

As the IC50 value for wortmannin inhibition of glucose uptake was similar to those for GLUT4 exocytosis, the activation of MAP kinase pathways following insulin stimulation was examined in order to see whether there was a link between glucose uptake and p38 MAP kinase activation. MAP kinases are activated by dual phosphorylation at their regulatory 'core signalling module', a Thr-X-Tyr motif in the activation loop within the kinase domain (Boulton *et al.*, 1990; Derijard *et al.*, 1994; Raingeaud *et al.*, 1995). Activation of MAP kinases was detected by western blotting of adipocyte extracts with antibodies raised against peptides containing the phosphorylated 'core signalling modules' as described in Section 2.11.

A.

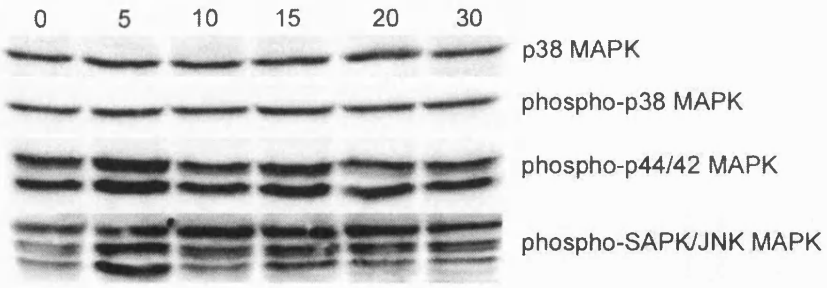

B.

Insulin (mins)	0	5	10	15	20	30
Phospho-p38 MAPK	1.00±0.00	1.13±0.14	1.32±0.11*	1.35±0.14	1.10±0.08	1.12±0.13
Phospho p44/42 MAPK	1.00±0.00	2.60±0.32*	1.49±0.19*	1.28±0.12	1.20±0.09	0.72±0.09
Phospho SAPK/JNK	1.00±0.00	2.80±0.42*	1.98±0.13*	1.47±0.26	1.38±0.24	1.12±0.44

Figure 3.5. Insulin stimulated MAP kinase activation in rat adipocytes. A. Rat adipocytes were stimulated with 20 nM insulin for the times indicated. Lysates were analysed by SDS-PAGE and western blotting with phospho-specific MAPK antibodies and a p38 MAP kinase antibody as a loading control. The blots shown are representative of at least three independent experiments. **B.** Mean band inensities from the experiments represented in **A**, corrected for loading differences and normalised to basal values, ± standard error of means (S.E.M.). * indicates that the value differs significantly from the value in the absence of insulin (i.e. $p<0.05$, paired, two-tailed t test).

A.

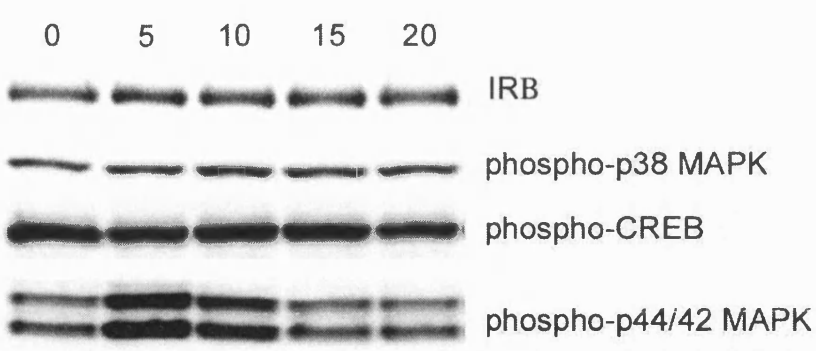

B.

Insulin (mins)	0	5	10	15	20
Phospho-CREB	1.00±0.00	0.95±0.10	1.01±0.05	0.98±0.02	0.93±0.12

Figure 3.6. Phosphorylation of CREB, a downstream effector of p38 MAP kinase in response to insulin. A. Rat adipocytes were stimulated with 20 nM insulin for the times indicated. Lysates were analysed by SDS-PAGE and Western blotting with phospho-specific p38 MAP kinase and CREB antibodies, and antibodies to the β-subunit of the insulin receptor (IRβ) as a loading control. This blot is representative of three independent experiments. **B.** Mean band intensities from the experiments represented by **A**, corrected for differences in loading and normalised to basal values, ± S.E.M.

Following insulin treatment there was a rapid rise in p44/42 Erk MAP kinase phosphorylation that peaked at 2.60 ± 0.32 times the basal value. This returned to basal levels within 15 min after insulin treatment began. Phosphorylation of SAPK/JNK also peaked at 5 min following insulin treatment at 2.80 ± 0.42 times basal levels and returned to basal levels 20 min after insulin treatment began. Phospho-p38 MAP kinase levels peaked after 15 min of insulin treatment at 1.35 ±

0.14 times basal levels and had returned to basal levels after 20 min of insulin treatment (Figure 3.5).

There was no detectable change in phosphorylation of the p38 MAP kinase substrate CREB in response to insulin (Figure 3.6).

3.2.5. Effect of glucose in buffers used for isolation of rat adipocytes

Through indirect comparisons of western blots from different experiments carried out in this laboratory (not shown), it was observed that in the absence of insulin, levels of phosphorylated p38 MAP kinase in rat adipocytes appeared to be at least an order of magnitude higher those observed in an equivalent amount of protein extracted from 3T3-L1 adipocytes. The possibility that the elevated basal p38 MAP kinase phosphorylation in rat adipocytes compared to 3T3-L1 adipocytes was a result of the isolation procedure was considered.

In a report by (Ruan *et al.*, 2003), a number of signaling pathways were observed to be activated during the isolation of mouse adipocytes, including by implication MAP kinase pathways. Direct comparison is difficult however, because the protocol described was much longer than that used to isolate rat adipocytes in the experiments described in this thesis. Nevertheless, the possibility of unintended activation of signalling pathways was considered. AMPK is activated in response to the change in [AMP]/[ATP] under conditions of low glucose in muscle cells. It has also been reported that AMPK activation can stimulate GLUT1-mediated glucose uptake in clone9 cells (Barnes *et al.*, 2002). However, (Xi *et al.*, 2001) showed that there was no link between AMPK activation and that of p38 MAP kinase in rat adipocytes. Nevertheless, the possibility that basal p38 MAP kinase phosphorylation

A.

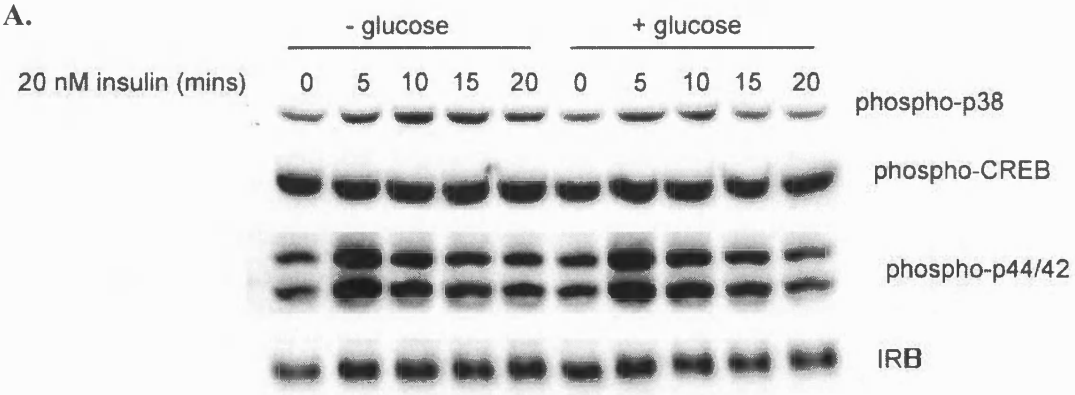

B.

Glucose	-		+	
Insulin	-	+	-	+
Phospho-p38 MAPK	1.00±0.00	1.40±0.21	1.00±0.00	1.20±0.06
Phospho-CREB	1.00±0.00	1.01±0.05	1.00±0.00	1.03±0.07

Figure 3.7. Effect of the presence of glucose during preparation of rat adipocytes on MAP kinase phosphorylation. A. Rat adipocytes were prepared either with the usual buffers or with 0.1% glucose in the wash buffer. Cells were stimulated with 20 nM insulin for the times indicated, lysed and analysed by SDS-PAGE and Western blotting with phospho-specific antibodies for p38 MAP kinase, CREB, p44/42 MAPK, and antibodies to the β-subunit of the insulin receptor (IRβ) as a loading control. This blot is representative of three different experiments. **B.** Mean band intensities at the 10-minute timepoints of the experiments represented in **A**. Intensities were corrected for loading differences and normalised against the basal values, ± S.E.M.

may be elevated as a result of the absence of glucose in the buffers used to wash and maintain the adipocytes following isolation was considered. However, the presence or

absence of glucose in these buffers had no effect on either basal p38 MAP kinase phosphorylation or its response to insulin (Figure 3.7).

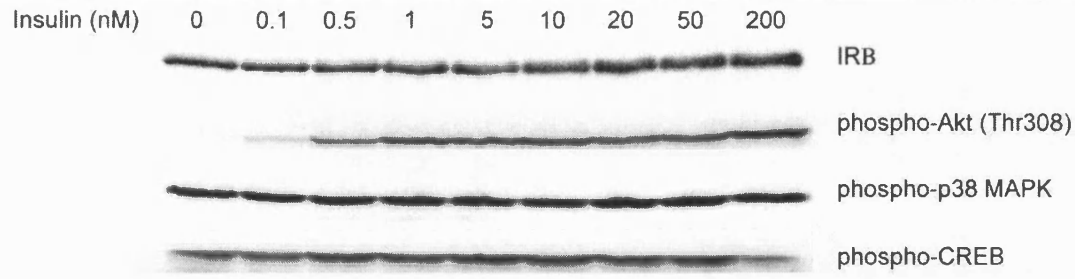

Figure 3.8. p38 MAP kinase response to varying concentrations of insulin. Rat adipocytes were stimulated with different concentrations of insulin for 10 min, lysed, and analysed by SDS-PAGE and Western blotting with antibodies to the β subunit of the insulin receptor (IRB) as a loading control, and phospho-specific antibodies to Akt(Thr308), p38 MAP kinase and CREB. This blot is representative of two different experiments.

3.2.6. Effect of insulin concentration on p38 MAP kinase activation

The effect on the phosphorylation of p38 MAP kinase of treating adipocytes with different concentrations of insulin was examined. As well as stimulating the insulin receptor, high concentrations of insulin such as those used to stimulate 3T3-L1 adipocytes may also stimulate related receptors, such as the IGF1 receptor, whose ligand is reported to stimulate p38 MAP kinase. There was no apparent increase in p38 MAP kinase phosphorylation between cells treated with 20 nM and 200 nM insulin (Figure 3.8).

3.2.7. Effect of SB203580 on glucose uptake and GLUT4 exocytosis

Treatment of adipocytes with 10 μM SB203580 inhibited insulin-stimulated 3-OMG uptake by 35.24% ± 0.05% (Figure 3.9). This is slightly smaller than the ~50%

inhibition reported in 3T3-L1 adipocytes by Sweeney *et al.* (1999). However, in contrast to the lack of inhibition of GLUT4 exocytosis reported by Sweeney *et al.* (1999), labelling of transporters at the cell surface with Bio-LC-ATB-BGPA photolabel (Section 2.9.1.) was also inhibited by 29.6% ± 4.1% following treatment with 10 μM SB203580 (Figure 3.10).

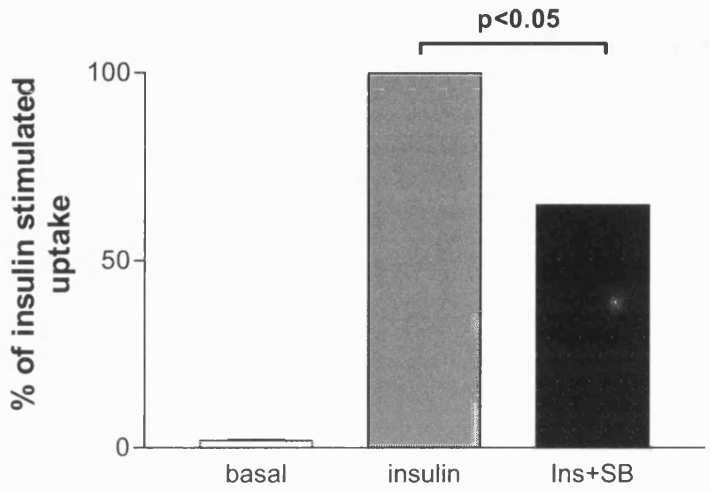

Figure 3.9. Inhibition of insulin stimulated glucose uptake by SB203580. Rat adipocytes were treated with 10 μM SB203580 for 20 min followed by 20 nM insulin for a further 20 min. Uptake was measured by the 3-OMG uptake assay. The chart shows means from four experiments. SB203580 had a statistically significant effect ($p < 0.05$) on insulin stimulated uptake, as measured by paired, two-tailed t test. Error bars are present but cannot be seen due to the small variation between experiments.

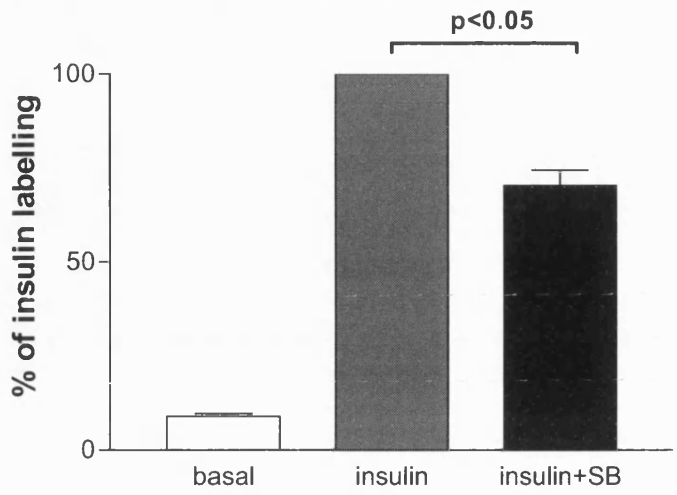

Figure 3.10. Inhibition of GLUT4 photolabelling by SB203580. Rat adipocytes were trerated with 10 μM SB203580 for 20 min, followed by a further 20 min with 20 nM insulin. Cell surface GLUT4 was labelled with Bio-LC-ATB-BGPA photolabel as described in General Methods and Streptavidin agarose precipitates were analysed by SDS-PAGE and western blot with anti-GLUT4 rabbit serum. GLUT4 bands from six experiments were quantified. SB203580 had a statistically significant effect ($p < 0.05$) on uptake, as measured by paired, two-tailed t test.

3.2.8. Effect of SB203580 on activation of p38 MAP kinase and Akt

Extracts from rat adipocytes treated with 10 μM SB203580 with and without insulin treatment were analysed for activation of p38 MAP kinase and Akt by western blotting. Akt is activated by phosphorylation on Thr308 and Ser473 (Alessi *et al.*, 1996), and phosphorylation on these residues can be detected with specific antibodies. Treatment with 10 μM SB203580 reduced basal and insulin-stimulated p38 MAP kinase phosphorylation by 35% and 42% respectively. There was no change in either CREB phosphorylation or phosphorylation of Akt on Thr308. Both basal and insulin stimulated phosphorylation of Akt on Ser473 were consistently reduced following

treatment with 10 μM SB203580, although this was not found to be statistically significant (Figure 3.11).

A.

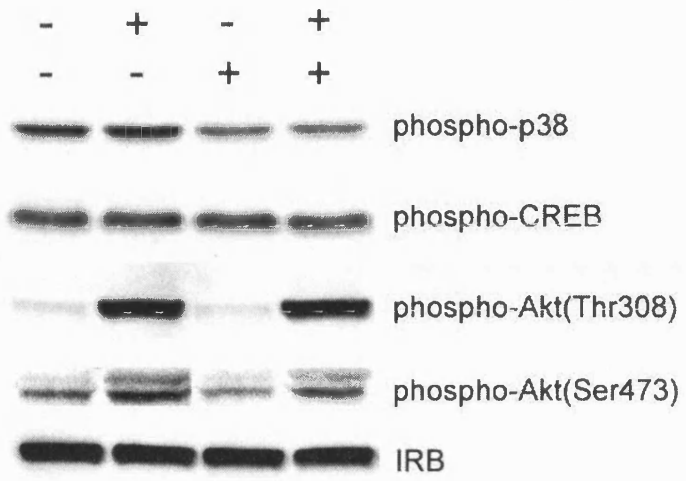

B.

	-SB		+SB	
	Basal	Insulin	Basal	Insulin
P-p38 MAPK	1.00±0.00	1.13±0.03	0.65±0.06*	0.65±0.02*
P-CREB	1.00±0.00	1.00±0.00	1.07±0.03	0.97±0.03
P-Akt (Ser473)	1.00±0.00	6.80±0.76	0.94±0.04	6.37±0.90
P-Akt (Thr308)	1.00±0.00	11.67±1.20	1.00±0.00	11.67±0.67

Figure 3.11. Effect of SB203580 on insulin stimulated phosphorylation of Akt at Thr308 and Ser473. A. Isolated rat adipocytes were stimulated for 10 min with 20 nM insulin with or without 20 min prior treatment with 10 μM SB203580. Cell lysates were analysed by SDS-PAGE and Western blotting with phospho-specific antibodies to p38 MAP kinase, CREB, Akt(Thr308), Akt(Ser473), and the β subunit of the insulin receptor (IRB). Blots shown are representative of three different experiments. **B.** Mean band intensities from the experiments represented in **A**, adjusted for loading differences and normalised to basal values, ± S.E.M. * indicates that treatment with SB has a significant effect ($p<0.05$, paired, two-tailed t test).

3.3. Discussion

Low nanomolar concentrations of wortmannin have previously been shown to differentially inhibit insulin stimulated glucose transport and GLUT4 exocytosis in 3T3-L1 adipocytes (Hausdorff *et al.*, 1999; Somwar *et al.*, 2001b). However, similar experiments carried out in our laboratory failed to detect any differences in the inhibition of these two processes by wortmannin in the same cell type (Clarke *et al.*, 1994). A possible explanation for the different results between the groups is in the methods used to measure GLUT4 exocytosis. Somwar *et al.* (2001) and Hausdorff *et al.* (1999) detected GLUT4 tagged with Myc on the extracellular domain. Clarke *et al.* (1994) however, used a biotinylated affinity label containing a glucose moiety designed to bind to GLUT4 at the cell surface. (Ferrara and Cushman, 1999) showed that this photolabel was unable to bind external GLUT4 in adipocytes that had been treated with the adrenergic agent isoproterenol. GLUT4 at the surface of cells treated with wortmannin or isoproterenol may be altered in some way and therefore have a lower affinity for the glucose moiety of the photolabel, thereby making the inhibited GLUT4 effectively invisible to the photolabelling assay.

The wortmannin inhibition experiments reported here included a modified exocytosis assay designed to ensure that all GLUT4 molecules on the cell surface were quantifiable (Section 2.9.3., Figure 3.3). Measurement of insulin-stimulated 3-OMG uptake, GLUT4 vesicle translocation (Figure 3.2) and exocytosis (using the modified photolabelling protocol, Figure 3.3) in rat adipocytes showed that wortmannin inhibited these three processes with similar IC50s of ~8 nM (Figure 3.4). A single target may therefore be responsible for the inhibition of all three processes by wortmannin. By implication, this target must therefore be upstream of GLUT4 translocation. These results do not necessarily imply that insulin does not regulate the

catalytic activity of GLUT4, only that GLUT4 exocytosis and glucose uptake cannot be separated at low concentrations of wortmannin, unlike in previous reports of experiments in cultured muscle and fat cells (Hausdorff *et al.*, 1999; Somwar *et al.*, 2001b).

There was less inhibition of insulin stimulated GLUT4 vesicle translocation than of glucose transport or GLUT4 exocytosis at wortmannin concentrations of 5 nM or less. The slope of the glucose uptake and GLUT4 exocytosis inhibition curves was also gentler and less sigmoidal in character than the GLUT4 translocation curve (Figure 3.4). This implies that exocytosis and glucose uptake are being inhibited at multiple steps, consistent with the existence an additional wortmannin-sensitive step after translocation but prior to fusion of GLUT4 vesicles with the plasma membrane. These results contradict the reported high affinity wortmannin target regulating transporter activity, but are consistent with more recent reports of a late pre-fusion step that is inhibited by the PI 3-kinase inhibitor LY294002 (Bose *et al.*, 2004) and is dependent on Akt activity (van Dam *et al.*, 2005).

The IC50 values for wortmannin inhibition of insulin stimulated glucose uptake, GLUT exocytosis and GLUT4 vesicle translocation in these experiments lies in between the values for the high and low affinity wortmannin targets reported by (Somwar *et al.*, 2001b) and (Hausdorff *et al.*, 1999). Some of these differences may be dependent on cell type. It is thought that wortmannin competes with ATP for its binding site on PI 3-kinase. Differences in sensitivities of different cell types to wortmannin may therefore be a result of differences in local ATP concentrations. Such differences in sensitivity may also be because different PI 3-kinase isoforms are responsible for the effects being measured. Wortmannin inhibits class I, class II, C2β and C2γ PI 3-kinase isoforms with IC50s in the narrow range between 1 and 10 nM,

and therefore cannot be used to distinguish between effects of different PI 3-kinase isoforms. In order to attribute functions to specific PI 3-kinase isoforms, other approaches such as dominant negative mutants, knockouts, and RNA interference are required.

It has also been suggested that the postulated high affinity target of wortmannin may not be a PI 3-kinase. This proposed high affinity wortmannin target has not been identified, but a series of papers from Amira Klip's laboratory has put forward evidence that the p38 MAP kinase pathway is involved in upregulating the catalytic activity of GLUT4 in response to insulin in muscle cells and in 3T3-L1 adipocytes and that this step is wortmannin-sensitive (Sweeney *et al.*, 1999; Somwar *et al.*, 2000; Konrad *et al.*, 2001; Somwar *et al.*, 2001a; Somwar *et al.*, 2001b; Somwar *et al.*, 2002).

The activation of the p38 MAP kinase pathway was examined in order to determine its possible involvement in insulin stimulated glucose transport. Insulin treatment of adipocytes resulted in a small transient increase in dual-phosphorylated p38 MAP kinase that peaked at an additional 35% over the basal value after 15 min of treatment and returned to basal levels after 20 min of insulin treatment (Figure 3.5). These changes are relatively small compared to the ~2.5-fold increases in p38 phosphorylation in muscle cells and 3T3-L1 adipocytes previously reported (Konrad *et al.*, 2001). No change was seen in phosphorylation of the p38 MAP kinase substrate CREB following insulin treatment (Figure 3.6). Adding glucose to the buffers used to wash and store our cells or increasing the insulin concentration had no effect on the magnitude of the insulin effect on p38 MAP kinase activation (Figure 3.7). However, changes in p38 MAP kinase activation following insulin treatment also appear to vary according to cell type and species, as primary human adipocytes show no increase at

all in p38 MAP kinase phosphorylation following insulin treatment (Carlson *et al.*, 2003).

The link between insulin stimulated glucose transport and p38 MAP kinase activation was examined in a series of experiments with the p38 MAP kinase inhibitor SB203580. 10 μM SB203580 inhibited insulin-stimulated 3-OMG uptake by 35% (Figure 3.9). SB203580 reduced p38 MAP kinase phosphorylation by 35% in the basal state and by 41% following insulin treatment (Figure 3.11). However, surface GLUT4 photolabelling was also reduced by 30% in insulin-treated rat adipocytes that had been preincubated with 10 μM SB203580 (Figure 3.10), contradicting the reports that SB203580 inhibits insulin-stimulated glucose transport independently of GLUT4 exocytosis. Again, it might be argued that the photolabelling assay only measures GLUT4 at the cell surface that is able to bind the glucose moiety of the label, and that a GLUT4 molecule that is being negatively regulated (by allosteric alteration of the glucose binding site, for example) may not be able to bind the label efficiently.

Following the completion of this work, a direct comparison of several different methods of measuring cell surface GLUT4 in 3T3-L1 adipocytes was reported. These studies showed that the mannose photolabelling method underestimated cell surface GLUT4 in cells treated with insulin and SB203580 when compared to direct cell surface protein biotinylation or detection of ectopically expressed GLUT4 containing a tag on the first extracellular loop (Bazuine *et al.*, 2005). Further work carried out in our laboratory following completion of the experiments described here also showed that SB203580 acted as a non-competitive inhibitor to glucose transport into the cell and as a competitive inhibitor to glucose transport out of the cell (Ribe *et al.*, 2005). Taken together, these studies strongly

suggest that the presence of SB203580 in cells reduces the ability of the extracellular domain of GLUT4 to bind glucose.

When lysates from insulin and SB203580 treated rat adipocytes were blotted for activated Akt, Thr308 phosphorylation was found to be unaffected by the inhibitor. Ser473 phosphorylation however, was consistently lower in SB treated cells than in control cells (Figure 3.11). As Akt activity requires phosphorylation on Thr308 and Ser473 mediated by PDK1 and PDK2 respectively (Alessi *et al.*, 1997; Anderson *et al.*, 1998), the fact that phosphorylation of Akt at one of these sites may be reduced in the presence of SB203580 makes it impossible to attribute the effects of the inhibitor on glucose uptake to inhibition of p38 MAP kinase. Akt was inhibited by 38% in the presence of 10 μM SB203580 in an *in vitro* phosphorylation assay (Davies *et al.*, 2000). Additionally, (Lali *et al.*, 2000) have shown that SB203580 inhibits phosphorylation of Akt on Ser473 by directly inhibiting PDK1 at micromolar concentrations in T cells. Furthermore, (Rane *et al.*, 2001) found that PDK2 activity in human neutrophils - and therefore phosphorylation of Akt on Thr308 - was also inhibited by SB203580 at concentrations similar to the IC50 for p38 MAP kinase. The target for SB203580 inhibition of PDK2 activity was identified as MAPKAPK-2, itself a p38 MAP kinase substrate. Also, the p38 MAP kinase inhibitor PD169316 reportedly has no effect on insulin stimulated glucose uptake in 3T3-L1 adipocytes even when applied at 50 times the IC50 for p38 MAP kinase inhibition (Kayali *et al.*, 2000). Together, these results suggest that the effects on insulin stimulated glucose uptake previously attributed to inhibition of p38 MAP kinase may in fact be due to inhibition of Akt.

The specificity of SB203580 is reported to improve when it is used at the lower concentration of 1 μM, but the data presented by Somwar *et al.* (1999)

supporting p38 MAP kinase involvement shows no inhibition of insulin stimulated glucose transport at this concentration of SB203580 (over double the IC50 value). (Somwar *et al.*, 2002) addressed the question of specificity of SB203580 by substituting two novel azaazulene p38 MAP kinase inhibitors for SB203580, producing similar inhibition of glucose uptake without inhibition of GLUT4 exocytosis. These novel inhibitors are otherwise uncharacterized in the literature, and given the evidence against p38 MAP kinase involvement in insulin stimulated glucose transport (Kayali *et al.*, 2000; Fujishiro *et al.*, 2001; Carlson *et al.*, 2003), doubts about their specificities must persist until their effects on other known components of the insulin signaling pathway have been demonstrated.

It is difficult to reconcile the apparently contradictory accounts of the role of p38 MAP kinase in insulin stimulated glucose uptake in 3T3-L1 adipocytes offered by (Somwar *et al.*, 2002) and (Fujishiro *et al.*, 2001). Insulin produced only a two-fold increase in exocytosis of Myc-GLUT4 in the study by the Klip laboratory (Somwar *et al.*, 2002). This response is unusually small for this type of cell, and is similar in magnitude to that seen when CHO cells, which lack a specialized GLUT4 compartment, express Myc-GLUT4 (Kanai *et al.*, 1993). These results may be affected by the increased GLUT4 expression levels, as changes in GLUT4 expression levels in adipocytes reportedly alter trafficking of GLUT4 and expression levels of proteins involved in GLUT4 trafficking (Carvalho *et al.*, 2004). Moreover, studies in which expression or activity of p38 MAP kinase are altered may also be misleading, as p38 MAP kinase has been shown to be a strong inducer of GLUT4 expression (Montessuit *et al.*, 2004).

In summary, the results presented in this chapter show that, unlike in recent reports of similar experiments in 3T3-L1 cells, wortmannin is unable to differentially

inhibit insulin stimulated glucose transport and GLUT4 exocytosis. The results of the wortmannin inhibition experiments on GLUT4 vesicle translocation, GLUT4 exocytosis and glucose uptake do not support the concept of a wortmannin sensitive step that leads to a change in the catalytic activity of GLUT4. The results suggest the existence of a wortmannin sensitive step between GLUT4 vesicle translocation and GLUT4 exocytosis. A small increase in p38 MAP kinase phosphorylation was observed following stimulation with insulin, but no detectable change in phosphorylation of CREB, a substrate of p38 MAP kinase was detected. Both insulin stimulated glucose uptake and cell surface GLUT4 labelling were inhibited by 10 μM SB203580, as was p38 MAP kinase phosphorylation. Insulin stimulated phosphorylation of Akt at Ser473 was also inhibited by 10 μM SB203580. The direct and indirect effects of SB203580 on Akt activity may therefore contribute to the reduction in insulin stimulated glucose transport, although more recent work has indicated that SB203580 is likely to inhibit GLUT4 transporter activity directly.

Chapter 4 – Quantitation and distribution of syntaxin4, SNAP23, VAMP2 and Munc18c in rat adipocytes

4.1. Introduction

The fusion of GLUT4 vesicles with the plasma membrane is the final step in insulin-stimulated translocation of GLUT4 to the plasma membrane. The cellular machinery controlling intracellular membrane fusion, introduced in Section 1.7., is common to all eukaryotes and includes NSF, the SNAP proteins, SNAP receptors (SNAREs) and Sec1/Munc18 homologs (SM proteins) (Mayer, 2002). Syntaxin4 and SNAP23 are present on adipocyte plasma membranes and act as t-SNAREs when GLUT4 vesicles fuse with the plasma membrane in response to insulin (Timmers *et al.*, 1996; Olson *et al.*, 1997; Rea *et al.*, 1998; St Denis *et al.*, 1999). VAMP2 is present on the insulin-responsive intracellular GLUT4 compartment and is thought to be the v-SNARE in the fusion reaction with the plasma membrane (Sevilla *et al.*, 1997; Millar *et al.*, 1999). These three SNAREs form a ternary complex *in vitro* and are present together in complexes isolated from adipocytes, which also include NSF and αSNAP (Timmers *et al.*, 1996; Olson *et al.*, 1997; Rea *et al.*, 1998).

The recruitment of insulin-responsive GLUT4 vesicles to the plasma membrane is regulated not only by availability of GLUT4 vesicles near the plasma membrane (by translocation) but also on the respective membranes. For instance, VAMP2 from GLUT4 vesicles formed SNARE complexes more readily on plasma membranes from insulin-treated adipocytes than on plasma membranes isolated from basal cells (Timmers *et al.*, 1996; Inoue *et al.*, 1999). Also, association of plasma membranes and GLUT4 vesicles from 3T3-L1 adipocytes *in vitro* increased when either was isolated from insulin-treated cells (Inoue *et al.*, 1999). Furthermore, insulin

treatment increased co-immunoprecipitation of GLUT4 vesicle proteins with the cytosolic domain of syntaxin4 in 3T3-L1 adipocytes (Olson *et al.*, 1997). These results suggest that SNARE complex formation may be a point of regulation by insulin, and that this regulation may take place on both the plasma membrane and the GLUT4 vesicle.

Munc18c is a potential mediator of this regulation by insulin. Munc18c is associated with syntaxin4 in 3T3-L1 adipocytes and blocked fusion of GLUT4 vesicles with the plasma membrane when overexpressed (Araki *et al.*, 1997; Thurmond *et al.*, 1998; Tamori *et al.*, 1998; Macaulay *et al.*, 2002), but paradoxically may also be required for the fusion reaction, as fusion was inhibited when its binding to syntaxin4 is disrupted by mutation or microinjection of inhibitory peptides (Thurmond *et al.*, 2000; Thurmond and Pessin, 2000). Unlike the neuronal Munc18a Munc18c could bind to a ternary SNARE complex (Widberg *et al.*, 2003). Insulin treatment disrupted the Munc18c/syntaxin4 complex in 3T3-L1 adipocytes (Thurmond *et al.*, 1998). This suggests that Munc18c may regulate the ability of syntaxin4 to form complexes with the other SNAREs. A recent report of experiments with adipocytes derived from Munc18c deficient mouse embryos indicated that Munc18c blocked GLUT4 exocytosis in a wortmannin sensitive manner. In the absence of Munc18c, insulin stimulated GLUT4 exocytosis was not wortmannin sensitive (Kanda *et al.*, 2005). This is an important development that directly links Munc18c and the membrane fusion machinery to the insulin signalling pathway.

Levels of syntaxin4, SNAP23, VAMP2 and Munc18c have previously been quantified in 3T3-L1 adipocytes (Hickson *et al.*, 2000). As the binary binding properties of these proteins are well characterised (Foster *et al.*, 1998), quantitating these proteins may be useful in identifying interactions that are likely to be under

regulation. For example, overexpression of SNAP23 stimulated GLUT4 exocytosis. This implies that the availability of SNAP23 limits the extent of fusion of GLUT4 vesicles with the plasma membrane (Foster *et al.*, 1999). However, the quantitative data showed that there were three times as many SNAP23 molecules as there were of its binding partner syntaxin4 (Table 4.1) (Hickson *et al.*, 2000). This suggests that the availability of SNAP23 may be tighly regulated and is potentially important in the regulation of insulin stimulated glucose transport.

Protein	Number of copies per cell
Syntaxin4	0.374×10^6
SNAP23	1.15×10^6
VAMP2	0.495×10^6
Munc18c	0.452×10^6

Table 4.1. Estimated numbers of syntaxin4, SNAP23, VAMP2 and Munc18c molecules in 3T3-L1 adipocytes. These estimates are based on the quantitative western blot analyses in the study by (Hickson *et al.*, 2000).

This study did not provide any information about the spatial distribution of the proteins in 3T3-L1 cells. Knowing how proteins are distributed within cells is important when considering the functional implications relative protein levels, as proteins that do not interact spatially are unlikely to interact functionally. The experiments in this chapter describe the quantification of syntaxin4, SNAP23, VAMP2 and Munc18c levels in rat adipocytes, in subcellular fractions and in SDS resistant complexes and the functional implications of the results are discussed.

4.2. Results

4.2.1. Characterisation of novel antibodies on western blots

Novel rabbit antibodies were raised against SNAP23, VAMP2 and Munc18c and prepared as described in Section 2.6. for use in the experiments described below. Adipocyte total lysates were run on SDS-PAGE and western blotted with the purified rabbit antibodies alongside commercial antibodies for the same proteins (Figure 4.1).

The major bands in the SNAP23 (at 27 kDa) and VAMP2 (16 kDa) blots were in the same positions as those detected by commercial antibodies directed against the same proteins. The SNAP23 antibody also detected an additional band at 36 kDa. This 36 kDa band was detected in the cytosol (Figure 4.5), and was not detected by the commercial antibody and is therefore unlikely to contain any SNAP23. The Munc18c antibody detected major bands at 59 and 65 kDa (Figure 4.1C). A western blot competition assay was performed to determine the specific band corresponding to Munc18c, as described in Section 2.2.6. Blots carried out in the absence of competing Munc18c showed the presence of the two bands at 59 and 65 kDa. In the presence of competing GST-Munc18c, the 65 kDa band disappeared, showing that this was the band corresponding to Munc18c (Figure 4.1C). This agreed with the molecular weight of the protein predicted from the amino acid sequence.

4.2.2. Quantification of syntaxin4, SNAP23, VAMP2 and Munc18c in rat adipocytes

GST-syntaxin4, NucA-SNAP23, NucA-$VAMP_{cyt}$ and GST-Munc18c were expressed and purified as described in Section 2.12. for use as protein standards for quantification of these proteins in adipocytes. Purities of the purified proteins were estimated by SDS-PAGE analysis and staining with coomassie blue (Figure 4.2).

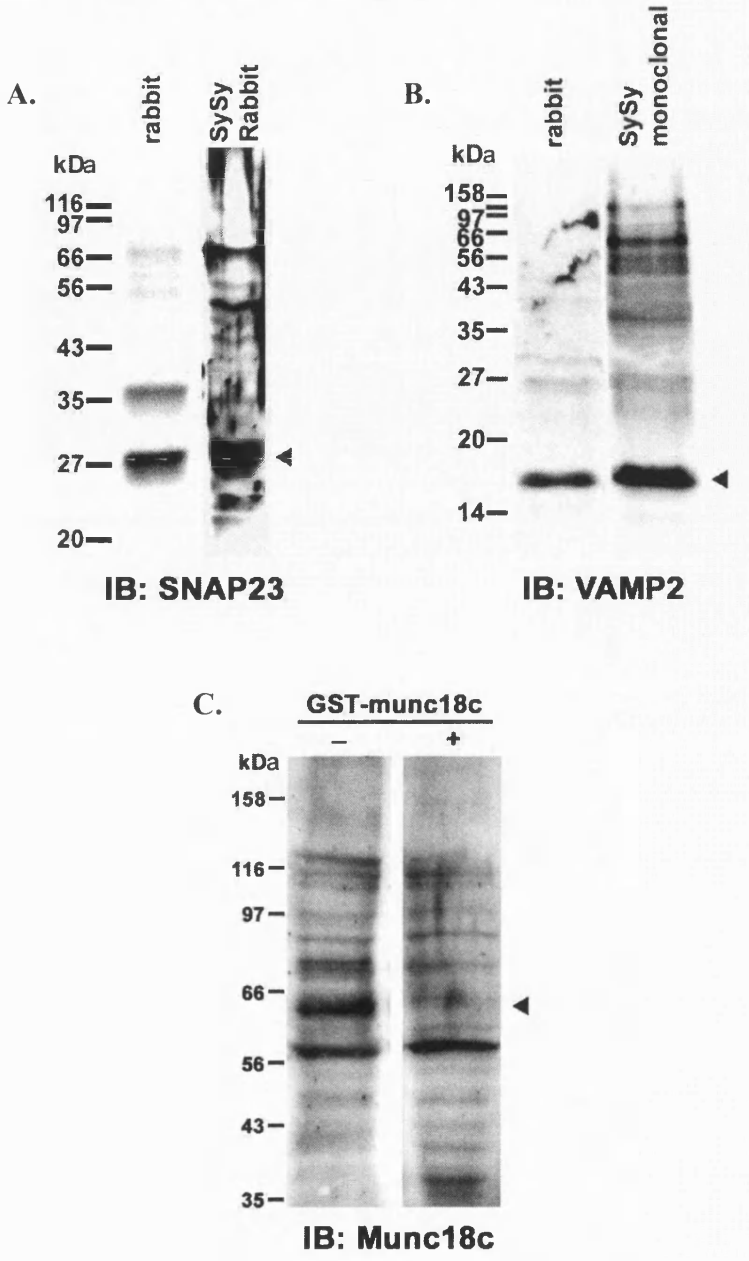

Figure 4.1. Specificities of affinity purified rabbit antibodies. Adipocyte lysates were western blotted with affinity purified rabbit antibodies from this laboratory (rabbit) and commercial equivalents for **A.** SNAP23 and **B.** VAMP2, both purchased from Synaptic Systems (SySy). **C.** Adipocyte lysates were western blotted with purified anti-Munc18c rabbit serum or with anti-Munc18c serum that had been preincubated with excess GST-Munc18. Arrowheads indicate expected positions of specific bands.

Band densities on the gels and total staining in each lane were measured from digital images of the backlit gels and used to provide an estimate of the purities of the protein standards using the method described in Section 2.12.1. and Figure 2.1. Purities of the protein standards were estimated at 74% (GST-syntaxin4), 81% (NucA-SNAP23, 88% (NucA-$VAMP_{cyt}$) and 95% (GST-Munc18c). The absolute concentration of specific protein in each standard was calculated from these estimates and the measurements of total protein concentrations.

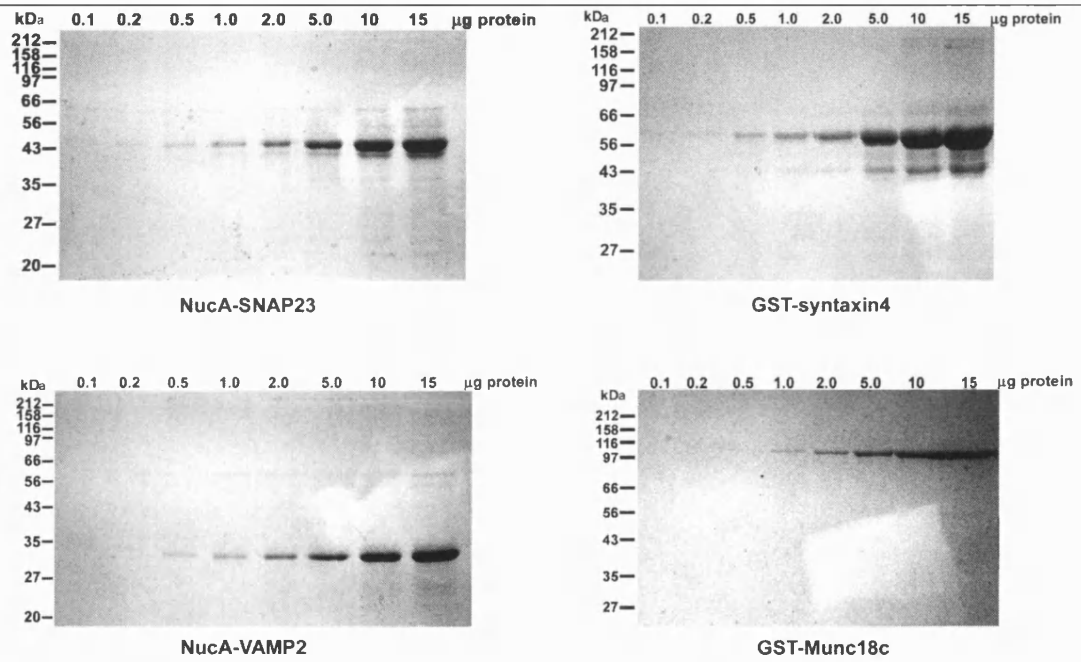

Figure 4.2. SDS-PAGE analysis of recombinant protein standards used for quantitation of adipocyte SNAREs. A range of amounts of each recombinant protein was analysed by SDS-PAGE and subjected to staining with coomassie blue. Protein purity was estimated from the band densities and the total staining in each lane. These proteins were used for subsequent quantification experiments.

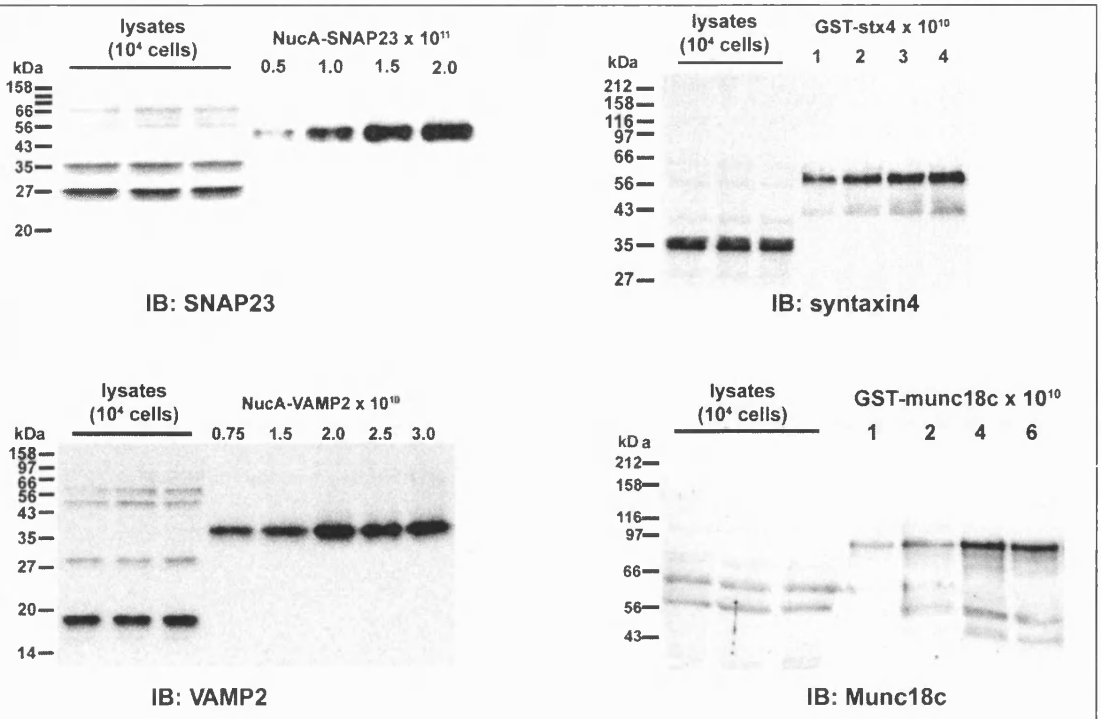

Figure 4.3. Quantification of SNAREs and Munc18c. Lysates from 10^4 cells, estimated from cell suspensions using a haemocytometer were run on SDS-PAGE in triplicate alongside known quantities of recombinant protein standards. Proteins were transferred to nitrocellulose and western blotted using purified rabbit sera against the respective proteins. Band densities were estimated and protein concentrations were calculated from calibration curves drawn from the standards. Representative blots from one of three separate experiments are shown here.

Lysates were made from adipocyte suspensions of known cell densities so that the recombinant protein standards could be compared to lysates from known numbers of cells. The lysate equivalent of 10^4 adipocytes was run in triplicate on SDS-PAGE alongside dilutions containing known numbers of the recombinant protein standard molecules (Section 2.12.2.). Proteins were then transferred to nitrocellulose and analysed by western blotting with the respective rabbit antibodies (Figure 4.3). Band intensities of the protein standards were quantified and used to construct a calibration

curve that was used to quantify the proteins in the lysate samples. The average number of copies of the proteins per adipocyte was determined from three separate experiments (Table 4.2).

Protein	Number of copies per cell (n=3)
Syntaxin4	$(2.5 \pm 0.3) \times 10^6$
SNAP23	$(8.9 \pm 1.7) \times 10^6$
VAMP2	$(1.9 \pm 0.3) \times 10^6$
Munc18c	$(1.0 \pm 0.2) \times 10^6$

Table 4.2. Estimated numbers of syntaxin4, SNAP23, VAMP2 and Munc18c molecules in rat adipocytes. Estimates of the numbers of protein molecules per adipocyte ± S.E.M. were calculated from band intensities of the blots represented in Figure 4.3.

4.2.3. Insulin induced redistribution of SNAREs and Munc18c on intracellular membranes

In order to select a suitable timepoint to track insulin induced changes in the distribution of syntaxin4, SNAP23, VAMP2 and Munc18c, the appearance of GLUT4 and VAMP2 on plasma membranes following insulin treatment was monitored by the plasma membrane lawn assay (Section 2.10.). Isolated adipocytes were treated with 20 nM insulin and processed for the plasma membrane lawn assay and labelled with rabbit anti-GLUT4 and mouse anti-VAMP2 antibodies. Immunofluorescence from fluorescent secondary antibodies was quantified as described in Section 2.10.4. The

time-course of trafficking of both proteins followed the same curve (Figure 4.4), as was to be expected if they trafficked in the same vesicles. There was a 1 min delay following insulin treatment followed by the rapid appearance of GLUT4 and VAMP2 on the membrane patches. The amount of the proteins on the lawns continued to increase for 20 min. By 40 min of insulin treatment, levels of both proteins on the plasma membrane patches had dropped to 70% of the maximum level.

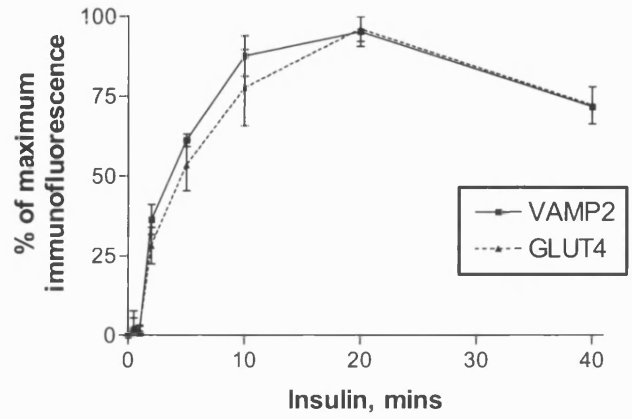

Figure 4.4. GLUT4 and VAMP2 appearance on plasma membrane lawns following insulin treatment. Adipocytes were treated with 20 mM insulin for the times indicated, adhered to coverslips and processed for the plasma membrane lawn assay. Lawns were probed with antibodies against GLUT4 and VAMP2. Immunofluorescence was quantified and plotted as a percentage of the maximum increase in intensity following insulin treatment. Results are means from three separate experiments except at t=40 min, where n=2.

Subsequent experiments were carried out with 20 min of insulin treatment so that cells were maximally stimulated as far as appearance of GLUT4 vesicles on the plasma membranes was concerned. In other words the cells had reached a steady state where GLUT4 vesicle translocation was exactly balanced by re-internalisation.

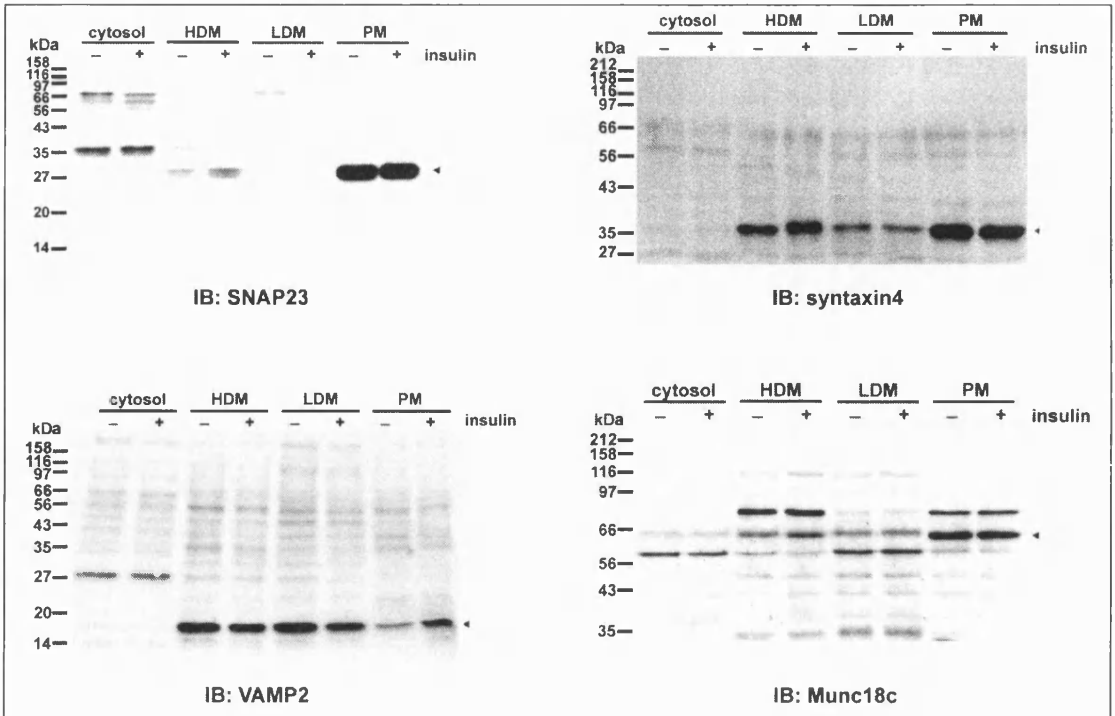

Figure 4.5. Distribution of SNAREs and Munc18c in rat adipocytes. Fractions prepared from adipocytes treated with and without 20 nM insulin were analysed by SDS-PAGE and western blotting with rabbit antibodies to SNAP23, syntaxin4, VAMP2 and Munc18c. The arrowheads show bands corresponding to these proteins in the cytosol, high density microsomes (HDM), low density microsomes (LDM), and plasma membranes (PM). Blots are representative of three separate experiments.

In order to monitor the distribution of the proteins in rat adipocytes, 20 μg of subcellular fractions from adipocytes that had been treated with insulin for 20 min were analysed by SDS-PAGE and western blotting alongside samples from non insulin-treated cells as described in Section 2.12.3. (Figure 4.5). Relative levels of the proteins in each fraction were calculated from the band intensities and the total protein content of the subcellular fractions.

		Syntaxin4	SNAP23	VAMP2	Munc18c
BASAL	PM	1940000±190000	8450000±280000	410000±110000	770000±140000
	LDM	172000±24000	79000±59000	919000±96000	74000±24000
	HDM	363000±8000	251000±177000	531000±16000	58000±1000
INSULIN	PM	1870000±130000	841000±40000	890000±200000	730000±160000
	LDM	138000±6000	112000±66000	696000±62000	85000±38000
	HDM	469000±11000	283000±18000	277000±118000	76000±23000

Table 4.3. Distribution of SNAREs and Munc18c in rat adipocytes. The table shows the estimated number of molecules of each protein ± S.E.M. in membrane fractions from adipocytes from three separate experiments, based on the band intensities from the blots represented in Figure 4.5 and the estimates of total numbers of molecules of each protein (Table 4.2).

All the proteins tested were concentrated in the HDM, LDM and PM fractions, with < 2% of the total detectable in cytosol and mitochondria/nuclei fractions (Table 4.3). SNAP23, syntaxin4 and Munc18c were predominantly localised to the plasma membrane with 95%, 78% and 75% of the respective cellular totals of these proteins in the plasma membrane. There was no change in Munc18c distribution following insulin treatment (Figure 4.6). There were small shifts of around 4% of the total syntaxin4 to the HDM following insulin treatment and of around 0.4% of the total SNAP23 to the LDM. VAMP2 was more evenly distributed, with 48% in the basal LDM, and the rest evenly split between HDM and PM fractions. Following insulin treatment, there was a redistribution of VAMP2 from the LDM to the PM, resulting in a 2.2-fold increase in VAMP2 in the plasma membrane.

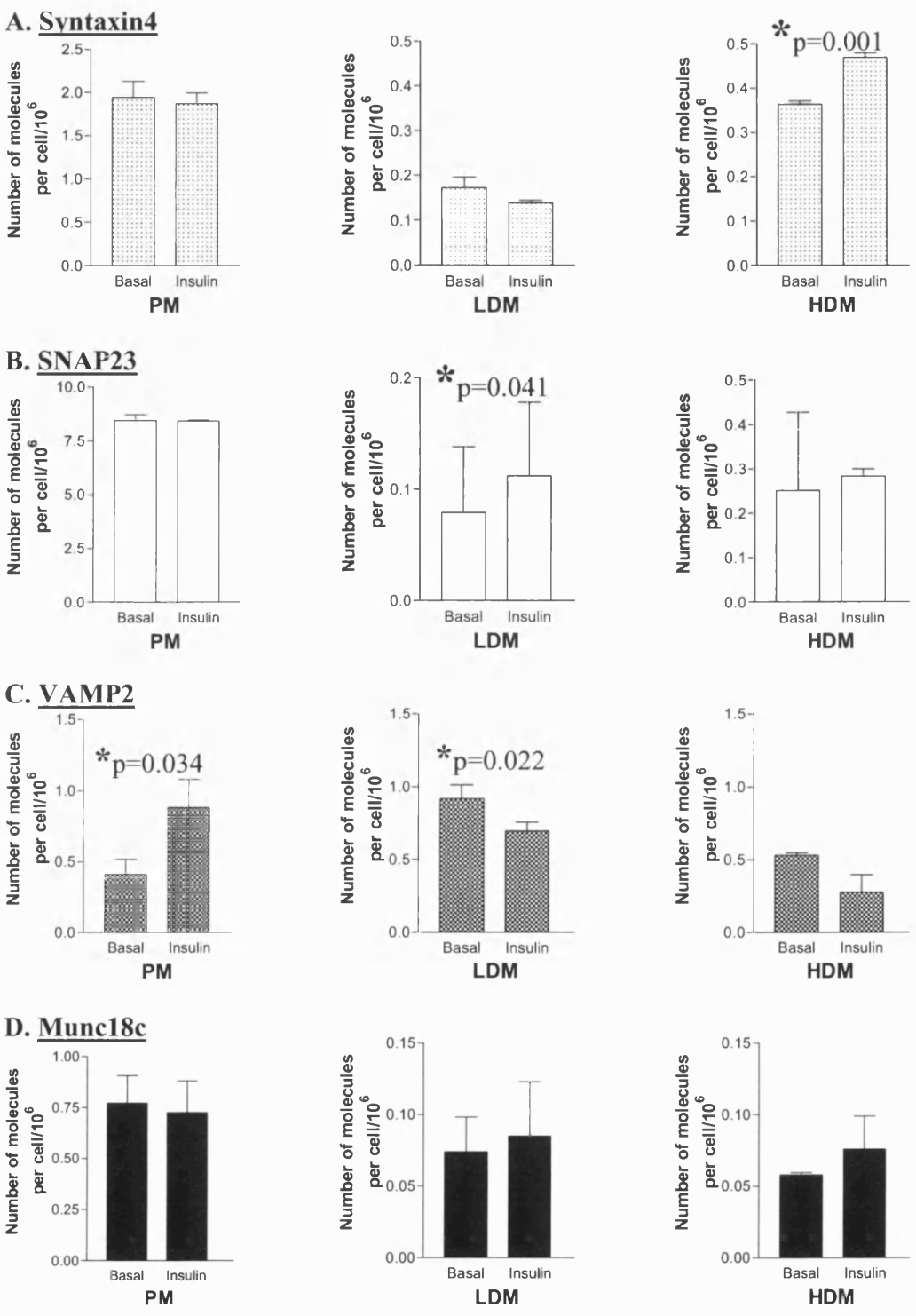

Figure 4.6. Changes in protein distribution with insulin treatment. The data from Figure 4.5 and Table 4.3 are presented to show changes in distribution of **A.** syntaxin4, **B.** SNAP23, **C.** VAMP2 and **D.** Munc18c that occured with insulin

treatment. Asterisks indicate where insulin causes a significant effect, determined by paired two-tailed t tests, where $p<0.05$.

4.2.4. SDS-resistant complexes

The presence of SNAREs in SDS-resistant complexes was inferred by the increase in detection of SNARE monomers following heat treatment of plasma membrane samples as described in Section 2.12.4. (Figure 4.7). Insulin treatment had no significant effect on the difference between heated and unheated samples ($p>0.05$ by paired, two-tailed t test). Detection of syntaxin4 and VAMP2 monomers increased by an average of 8% following heat treatment, and SNAP23 increased by an average of 32%.

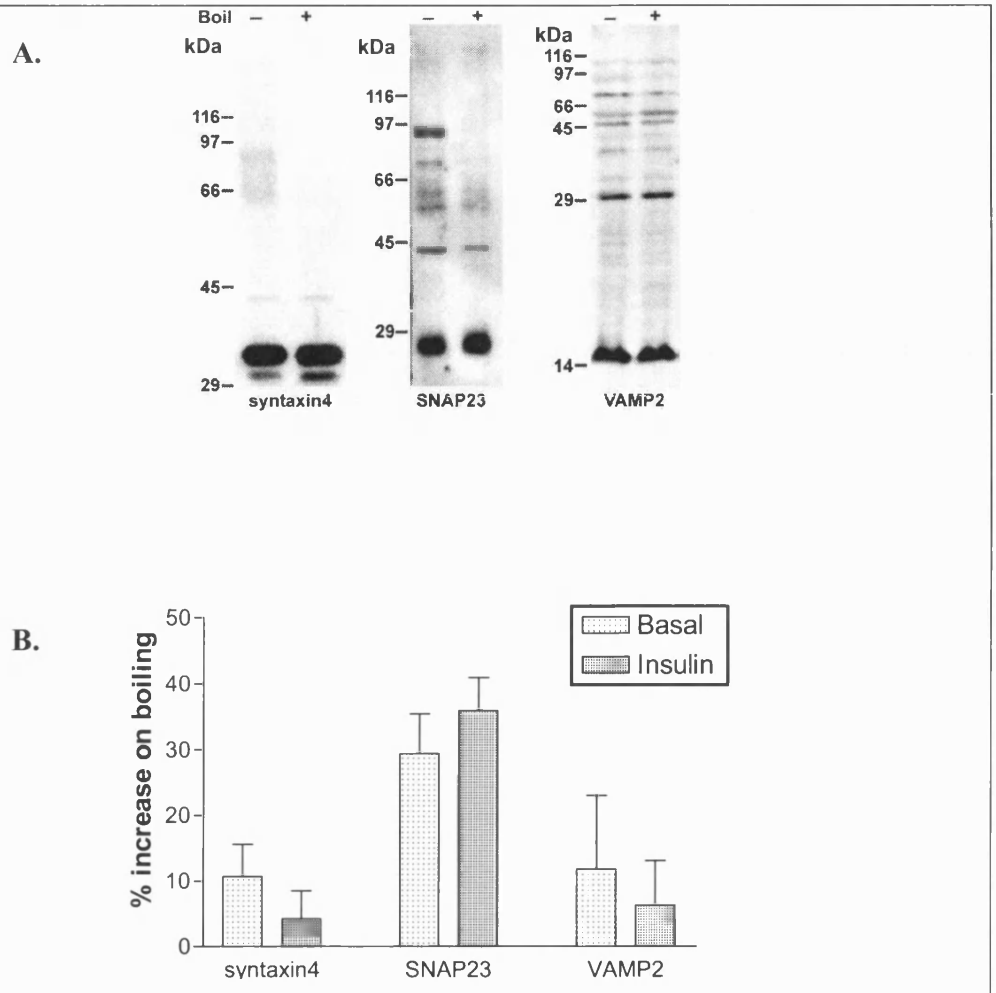

Figure 4.7. Effect of heat treatment on detection of SNAREs. (A) Plasma membranes from rat adipocytes were solubilised in sample buffer containing 0.1% SDS. They were then analysed by SDS-PAGE and western blotting with rabbit anti-syntaxin4 serum and SNAP23 and VAMP2 monoclonal antibodies, with or without 10 min prior heating of samples at 95°C. **(B)** Bands on blots of heat-treated samples were quantified and expressed as fractions of the band density of non heat-treated samples. Blots are representative of five separate experiments carried out with Dr. Alois Hodel.

4.3. Discussion

The results described here show that there were approximately 2,500,000 copies of syntaxin4, 8,900,000 copies of SNAP23, 1,900,000 copies of VAMP2 and 1,000,000 copies of Munc18c per adipocyte (Figure 4.3, Table 4.2). The relative expression levels of these proteins was in rough agreement with those previously measured in 3T3-L1 adipocytes (Hickson *et al.*, 2000), although absolute levels were around five-fold higher in the rat adipocytes.

The distribution of these proteins was detected by western blotting of subcellular fractions of basal and insulin treated adipocytes (Figure 4.5, Figure 4.6, Table 4.3). 95% of SNAP23 was located in the plasma membrane. Approximately 77% of syntaxin4 was found in the plasma membrane, 15% in the basal HDM fraction, and the remainder in the LDM. There was a shift of around 4% of the total syntaxin4 to the HDM fraction followong insulin treatment. The distribution agrees roughly with that seen in 3T3-L1 adipocytes and rat adipocytes by other groups (Rea *et al.*, 1998; St Denis *et al.*, 1999), although some groups have detected insulin-stimulated movement of syntaxin4 from the LDM to the plasma membrane in 3T3-L1 adipocytes (Volchuk *et al.*, 1996; Jagadish *et al.*, 1997; Tellam *et al.*, 1997).

There was a redistribution of 0.4% of the total cellular SNAP23 to the LDM following insulin treatment, in contrast with previous studies in both 3T3-L1 adipocytes and rat adipocytes that found no change in distribution following insulin treatment (Chen *et al.*, 1997; Wang *et al.*, 1997; Wong *et al.*, 1997; Rea *et al.*, 1998; St Denis *et al.*, 1999). Although consistent enough to be statistically significant, the measured insulin effect was much smaller than the variation in LDM SNAP23 content from experiment to experiment. This may have been because the bands on the western blots were of very low intensity compared to those on adjacent lanes. Furthermore, it

was unclear which of the other fractions accounted for the increase in LDM SNAP23. More detailed examination of the LDM in isolation and in direct comparison to each of the other fractions may be required to clarify this point.

VAMP2 was predominantly located in the LDM in the basal condition. On insulin stimulation there was a shift in distribution, predominantly from the LDM to the plasma membrane, which resulted in a 2.2-fold increase in VAMP2 at the plasma membrane. This is also consistent with previously published results (Cain *et al.*, 1992; Laurie *et al.*, 1993).

Munc18c was predominantly found in the plasma membrane, with the remainder distributed between the intracellular membrane and cytosolic fractions. There was no difference in Munc18c distribution between basal and insulin-treated cells in these experiments. There are reports of Munc18c trafficking to the plasma membrane following insulin stimulation of 3T3-L1 adipocytes, though this has not been confirmed in other reports (Tellam *et al.*, 1997; Thurmond *et al.*, 1998; Nelson *et al.*, 2002).

In previous reports of work in 3T3-L1 adipocytes, increasing SNAP23 levels increased insulin stimulated trafficking of GLUT4 to the plasma membrane as well as glucose uptake, suggesting that SNAP23 availability limits insertion of GLUT4 into the plasma membrane (Foster *et al.*, 1999). This finding implied that SNAP23 availability must be tightly regulated, as it was also present in excess compared to syntaxin4 in 3T3-L1 adipocytes, and had a similar distribution in those cells to that seen in rat adipocytes (Rea *et al.*, 1998; Hickson *et al.*, 2000). A proportion of SNAP23 was associated with a Triton-insoluble cytoskeletal fraction in 3T3-L1 adipocytes, and colocalised with vimentin in fibroblasts and HeLa cells (Foster *et al.*, 1999). SNAP23 also interacted with kinesin in a yeast two-hybrid assay and *in vitro*

(Diefenbach *et al.*, 2002). These cytoskeletal interactions may regulate availability of SNAP23 for SNARE complex formation.

Synaptic SNAREs assemble spontaneously *in vitro* into complexes that are resistant to SDS at temperatures up to 80°C. This assembly was prevented by cleavage of SNAP25 with BoNT E, in a manner which parallels BoNT E inhibition of calcium-evoked exocytosis (Hayashi *et al.*, 1994; Banerjee *et al.*, 1996). BoNT E inhibition of exocytosis was relieved by addition of a SNAP25 peptide that was incorporated into SDS-resistant complexes (Chen *et al.*, 1999), suggesting that these complexes may precede exocytosis. SDS-resistant complexes isolated from secretory cells migrate as a series of bands of different sizes when analysed by SDS-PAGE (Hayashi *et al.*, 1994; Otto *et al.*, 1997; Chen *et al.*, 1999). These may represent oligomers of ternary complexes, or different folding states of individual complexes (Tokumaru *et al.*, 2001; Lawrence and Dolly, 2002). Previous attempts have failed to detect SDS-resistant SNARE complexes between adipocyte SNAREs in 3T3-L1 cells (Foster *et al.*, 1998), although the recombinant proteins do form an SDS-resistant complex *in vitro* (Rea *et al.*, 1998).

SDS-resistant complexes were detected indirectly in plasma membranes of rat adipocytes by comparing the detection of SNARE monomers on western blots of heat and non-heat treated samples (Figure 4.7). The intensities of all three SNARE monomer bands increased with heat treatment, implying the existence of SDS-resistant states with altered mobility on SDS-PAGE. A number of additional minor bands were also detected on the gels. Of these, the band at ~94 kDa was common to blots with antibodies against all three SNAREs (Figure 4.6A). This band also decreased in intensity in the heat-treated samples, although the decrease was greater in blots against SNAP23 and syntaxin4 compared VAMP2.

Using the estimates of numbers of each SNARE in the plasma membrane, the increase in number of SNAP23 monomers following heat treatment was estimated as being in excess of twenty times the increase in number of syntaxin4 monomers. This lopsided distribution suggests that the SDS-resistant states of syntaxin4 and SNAP23 are not simply multiple heterodimers of the two proteins. SNAP23 must therefore be associated with proteins other than syntaxin4 in the SDS-resistant complexes. A proportion of the SDS-resistant states of SNAP23 may therefore represent protein that is unavailable for binding to other SNAREs, supporting the limited availability model.

The amount of SNARE monomers released following heat treatment did not differ between basal and insulin-treated cells (Figure 4.7). No changes were detected in the amount of SDS-resistant SNARE complexes during neurotransmitter release in nerve terminals or granule release in chromaffin cells either (Mehta *et al.*, 1996; Leveque *et al.*, 2000; Lawrence and Dolly, 2002), so it is not certain that changes would be detected following insulin treatment. It is thought that this is because SNAREs go through a variety of folded states and complexes prior to membrane fusion, and those states that occur immediately prior to fusion may be short lived and relatively rare in a snapshot view of the population.

Previously reported results have indicated that participation of plasma membrane syntaxin4 in SNARE complexes may also be regulated. Only half the syntaxin4 precipitated from rat adipocyte plasma membranes was in a complex with SNAP23 (St Denis *et al.*, 1999). This is interesting because in the experiments described above, there are half as many copies of Munc18c on the plasma membrane as there are of syntaxin4. It is therefore possible that Munc18c is associated exclusively with one half of the syntaxin4 population. Munc18c co-immunoprecipitated with SNAP23 and syntaxin4 in platelets, and with syntaxin4 but

not with SNAP23 in 3T3-L1 adipocytes (Tamori *et al.*, 1998; Schraw *et al.*, 2003). Munc18c also inhibits the complex between syntaxin4 and SNAP23 when all three proteins are expressed together in COS cells (Araki *et al.*, 1997). The quantitative data shown here support a model where syntaxin4/Munc18c complexes and syntaxin4/SNAP23 complexes are mutually exclusive and each account for half of the syntaxin4 in the plasma membrane.

Insulin stimulated GLUT4 exocytosis was inhibited and GLUT4 vesicles accumulated adjacent to the plasma membrane when the syntaxin4-Munc18c interaction was disrupted by a blocking peptide (Thurmond *et al.*, 2000). One interpretation of this result is that the Munc18c/syntaxin4 interaction is required for the fusion reaction. An alternative explanation which may better fit with the data on Munc18c inhibiting SNARE complex formation is that Munc18c bound to non-SNAP23 bound syntaxin4 molecules in the basal state, and prevents them combining with VAMP2. Blocking Munc18c binding to syntaxin4 may allow syntaxin4 to bind VAMP2 on GLUT4 vesicles in the absence of SNAP23, thereby competing with ternary syntaxin4/SNAP23/VAMP2 complex formation. Recent reports from *in vitro* assays and SNAP25 knockout work have suggested that syntaxin1/VAMP complexes may support slow constitutive exocytosis but not fast calcium-evoked exocytosis (Woodbury and Rognlien, 2000; Washbourne *et al.*, 2002; Bowen *et al.*, 2004). Therefore increasing syntaxin4/VAMP2 complexes at the expense of syntaxin4/SNAP23/VAMP2 complexes by disrupting the Munc18c-syntaxin4 complex with a blocking peptide may reduce the overall rate of fusion of GLUT4 vesicles with the plasma membrane (Thurmond *et al.*, 2000). The relationship between the amount of available SNAP23 and Munc18c may therefore be a crucial

determinant of the insulin response, and suggests that regulation of insulin-stimulated GLUT4 translocation may occur at this level.

The number of VAMP2 molecules on the plasma membrane in the insulin-stimulated state was also found to be approximately half the total number of syntaxin4 molecules (Table 4.3). This is the same as the number of syntaxin4/SNAP23 complexes (St Denis *et al.*, 1999), consistent with VAMP2 from GLUT4 vesicles being recruited to syntaxin4/SNAP23 complexes on insulin stimulation. The Syntaxin4/SNAP23 complex as a whole is therefore likely to be rate-limiting for GLUT4 docking with the plasma membrane.

As well as regulation of SNARE complex formation, another function that has been attributed to Munc18 proteins is in the trafficking of syntaxins through the cell (Rowe *et al.*, 1999; Rowe *et al.*, 2001). Syntaxin4 trafficking to the plasma membrane was disrupted when syntaxin4 was overexpressed in a number of cell types. Trafficking was restored when Munc18c was co-expressed in the same cells (Takuma *et al.*, 2002). These results suggest that Munc18c participates in the trafficking of syntaxin4 by preventing undesirable interactions with other proteins. In rat adipocytes however, syntaxin4 was present in large excess over Munc18c in the intracellular membrane fractions (Table 4.3). This suggests that Munc18c does not play a major role in preventing premature interactions with syntaxin4 in these membranes.

In summary, syntaxin4, SNAP23, VAMP2 and Munc18c were quantified in rat adipocytes and in intracellular fractions. The proteins were expressed at approximately five times the levels previously seen in 3T3-L1 adipocytes, though expression levels of the proteins relative to each other were similar in both cell types. Syntaxin4, SNAP23 and Munc18c were predominantly localised to the plasma membrane. A small proportion of syntaxin4 and SNAP23 were redistributed to the

HDM and LDM respectively following treatment of adipocytes with insulin. VAMP2 was predominantly intracellular, and its presence on the plasma membrane increased 2.2-fold in response to insulin. The relative proportions of these proteins suggest that SNAP23 availability is tightly regulated and that Munc18c does not play a major role in syntaxin4 trafficking. There was also a large excess of SNAP23 over syntaxin4 and VAMP2 in SDS-resistant complexes isolated from adipocyte plasma membranes. Insulin treatment had no effect on the number of these proteins segregated into SDS-resistant complexes. The stoichiometry of these complexes suggested that they were not directly linked to membrane fusion.

Chapter 5 - Expression, purification and reconstitution of bacterially-expressed adipocyte SNAREs into liposomes for *in vitro* fusion experiments

5.1. Introduction

The fusion of GLUT4 vesicles with the plasma membrane of adipocytes is an important step in exposing GLUT4 to the exterior of the cell, thus enabling it to transport its hexose substrate into and out of the cell (Sections 1.3. and 1.7.). There is evidence that insulin as well as stimulating translocation of GLUT4 vesicles to the plasma membrane, also directly promotes docking of vesicles at the plasma membrane (Timmers *et al.*, 1996; Inoue *et al.*, 1999). This upregulation of docking by insulin occurs both on the plasma membrane and on GLUT4 vesicles. Membrane fusion itself is also a target of regulation by insulin. Insulin treatment affects intracellular pH (Yang *et al.*, 2002), interactions of SNAREs with proteins such as Munc18c and synip (Tellam *et al.*, 1997; Min *et al.*, 1999), and calcium ion concentration (Whitehead *et al.*, 2001), all of which affect membrane fusion. Insulin treatment of cells increased the ability of syntaxin4 to bind GLUT4 vesicles (Olson *et al.*, 1997), and also increased the ability of VAMP2 on GLUT4 vesicles to form complexes with plasma membrane SNAREs (Timmers *et al.*, 1996).

Syntaxin4, SNAP23 and VAMP2 have been shown to bind pairwise *in vitro* with affinities similar to those of the neuronal homologs (Foster *et al.*, 1998). They also form a ternary complex *in vitro* (Rea *et al.*, 1998; Widberg *et al.*, 2003) and are present together in 20S SNARE complexes from adipose cells (St Denis *et al.*, 1999).

It is known that trans-SNARE complex assembly functions upstream of membrane fusion (Section 1.7.2.), but whether the complex itself catalyses the fusion

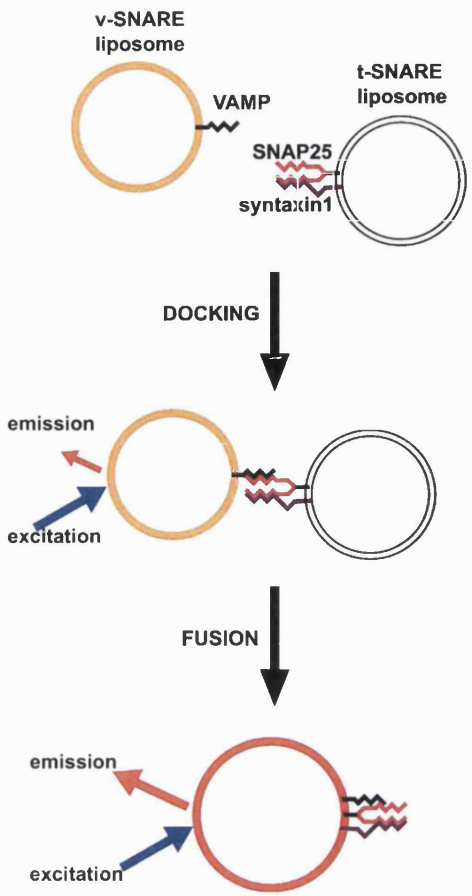

Figure 5.1. Reconstitution of membrane fusion with liposomes and recombinant SNAREs. Recombinant VAMP2 is reconstituted into liposomes containing a mixture of fluorescent and quenching lipid head groups. The t-SNARE complex of syntaxin1 and SNAP25 is reconstituted into non-fluorescent liposomes. When mixed, liposomes containing complementary SNAREs dock and fuse. Subsequent fusion of the liposomes causes an increase in fluorescence as a result of dilution of the quenching lipid from the v-SNARE liposomes (Weber *et al.*, 1998).

reaction is still a matter of debate (Szule and Coorssen, 2003). *In vitro* assays show that SNARE proteins are able to catalyse fusion between artificial lipid bilayers, and that this reaction retains many of the properties that characterise *in vivo* membrane fusion (Weber *et al.*, 1998). Figure 5.1 shows an assay that has been used to demonstrate liposome fusion by SNAREs. Aside from lipid mixing, similar liposome-based assays have used content mixing to demonstrate full fusion between liposomes (Nickel *et al.*, 1999). Although SNARE proteins are promiscuous, in that they are able to form complexes *in vitro* with SNAREs that they do not encounter *in vivo* (Fasshauer *et al.*, 1999; Yang *et al.*, 1999), only combinations that are partners in *in*

vivo trafficking events are able to catalyse fusion between liposomes (Parlati *et al.*, 2002). This suggests that the function of SNAREs in fusion is separate from their ability to form complexes.

Although this assay shows that SNARE proteins are able to facilitate lipid mixing *in vitro*, it does not necessarily mean that they carry out the same function *in vivo*. Structural studies of VAMP show that a number of residues in the carboxy-terminal part of the SNARE motif are buried in the membrane (Kweon *et al.*, 2002). This makes VAMP unable to bind soluble syntaxin or SNAP25. Furthermore, no lipid mixing was observed between VAMP-containing liposomes and liposomes containing syntaxin and SNAP25 isolated from bovine brain, and VAMP from synaptic vesicles was unable to form complexes with soluble syntaxin and SNAP25 (Hu *et al.*, 2002). Some argue that the fusion observed between v- and t-SNARE liposomes in the assay by the Rothman group may be an artefact caused by the high ratio of VAMP:lipid molecules (~1:20) in the liposomes. This is around 30 times the density in synaptic vesicles (Walch-Solimena *et al.*, 1995a). The VAMP may not be able to interact fully with the membrane in these conditions. However, SNARE density was nearer physiologically relevant levels in the liposome based assays performed with yeast SNAREs, and in studies that observed fusion between cells that were made to express VAMP and syntaxin/SNAP25 on their outer surfaces (McNew *et al.*, 2000a; Parlati *et al.*, 2002; Hu *et al.*, 2003).

Despite these doubts, this liposome-based assay has provided the basis for studies on structural requirements of SNAREs and regulation of fusion (Parlati *et al.*, 2000; Weber *et al.*, 2000; McNew *et al.*, 2000b; Melia *et al.*, 2002), the role of calcium and synaptotagmin in membrane fusion (Hu *et al.*, 2002; Mahal *et al.*, 2002;

Tucker *et al.*, 2004; Jeremic *et al.*, 2004) and the role of Sec1 in stimulating fusion (Scott *et al.*, 2004).

This chapter describes the adaptation of the liposome-based assay of SNARE-mediated fusion shown in Figure 5.1 to the GLUT4 vesicle-plasma membrane system using recombinant syntaxin4, SNAP23, and VAMP2. The aim of developing this assay is to demonstrate whether these SNAREs are capable of catalyzing fusion between artificial liposomes. If this is so, it will be used as a model in studies of the regulation of fusion of GLUT4 vesicles with the plasma membrane. This means that there will be a defined starting point for experiments examining the effects of altering parameters such as mutations of the SNAREs, pH, metal ion concentration or the effects of addition of recombinant proteins or cellular components such as cytosol or peripheral membrane proteins on membrane fusion. This information can then be related to data obtained on the fusion apparatus from insulin-responsive cells to increase our understanding of the regulation of GLUT4 vesicle fusion with the plasma membrane by insulin.

5.2. Results

5.2.1. Reconstitution of recombinant t-SNAREs into liposomes

5.2.1.1. Expression and purification of syntaxin4

A number of approaches to expressing, purifying and reconstituting t-SNAREs into liposomes were examined. The first step towards enabling bacterial expression of syntaxin4 was to clone the coding sequence of syntaxin4. Two independent clones coding for full length syntaxin4 were obtained by RT-PCR from rat adipocyte mRNA as described in Section 2.4.1.1. The coding sequence of both syntaxin4 clones was

identical to that of rat syntaxin4 (NM_031125) except for the substitution of the bases gc for cg at bases 647 and 648. This corresponds to the substitution of a serine for a threonine at residue 216 in the translated protein.

The syntaxin4 coding sequence was ligated into pET28a to produce pET28a-stx4 (Section 2.4.1.2.). The fusion protein expressed from this plasmid should resemble endogenous syntaxin4 on the cytosolic domain, but would contain the his-tag on the lumenal domain as shown in Table 5.1. The cytosolic domain is thought to be important in the protein-protein interactions that precede membrane fusion. The lumenal affinity tag should therefore not affect the function of the molecule in fusion assays.

Total syntaxin4-his expression from pET28a-transformed *E. coli* is described in Section 2.5.1. and was estimated at 0.7 mg per l of culture. Of this total, an estimated 0.45 mg per l of culture was soluble protein (Figure 5.2A). The soluble syntaxin4-his bound to Ni-NTA as predicted, but only partially eluted in buffer containing 250 mM imidazole (Figure 5.2B). The protein eluted on a pH step gradient at pH 6, consistent with a monomeric his-tag interaction with the nickel ions on the resin (Figure 5.2C). The total recovery of syntaxin4-his was estimated at 0.23 mg per l of culture in a volume of 10 ml.

Plasmid name	Expressed proteins
pET28a-stx4	
pDRSN1-stx4	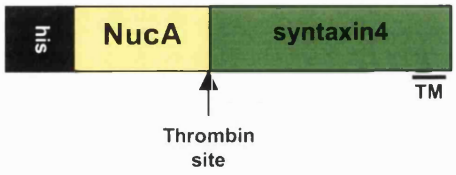
pGEX-SNAP23	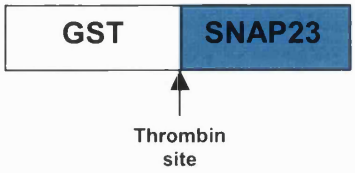
pGEX-tSNAREs	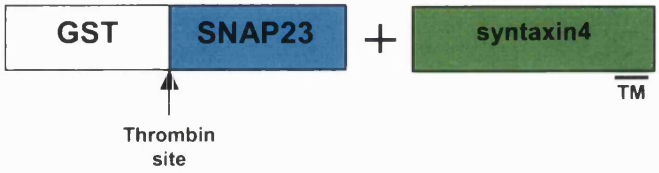
PGEX-tSNAREs(NucA)	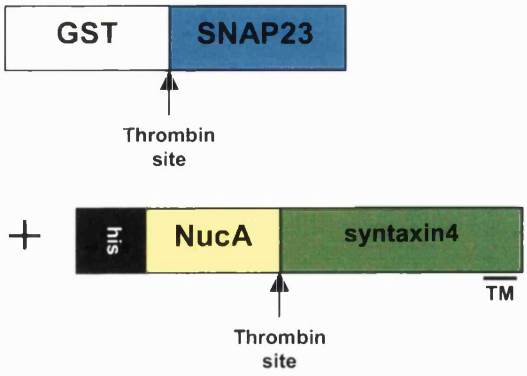
pET28a-VAMP2	
pDRSN1-VAMP2	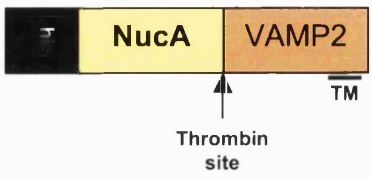

Table 5.1. Bacterial expression of adipocyte SNARE proteins. Schematic of the plasmids and recombinant SNARE proteins that were expressed for reconstitution studies described in this chapter. TM indicates the position of the transmembrane domain and arrowheads show the position of thrombin cleavage sites.

A final concentration 1-2 mg/ml of syntaxin was used when reconstituting the protein into liposomes in previously published studies (Weber *et al.*, 1998). This was approximately 40 times the concentration of syntaxin4 purified from *E. coli* containing pET28a-stx4. Massive scaling up of the expression and purification steps would be required in order to achieve this final concentration with this syntaxin4 expression system.

In an attempt to increase the yield and concentration of recovered syntaxin4, a vector was constructed with the aim of expressing of the protein as a fusion with the *Staphylococcus aureus* NucleaseA protein (NucA). As well as facilitating high expression levels in *E. coli*, NucA fusion proteins have the advantage of having a calcium-dependent endonuclease activity. This allows digestion of genomic DNA to reduce viscosity of bacterial lysates under mild conditions, minimising possible denaturation of the recombinant protein. NucA fusion proteins tend to be sequestered into inclusion bodies, which reduces the potential toxic effects of hydrophobic domains on the host cells, potentially increasing expression levels (Laage and Langosch, 2001).

The syntaxin4 coding sequence was cloned into pSNiR3, which was then modified to reduce the glycine spacer at the N-terminus of syntaxin4 and to remove the HA tag that is coded for by the plasmid (Section 2.4.1.3.). The resulting plasmid, pDRSN1-stx4 coded for syntaxin4 with a thrombin-cleavable NucA moiety at its

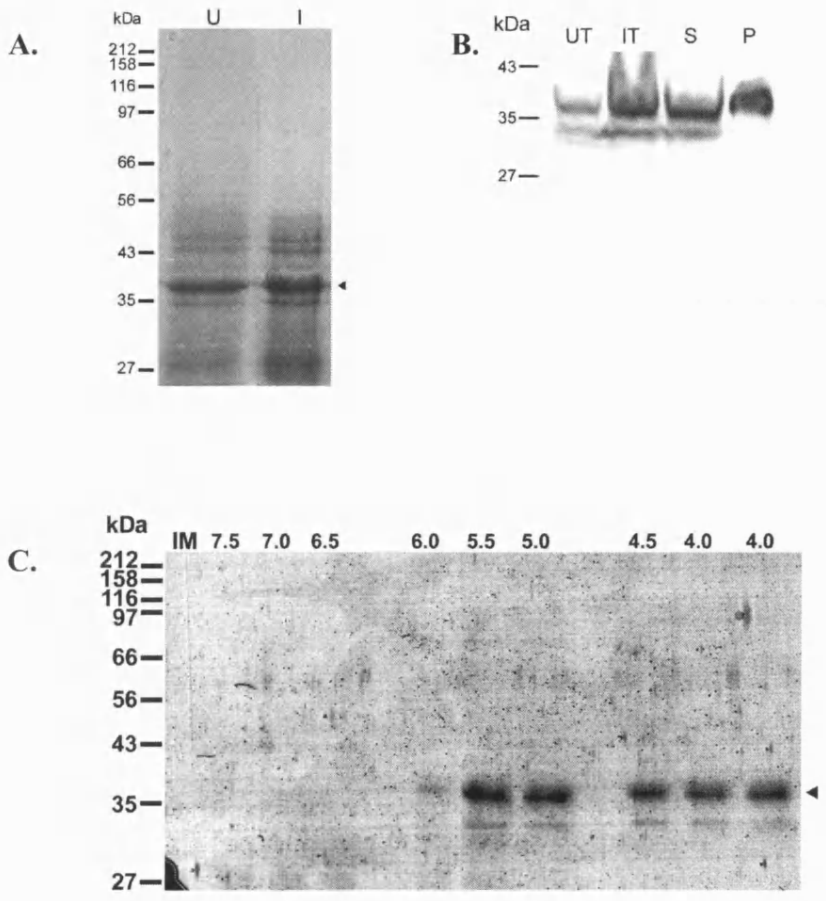

Figure 5.2. Syntaxin4-his expression in Rosetta (DE3)pLysS. A. Total lysates from cells that were either uninduced (U) or induced (I) with 1 mM IPTG were separated by SDS-PAGE and stained with coomassie blue. **B.** Total lysates from uninduced cells (UT), induced cells (IT), proteins soluble in 25 mM phosphate buffer pH 8, 1 M NaCl, 4% TritonX-100 (S), and the insoluble pellet (P) were analysed by SDS-PAGE and blotted with anti-syntaxin4 rabbit serum. **C.** Coomassie stained gel showing syntaxin4-his eluted from Ni-NTA with 250 mM imidazole (IM) or a pH gradient of 50 mM phosphate and phosphate-citrate buffers containing 300 mM KCl and 1% n-octylglucoside. The arrowheads indicate the expected position of syntaxin4-his.

amino terminus (Table 5.1). Cells transformed with this plasmid expressed an estimated 18 mg of NucA-syntaxin4 per l of culture when induced as described in Section 2.5.2. All of this protein was soluble in a high salt detergent buffer designed to solubilise inclusion bodies (Figure 5.3A). In a typical experiment, NucA-syntaxin4 made up an estimated 70% of the total protein in the washed and solubilised inclusion body fraction (Figure 5.3B). The concentration of NucA-syntaxin4 in the final solubilised inclusion body fraction was typically 3.6 mg/ml. This was equivalent to 2.4 mg/ml of syntaxin4.

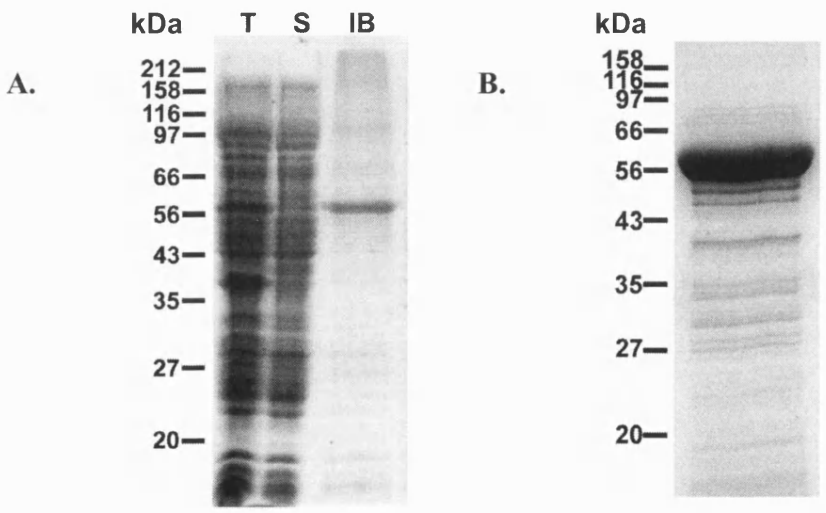

Figure 5.3. Solubilisation of NucA-syntaxin4. A. Coomassie stained gel showing total lysates of cells expressing NucA-syntaxin4 (T), proteins soluble in 50 mM phosphate buffer pH 8 (S), and inclusion bodies solubilised in IB buffer (25 mM phosphate buffer pH 8, 1.5 M NaCl, 1% n-octylglucoside) (IB). **B.** Inclusion bodies washed three times in 50 mM sodium phosphate buffer pH 7.5, 1 mM EDTA, 1% n-octylglucoside and solubilised in IB buffer. NucA syntaxin4 migrated at the theoretical molecular weight of 55 kDa.

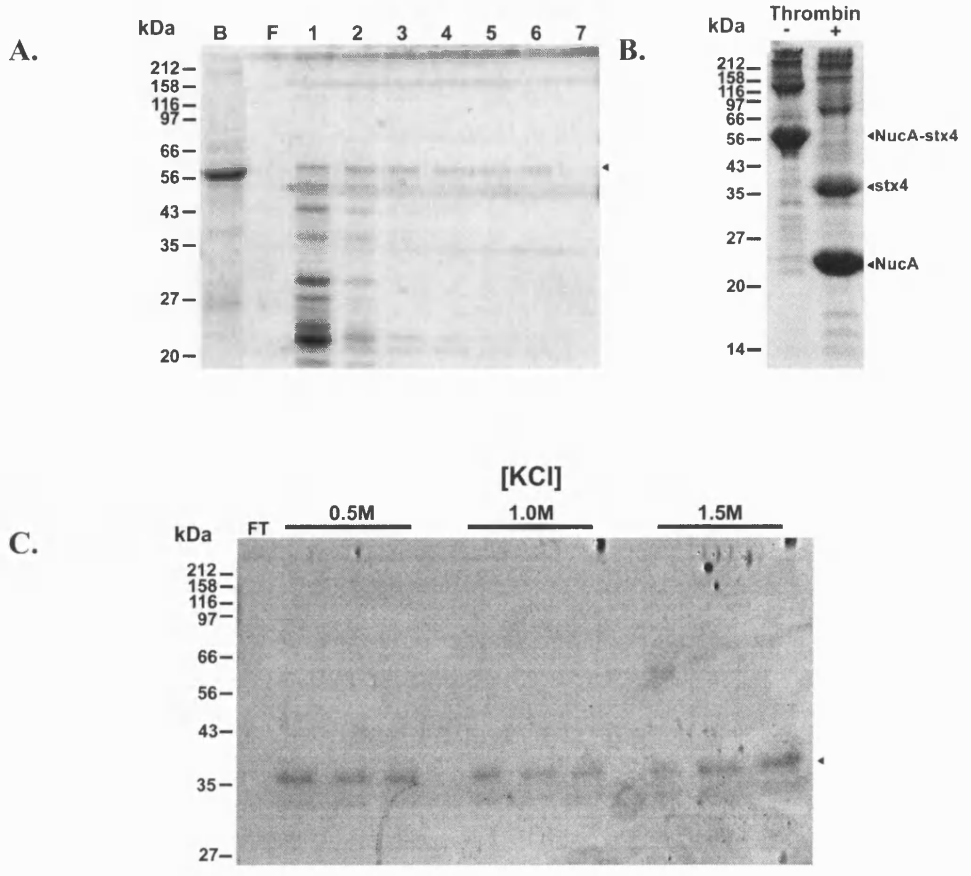

Figure 5.4. Purification of NucA-syntaxin4. A. Inclusion bodies were solubilised and bound to Ni-NTA agarose. The following samples were run on SDS-PAGE and stained with coomassie blue: an aliquot of the agarose beads boiled in sample buffer (B), flow through from beads washed with IB buffer (F), successive fractions eluted with 500 mM imidazole in IB buffer (1-7). **B.** An inclusion body preparation was bound to Ni-NTA agarose, washed, then digested with thrombin. Lanes show proteins eluted from beads boiled in SDS-sample buffer. **C.** Proteins in the supernatant following digestion with thrombin. Proteins were washed off with increasing KCl concentrations in 25 mM phosphate buffer pH 7, 250 mM NaCl, 1% n-octylglucoside.

Solubilised inclusion bodies were bound to Ni-NTA agarose in an attempt to purify the protein further. However the protein did not elute from the agarose in buffer containing 500 mM imidazole (Figure 5.4A). Thrombin digestion showed that the syntaxin4 moiety adhered to Ni-NTA agarose even when the NucA moiety that contained the His-tag had been cleaved away (Figure 5.4.B). Syntaxin4 eluted from the Ni-NTA agarose at low concentrations in a buffer containing large amounts of KCl (Figure 5.4C). In a typical experiment, 1 mg of syntaxin4 was recovered from each l of culture by this method.

In the interest of maximising yield and concentration of syntaxin4, the washed and solubilised inclusion body fraction was used in subsequent reconstitution experiments.

5.2.1.2. Expression and purification of SNAP23

SNAP23 was expresed as a fusion with glutathione-S-transferase (GST). GST is useful as a fusion protein because it aids high level expression in bacteria, increases the solubility of fusion proteins, and can be purified on immobilized glutathione (Smith and Johnson, 1988). The plasmid pGEX-SNAP23 was designed to express SNAP23 with an amino terminal thrombin-cleavable GST tag (Table 5.1). Cells transformed with this plasmid expressed around 12 mg of soluble GST-SNAP23 per l of culture (Section 2.5.3.). This could be purified on glutathione-sepharose and recovered in a total volume of 4 ml (Figure 5.5). This was equivalent to 5 mg of SNAP23 per l of cultured cells.

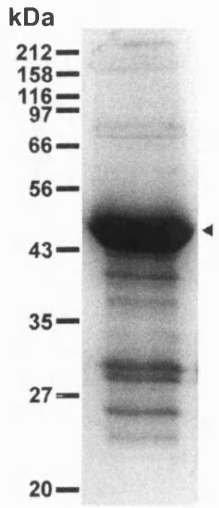

Figure 5.5. Purified GST-SNAP23. Lysates from cells expressing GST-SNAP23 were bound to glutathione sepharose, washed in 50 mM Tris buffer pH 8 containing 500 mM NaCl, 10 mM DTT. Bound proteins were eluted in 50 mM borate buffer pH 9, 500 mM NaCl, 10 mM DTT, 20 mM glutathione. Eluted proteins were analysed by SDS-PAGE and coomassie staining. GST-SNAP23 ran at the predicted molecular weight of 50 kDa.

5.2.1.3 Reconstitution of syntaxin4 into liposomes

Liposomes were prepared by dissolving lipids in a detergent solution containing NucA-syntaxin4, followed by rapid dilution of the detergent below it critical micellar concentration (CMC), as described in Section 2.13.1. Liposomes were harvested by density gradient centrifugation. Following centrifugation, liposomes were visible as a closely spaced doublet of faint white bands above the 30% Optiprep layer. They were recovered by careful pipetting of the different layers, which were then analysed by SDS-PAGE. The NucA-syntaxin4 concentrated in the two white bands on the gradient. No bands other than NucA-syntaxin4 were detectable on the gel, indicating that the lipids had effectively partitioned the NucA-

syntaxin4 from the other proteins in the inclusion bodies (Figure 5.6A). The NucA-syntaxin4 containing layers were pooled, making a total of 550 µl of NucA-syntaxin4 at a concentration of 3 mg/ml, equivalent to 2 mg/ml of syntaxin4. This accounted for >90% of the syntaxin4 that was initially mixed with the lipids. Thrombin digestion revealed that 75% of NucA- syntaxin4 reconstituted with the cytosolic domain of syntaxin facing outward, in the 'correct' orientation for the fusion experiments (Figure 5.6B).

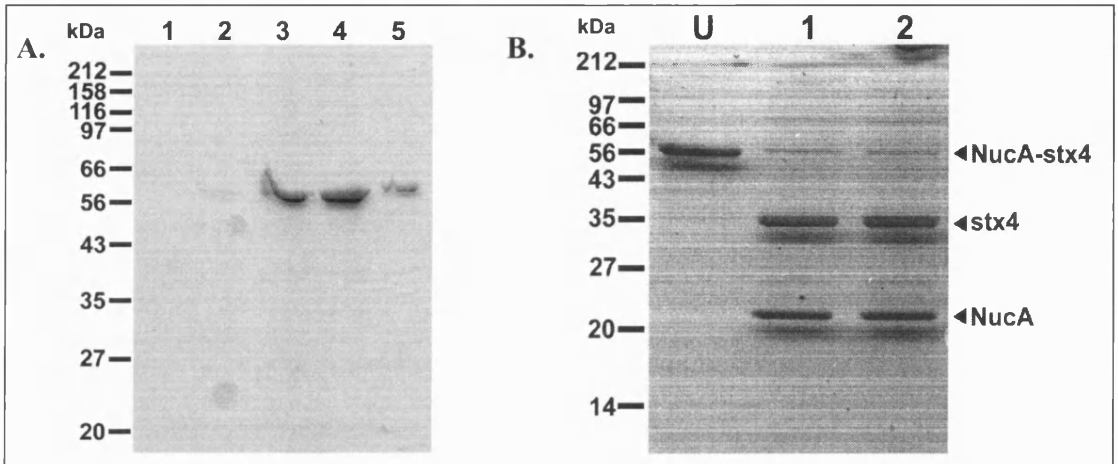

Figure 5.6. NucA-syntaxin4 reconstituted into liposomes. A. Liposomes were separated from unreconstituted proteins by flotation on a Optiprep step gradient. Samples were taken from various points on the gradient and analysed by SDS-PAGE and coomassie staining. Samples are labeled 1 to 5, with 1 being the bottom layer and 5 being the top of the gradient. **B.** 200 µl of NucA-syntaxin4 containing liposomes were digested with thrombin. Undigested liposomes (U) were run on SDS-PAGE alongside those incubated with 1 or 2 units of thrombin for 2 hours at room temperature. Note the volume of digested liposomes run on the gel was double that of the undigested liposomes.

5.2.1.4. Reconstitution of t-SNARES into liposomes

In order to form liposomes containing a t-SNARE complex, a second preparation was made, substituting a 2 mg/ml solution of GST-SNAP23 for detergent-free buffer at the stage where the lipid solution was diluted to form liposomes (Section 2.13.1).

The resulting liposomes were concentrated by gradient centrifugation and contained both NucA-syntaxin4 and GST-SNAP23 (Figure 5.7B). The molar ratio of SNAP23:syntaxin4 on the liposomes was estimated at approximately 1:5 by comparison of intensity of staining by coomassie blue. This preparation is not likely to be useful for reconstitution of fusion, as syntaxin4 is likely to compete with the syntaxin4/SNAP23 complex for binding to VAMP2. The interaction between SNAP23 and the cytosolic domain of syntaxin4 has an experimentally determined dissociation constant of 0.76 μM (Foster *et al.*, 1998). According to this figure more than 90% of syntaxin would be expected to be in a complex with SNAP23 in this experiment. Complexes were therefore not formed efficiently by this method.

5.2.1.5. Formation of t-SNARE complex on glutathione-sepharose

A second approach to forming the t-SNARE complex involved incubating 4 mg of GST-SNAP23 that had been pre-bound to 0.5 ml glutathione-sepharose with 3.6 mg of NucA-syntaxin4 inclusion body preparation containing detergent in 2 ml of IB buffer (Section 2.13.2.). The proteins were eluted with buffer containing glutathione. A small proportion of NucA-syntaxin4 co-eluted with GST-SNAP23. A sample of the glutathione sepharose was also boiled in SDS sample buffer following elution and analysed by SDS-PAGE. This showed that most of the NucA-syntaxin4 was still bound to the resin (Figure 5.7A).

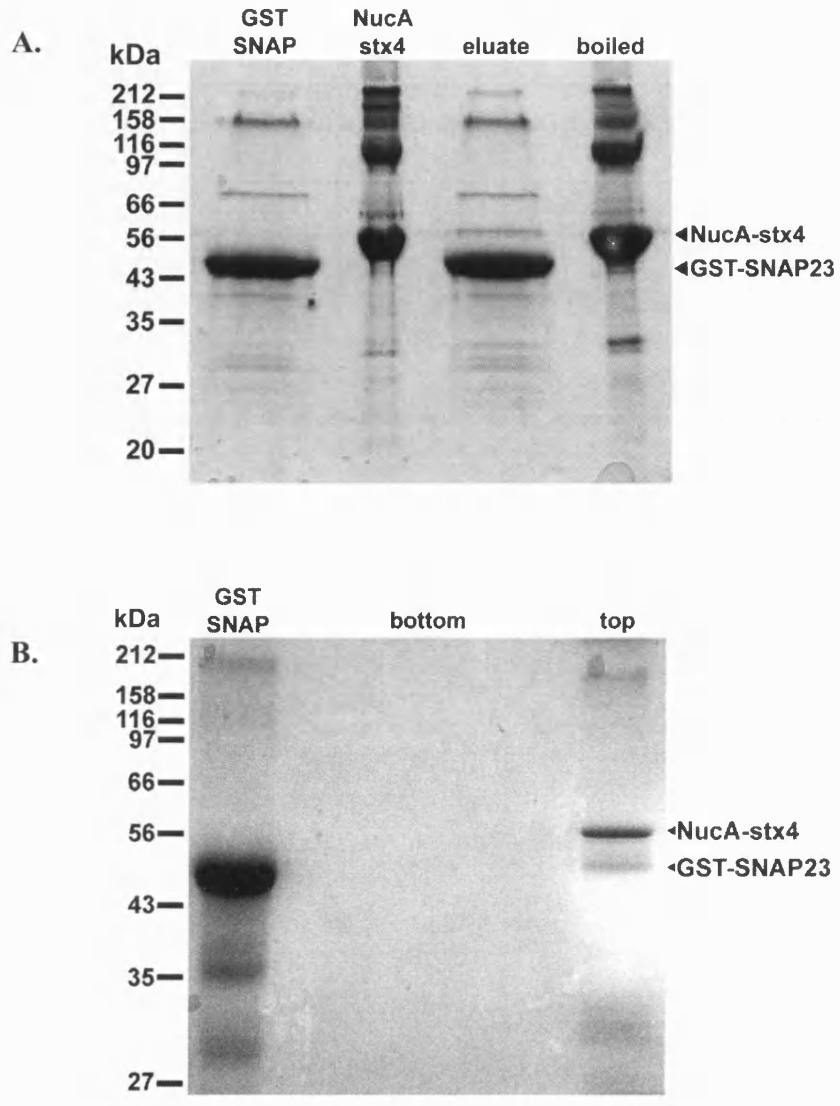

Figure 5.7. t-SNARE complex assembly. A. NucA-syntaxin4 (NucA stx) was incubated with immobilized GST-SNAP23 (GST SNAP) on glutathione-sepharose. Bound proteins were eluted with glutathione (eluate). Proteins remaining on the beads were eluted by boiling in SDS sample buffer (boiled). **B.** GST-SNAP23 (GST SNAP) was incubated overnight at 4°C with syntaxin4 following reconstitution into liposomes. Following dialysis, liposomes were isolated by flotation on an Optiprep step gradient. Samples were taken from the top and bottom of the gradient and separated by SDS-PAGE and stained with coomassie blue.

5.2.1.6. Co-expression of adipocyte t-SNAREs in bacteria

Due to the low recovery of t-SNARE complexes using the approaches described above, the strategy was changed to one where the adipocyte t-SNAREs were co-expressed in bacteria. GST-SNAP23 was co-expressed with untagged syntaxin4 or NucA-syntaxin4 from the plasmids pDRSN1-tSNAREs and pDRSN1-tSNAREs(NucA), described in Section 2.4.1.4. These plasmids were derived from pGEX-SNAP23, and code for bacterial expression of GST-SNAP23 and syntaxin4 or NucA-syntaxin4 under the control of a single *tac* promoter (Table 5.1).

Inclusion body preparations were made from bacterial cultures transformed with either plasmid as described in Section 2.5.4. These were analysed by SDS-PAGE and Coomassie staining. A number of protein bands in the solubilised inclusion bodies were common to both sets of expressed proteins, implying that they were either bacterial proteins, degradation products or truncated products of GST-SNAP23 (Figure 5.8A). Each plasmid however also produced a unique band at the predicted molecular weight of the translated products. Inclusion body preparations from cells transformed with pGEX-tSNAREs contained an estimated 10 mg of GST-SNAP23 and 1.5 mg of syntaxin from 1 l of culture. Cells transformed with pGEX-tSNAREs(NucA) produced around 15 mg of GST-SNAP23 and 10 mg of NucA-syntaxin4 in inclusion bodies from 1 l of culture.

5.2.1.7. Reconstitution of coexpressed t-SNAREs into liposomes

Solubilised inclusion bodies from cells transformed with pGEX-tSNAREs were used to form liposomes by dilution of lipids as described for NucA-syntaxin4 liposomes. Following flotation on an Optiprep gradient, GST-SNAP23 and syntaxin4 were detected at the top of the gradient by coomassie staining and western blot,

coinciding with the visible band of lipid on the gradient (Figure 5.8B). Syntaxin4 concentration in the final liposome fraction was estimated at 0.025 mg/ml. These liposomes were used for the fusion assays described below.

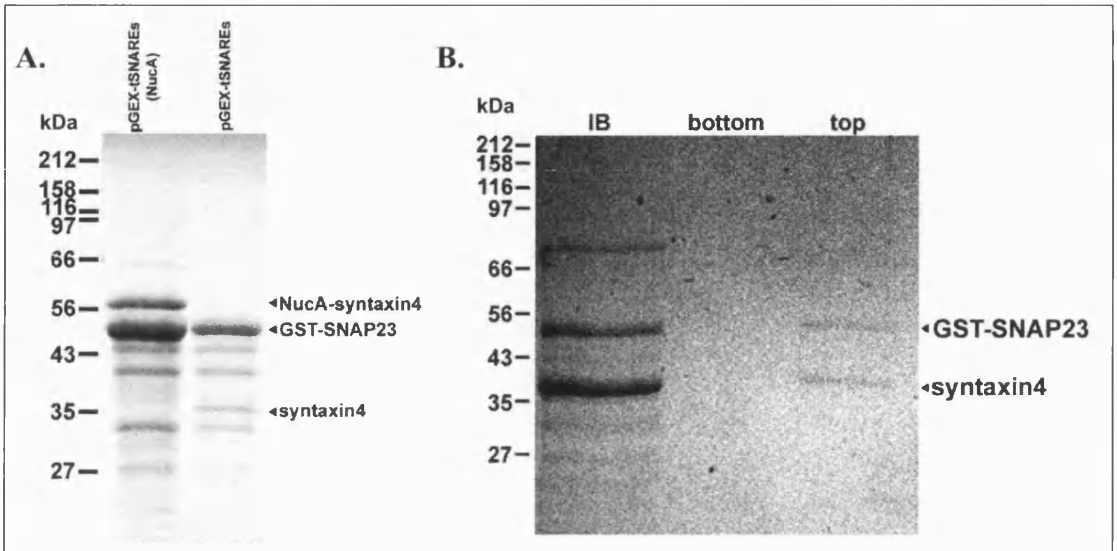

Figure 5.8 Coexpression and reconstitution of recombinant t-SNAREs. A. Inclusion bodies from Rosetta(DE3)pLysS cells transfected with the indicated plasmids were solubilised in 6 M guanidine hydrochloride, 10 mM DTT, 1% n-octylglucoside, run on SDS-PAGE and coomassie stained. **B.** Solubilised inclusion bodies from bacteria coexpressing GST-SNAP23 and syntaxin4 were mixed with lipid followed by rapid dilution, dialysis and flotation in an Optiprep gradient to form liposomes as described in the text. Samples of the protein mixture that was initially mixed with the lipids (IB), the bottom of the gradient (bottom), and the top of the gradient (top) were run on SDS-PAGE and stained with coomassie blue. Arrowheads indicate the expected migration of the recombinant proteins.

5.2.2. Reconstitution of VAMP2 into liposomes

5.2.2.1. Expression of VAMP2 in bacteria

VAMP2 was cloned by PCR from a rat adipocyte cDNA library made by Dr Paul Whitley (Whitley *et al.*, 2003), as described in Section 2.4.2.1. Sequence analysis showed that the cloned VAMP2 sequence was identical to the rat VAMP2 mRNA sequence (M24105). This coding sequence was ligated into pET28a to form pET28a-VAMP2 (Section 2.4.2.2.). This plasmid was used to express VAMP2 with a carboxy-terminal his-tag on the lumenal side of the membrane, ensuring minimal interference with interactions of the cytosolic domain.

Protein expressed by *E. coli* transformed with this plasmid was bound to Ni-NTA agarose as described in Section 2.5.5. VAMP2 was not detected in imidazole elutions from the resin (Figure 5.9A). The protein eluted from the resin at pH 4.8 on a pH gradient (Figure 5.9B), suggesting that the protein was eluting as an homo-oligomer, consistent with previous reports (Laage and Langosch, 1997). A total of ~0.5 mg of VAMP2-his was eluted by the pH gradient in a total volume of 20 ml from an initial culture volume of 2 l.

In order to increase the yield of VAMP2, the protein was also expressed as a NucA fusion from the plasmid pDRSN1-VAMP2 (Table 5.1), that was constructed as described in Section 2.4.2.3. *E. coli* transformed with this plasmid expressed ~16 mg of NucA-VAMP2 per l of culture, all of which was recovered in the inclusion body fraction (Figure 5.10A). The protein bound to Ni-NTA and could be recovered by elution with imidazole (Section 2.5.6., Figure 5.10B). Alternatively, digestion with thrombin released VAMP2 into the bead supernatant. Purity of this VAMP2 was estimated at > 90% by coomassie staining (Figure 5.10C). Typically, 1 l of culture yielded ~6 mg of VAMP2 in a final volume of 1 ml by digestion from Ni-NTA

agarose. This VAMP2 preparation was used in the reconstitution experiments described below.

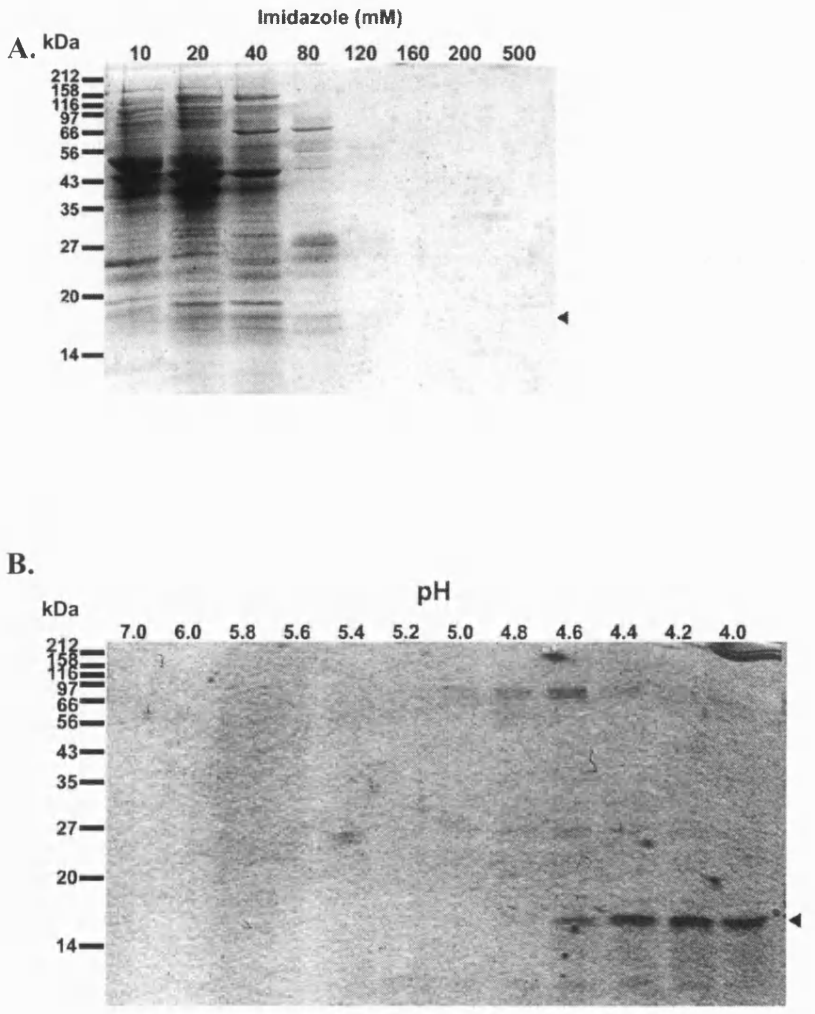

Figure 5.9. Expression and purification of VAMP2-his. Lysates from bacteria expressing VAMP2-his were incubated with Ni-NTA agarose. Bound proteins were eluted with **A.** increasing concentrations of imidazole, or **B.** a gradient of phosphate and phosphate-citrate buffers of decreasing pH. Fractions were collected and analysed by SDS-PAGE and coomassie staining.

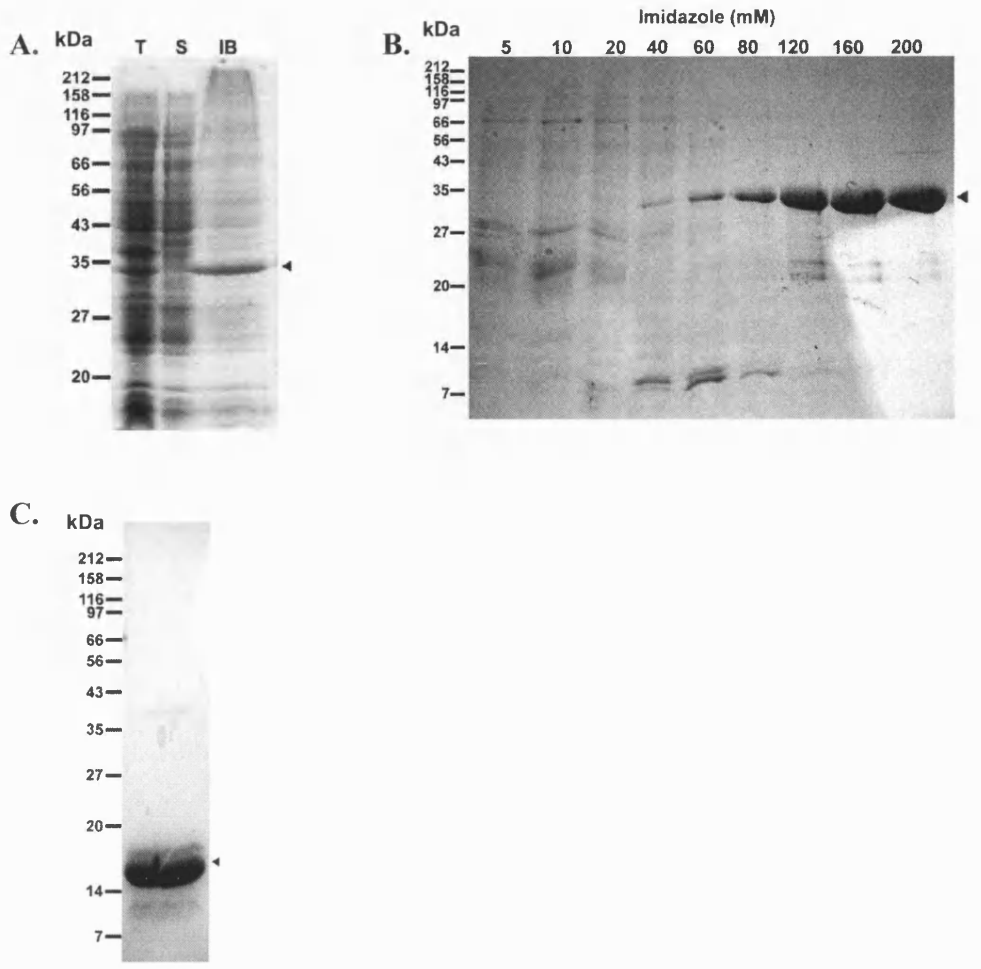

Figure 5.10. Expression and purification of NucA-VAMP2. A. Total lysates (T) from cells expressing VAMP2 were run on SDS-PAGE alongside proteins soluble in 50 mM phosphate buffer pH 8 (S) and inclusion bodies solubilised in 25 mM phosphate buffer, 1.5 M NaCl, 1% n-octylglucoside (IB). **B.** Solubilised inclusion bodies were bound to Ni-NTA agarose and bound proteins were eluted in IB buffer containing increasing concentrations of imidazole. **C.** Supernatant from beads following thrombin digestion. Arrowheads indicate expected positions of NucA-VAMP2 in **A** and **B**, and of VAMP2 in **C**.

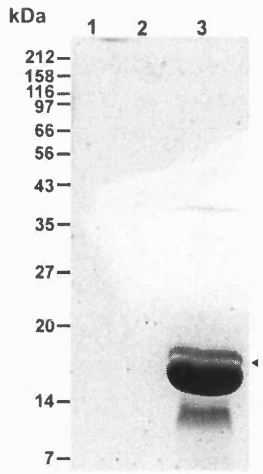

Figure 5.11. VAMP2 reconstituted into liposomes. VAMP2 purified by thrombin digestion of NucA-VAMP2 on Ni-NTA agarose was mixed with dried lipids in detergent solution. Liposomes were prepared by rapid dilution and isolated by flotation on an Optiprep step density gradient. Samples were taken from points on the gradient. Fractions are numbered 1-3 where 1 was the lowest layer in the gradient.

5.2.2.2. Reconstitution of VAMP2 into liposomes

Fluorescent liposomes containing VAMP2 were made by solubilizing the fluorescently labeled lipids in the VAMP2 solution followed by rapid dilution of the detergent below its CMC as described in Section 2.13.4. Liposomes were concentrated by centrifugation on a density gradient. All VAMP2 co-migrated with the lipid band near the top of the gradient (Figure 5.11). The reconstituted protein was recovered in a volume of 250 μl, containing 0.6 mg of VAMP2. These liposomes were used in subsequent trial fusion assays.

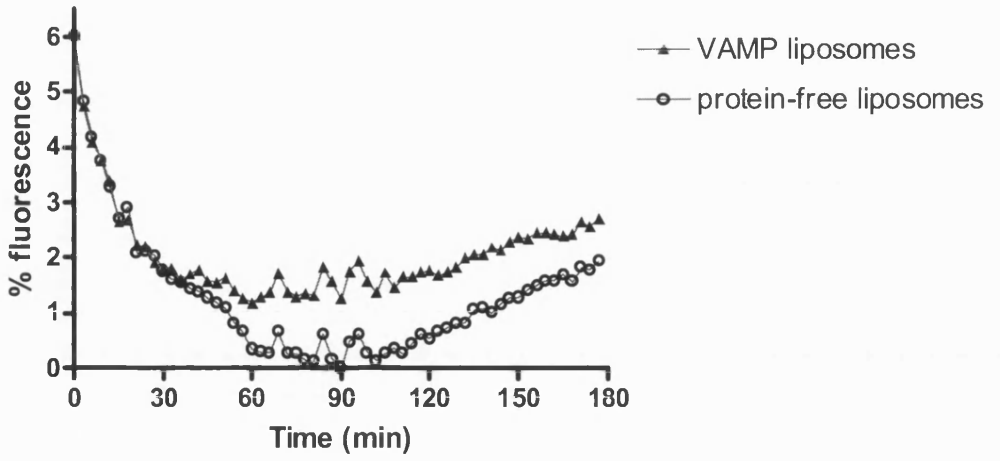

Figure 5.12. Fusion between liposomes containing adipocyte t-SNAREs and VAMP2. Liposomes containing VAMP2 and a mixture of fluorescent and quenching lipids were incubated with liposomes containing syntaxin4 and SNAP23 for 16 h at 4°C. A second experiment was set up with liposomes lacking the VAMP2. NBD fluorescence was monitored at 37°C for 3 h. Following measurements, TritonX-100 was added to 0.4% (w/v) and fluorescence was measured again. The lowest reading was set as a baseline and fluorescence was expressed as a percentage of the value following addition of TritonX-100. The graph shown is representative of results from two separate experiments.

5.2.3. Fusion Assays

t-SNARE liposomes were mixed with either VAMP-containing or protein-free fluorescent liposomes and incubated for 16 h at 4°C to allow liposomes to dock together. Fusion assays were carried out at 37°C as described in Section 2.13.5. Fluorescence was measured at 535 nm with the excitation filter set to 485 nm over a period of 3 h and plotted on a graph (Figure 5.12). There was a slow initial decrease in fluorescence up to about 90 min in both VAMP2 and protein-free donor liposome

wells. The fluorescence in VAMP2-containing wells remained above that of protein-free wells throughout the duration of the experiment, although from around 100 min to the end of the experiment, the rate of increase of the reading from the protein-free donor liposome was greater than that from the VAMP liposomes. This was also true of a second experiment carried out with the same t-SNARE liposomes and a fresh preparation of donor liposomes two days after the first experiment.

5.3. Discussion

This chapter describes the expression of full length syntaxin4, SNAP23 and VAMP2 in bacteria for use in an *in vitro* fusion assay. Bacterial expression of SNAP23 and VAMP2 have been described previously (Rea *et al.*, 1998; Weber *et al.*, 1998), but bacterial expression and purification of full length syntaxin4 has not been demonstrated before. Syntaxin4-his was expressed at comparatively low levels and was difficult to purify as it adhered to Ni-NTA agarose even under conditions of high imidazole and low pH (Figure 5.2). NucA-syntaxin4 was expressed at much higher levels and could be isolated from inclusion bodies and by reconstitution into artificial liposomes (Figure 5.3, Figure 5.6). Incubation of NucA-syntaxin4 with GST-SNAP23 produced smaller amounts of complex than that predicted by the k_d of the cytosolic domains (Foster *et al.*, 1998). This may be because of interference by the fusion proteins, or because of incorrect folding of the polypeptide chains. Alternatively, complex assembly may be hindered when syntaxin4 is associated with a lipid bilayer.

When syntaxin4 and GST-SNAP23 were coexpressed in bacteria the proteins sequestered into inclusion bodies, which were soluble in solution containing 6 M guanidine (Figure 5.8A). Following buffer exchange, approximately equimolar amounts of syntaxin4 and SNAP23 were successfully reconstituted into liposomes

(Figure 5.8B). A great deal of precipitation of protein was seen following buffer exchange, suggesting that the yield of soluble protein might be increased using a more sophisticated refolding strategy. Examples of suitable approaches to try include solubilisation followed by removal of denaturants and chaotropes such as urea or guanidine, solubilisation at high or low pH followed by gradual neutralisation, or chaperone-mediated refolding.

VAMP2 was expressed with a carboxy terminal his-tag and as a NucleaseA fusion protein. Once again the NucleaseA fusion protein was expressed at higher levels than the his-tagged version (Figure 5.9, Figure 5.10). VAMP2 could be purified by binding NucA-VAMP2 to Ni-NTA agarose and cleaving the fusion protein with thrombin. Purified VAMP2 successfully reconstituted into liposomes (Figure 5.11).

When t-SNARE liposomes where mixed with VAMP liposomes containing fluorescent and quenching lipids, there was an initial decrease in fluorescence (Figure 5.12). This was likely to be a result of the increase in temperature when the 96-well plate was transferred from incubation at 4°C to the chamber of the plate reader at 37°C, as NBD fluorescence is sensitive to temperature changes (Chapman *et al.*, 1995). The time taken for the temperature to equilibrate might be reduced by not preincubating the plates at 4°C. The preincubation step was used to maximise the initial signal, by allowing the liposomes to dock, ensuring that fusion commenced immediately on the temperature change (Weber *et al.*, 1998). However, even when the chamber in the fluorescent plate reader was pre-warmed, it took more than 30 min after the 96-well plate was inserted for the chamber temperature to return to 37°C.

Bearing this limitation in mind, wells containing donor liposomes with VAMP2 still showed higher fluorescence readings than protein-free donor liposomes as the experiments progressed, even though initial fluorescence was the same.

However, after ~100 min of incubation at 37°C, the rate of increase in fluorescence was greater with the protein-free vesicles. Though a specific SNARE-dependent effect cannot be discounted, it is possible that the initial increased fluorescence is simply an exaggeration of the background rate of increase due to the destabilising presence of large amounts of proteins in the donor liposomes. The existence of specific SNARE-dependent effects could be established by experiments with VAMP-cleaving toxins or by substituting VAMP with other transmembrane proteins.

The kinetics of fusion events mediated by the adipocyte SNAREs are unknown. Synaptic vesicle fusion occurs rapidly *in vivo*, and individual fusion events occur on a similar timescale (<100 ms) when VAMP is reconstituted into liposomes and t-SNAREs are reconstituted into a planar lipid bilayer (Fix *et al.*, 2004). This reaction is slower when both sets of SNAREs are in liposomes (Parlati *et al.*, 1999). The geometries of the lipid bilayers involved therefore affect the kinetics of reconstituted fusion. The appearance of GLUT4 on the plasma membrane of adipocytes follows soon after GLUT4 translocation, and has a $t_{1/2}$ of several min (Satoh *et al.*, 1993). The use of a temperature-sensitive Munc18c mutant however has shown that trafficking of GLUT4 to the plasma membrane and not membrane fusion is rate-limiting to the appearance of GLUT4 on the cell surface (Thurmond and Pessin, 2000). The rate at which fusion between liposomes containing adipocyte SNAREs could occur is therefore unknown. The combination of the liposome geometry and the low density of t-SNAREs in the acceptor liposomes used in the assay described above may slow fusion to the point where it is overtaken by the background increase in fluorescence in these assays.

Previous liposome-based fusion studies have used pre-formed binary t-SNARE complexes on one of the liposome populations. However, recent reports have

questioned the requirement for SNAP25 in this kind of assay. Reconstituted VAMP liposomes and synaptic vesicles are able to fuse with planar lipid bilayers containing only syntaxin1 (Woodbury and Rognlien, 2000; Bowen *et al.*, 2004). Furthermore, knockout mice lacking SNAP25 show normal vesicle docking and constitutive fusion, although stimulus dependent neurotransmitter release was abolished (Washbourne *et al.*, 2002). SNAP23 has been shown to function in modulating the calcium sensitivity of docking and fusion of secretory granules (Chieregatti *et al.*, 2004), and may therefore be involved in regulating fusion rather than directly participating in catalyzing fusion as previously thought. It may therefore be possible to reduce the assay further to one with VAMP2 donor liposomes and acceptor liposomes containing only syntaxin4.

The fusion reconstituted between VAMP liposomes and t-SNAREs in a planar bilayer may also be sensitive to divalent ion concentration (Fix *et al.*, 2004), although this effect was not duplicated in other similar studies (Bowen *et al.*, 2004); (Tucker *et al.*, 2004). In one study, high calcium concentrations were able to induce fusion between liposomes in the total absence of SNARE proteins (Jeremic *et al.*, 2004). Therefore fusion of the liposomes in the assay described here may require calcium ions. This would be consistent with the reported requirement for calcium at a late docking stage or fusion of GLUT4 vesicles with the plasma membrane in 3T3-L1 adipocytes (Whitehead *et al.*, 2001).

In summary, syntaxin4, SNAP23 and VAMP2 were expressed in bacteria and reconstituted into liposomes. Fusion assays based on these reconstituted proteins were not conclusive and may have been limited by the concentration of syntaxin4-SNAP23 complexes in acceptor liposomes, among other factors. Nevertheless, the work

described here provides material on which future studies on membrane fusion mediated by adipocyte SNAREs can be based.

Chapter 6 – Conclusions

This thesis set out to investigate the events at the plasma membrane that follow insulin stimulation of adipocytes and the roles played by SNAREs and other proteins involved in membrane fusion.

The experiments on activation of the p38 MAP kinase pathway in Chapter 3 showed a relatively small stimulation of p38 MAP kinase phosphorylation at the regulatory site by insulin (35% above basal levels), and no insulin effect at all on phosphorylation of the downstream molecule CREB. This contrasts with the more than two-fold activation of p38 MAP kinase seen in 3T3-L1 adipocytes and cultured muscle cells (Konrad *et al.*, 2001), and the complete lack of activation of p38 MAP kinase by insulin seen in human adipocytes (Carlson *et al.*, 2003). The marginal insulin stimulated increase in p38 MAP kinase activation seen in the rat adipocyte experiments may not be consistent with the large effect that it is reported to have on GLUT4 transporter activity.

The experiments with the p38 MAP kinase inhibitor SB203580 showed that insulin stimulated glucose uptake and labelling of cell surface GLUT4 were inhibited to similar degrees. This initially suggested that SB203580 was inhibiting GLUT4 exocytosis, consistent with the reported effects of the inhibitor on the Akt pathway. However, only a small activation of Akt is required for the full insulin effect on GLUT4 exocytosis (Whitehead *et al.*, 2001), meaning that it is unlikely that this small effect of SB203580 on Akt activation would noticeably affect GLUT4 exocytosis. Furthermore it has been shown that treatment with 10 μM SB203580 does not affect insulin stimulated GLUT4 exocytosis (Somwar *et al.*, 2002). Subsequent experiments have shown that SB203580 acts as a competitive inhibitor of glucose transport on the

intracellular surface of GLUT4 (Ribe *et al.*, 2005). Furthermore, a recent report demonstrated that treatment with SB203580 reduced affinity labelling of cell surface GLUT4 independently of insulin stimulated GLUT4 exocytosis (Bazuine *et al.*, 2005). These later experiments suggest that SB203580 binds to the intracellular face of GLUT4, displacing the hexose substrate from the intracellular binding site, and also prevents binding of the hexose moiety of the affinity label to the extracellular binding site on GLUT4. The discrepancy between GLUT4 labelling and exocytosis might have been detected if the modified GLUT4 exocytosis assay described in Section 3.2.2. had been used in the SB203580 experiments instead of the simpler affinity labelling assay.

The results of these experiments did not rule out a role for p38 MAP kinase in insulin stimulated GLUT4 translocation. They did however imply that SB203580 is not a good tool for studying p38 MAP kinase involvement in insulin stimulated glucose transport, because it interfered directly with GLUT4 function. The SB203580 evidence from previous studies cannot now be viewed as supporting the case for p38 MAP kinase activation of GLUT4 transport activity.

It has previously been shown that wortmannin was able to block insulin stimulated glucose uptake at lower concentrations than were needed to block GLUT4 vesicle translocation and GLUT4 vesicle fusion with the plasma membrane in 3T3-L1 adipocytes (Hausdorff *et al.*, 1999; Somwar *et al.*, 2001b). The inhibition experiments with wortmannin reported in Chapter 3 demonstrate that this was not the case in rat adipocytes. Instead they showed that at low wortmannin concentrations, insulin stimulated GLUT4 vesicle fusion and glucose uptake were blocked independently of GLUT4 vesicle translocation. This implied that there was a high affinity wortmannin target downstream of GLUT4 vesicle trafficking to the plasma membrane, but

upstream of GLUT4 incorporation into the plasma membrane. This is in agreement with recently reported studies that have shown that 1) PI 3-kinase inhibition blocks a late pre-fusion step in 3T3-L1 adipocytes (Bose *et al.*, 2004), 2) a late pre-fusion step is blocked under conditions that inhibit Akt activity (van Dam *et al.*, 2005), 3) that the function of synip, a protein that regulates the SNARE complex is regulated by Akt (Yamada *et al.*, 2005), 4) and that a PI 3-kinase dependent block at a late pre-fusion step is dependent on Munc18c, also a SNARE complex regulator (Kanda *et al.*, 2005). These reports give the membrane fusion machinery a major role in insulin stimulation of glucose uptake.

The quantitation of syntaxin4, SNAP23, VAMP2 and Munc18c in rat adipocytes (Chapter 4) was intended to provide a quantitative context for interpreting data on the membrane fusion machinery in these cells. The quantitative data suggested two key points. The first was that syntaxin4 outnumbered Munc 18c on intracellular membranes by a factor of four. This meant that it was unlikely that Munc18c was the main binding partner supporting syntaxin4 trafficking to the plasma membrane, as had been suggested by previous studies (Takuma *et al.*, 2002). The second point was that in the plasma membrane, SNAP23 was present at more than four-fold the levels of syntaxin4. This suggests that if the excess SNAP23 is not to compete with syntaxin4 by forming 'unproductive' SNARE complexes, SNAP23 availability must be tightly regulated. This was supported by the 20-fold excess of SNAP23 over syntaxin4 in SDS-resistant complexes that may represent a segregated state of SNAP23 that is unavailable for SNARE binding.

In a study on plasma membrane lawns made from PC12 cells, syntaxin1 was concentrated in numerous clusters of approximately 200 nm in size. Docking and fusion of secretory vesicles occurred within these clusters. SNAP25 was concentrated

in a different set of clusters that partially overlapped with the syntaxin1 clusters, and its distribution was more diffuse than that of syntaxin1. The majority of syntaxin1 clusters contained SNAP25, but there were many SNAP25 clusters that did not contain syntaxin1 (Lang *et al.*, 2001). This distribution may represent segregation of the excess SNAP25, as SNAP25 was expressed in 5 to 6-fold excess over syntaxin1 in these cells (Xiao *et al.*, 2004). It would be instructive to see if this kind of spatial segregation occurs in lawns prepared from adipocyte plasma membranes, and whether the 'segregated' SNAP23 pool colocalises with other proteins, such as the cytoskeletal proteins that are reported to bind to SNAP23 (Foster *et al.*, 1999; Diefenbach *et al.*, 2002).

Unfixed plasma membrane lawns from PC12 cells also support SNARE complex formation and exocytosis of secretory vesicles (Lang *et al.*, 2001; Holroyd *et al.*, 2002; Lang *et al.*, 2002). Similar membrane preparations from adipocytes could be used in combination with soluble recombinant VAMP2, purified GLUT4 vesicles, or recombinant VAMP2 reconstituted into liposomes to monitor SNARE complex formation and localisation of vesicle fusion. The usefulness of such a system could be extended by adding signalling molecules such as Akt or inhibitors such as wortmannin, for example. This type of assay, has a lot of potential for elucidating the regulation of the steps leading to membrane fusion.

This plasma membrane lawn based assay system would be an intermediate between observations of membrane fusion events in cells, and the entirely artificial fusion assay system that is described in Chapter 5. In the cell-free system, mixing of liposomes with reconstituted v- and t-SNAREs should produce a signal indicating that lipid mixing, or fusion has taken place. This assay is intended to enable studies of the SNAREs in isolation, or in combination with other proteins such as Munc18c and

synip. Again the system could be manipulated by adding external factors such as calcium ions, signalling proteins, inhibitors or cytosol. This type of 'minimal machinery' assay has been used to study the function of synaptotagmin in sensitizing SNARE-mediated fusion to calcium, the function of NSF/αSNAP and the function of Munc18 in synaptic SNARE-mediated fusion (Weber *et al.*, 2000; Tucker *et al.*, 2004; Scott *et al.*, 2004). The signal in the liposome assays reported in this thesis was very close to background. This was likely to be because of the low concentration of t-SNAREs in the acceptor liposomes. Although syntaxin4 and SNAP23 could be expressed at high levels and isolated individually, difficulties arose when attempting to form a t-SNARE complex from co-expressed or individually expressed syntaxin4 and SNAP23, either in solution or on liposomes. This may have been due to faulty refolding of the proteins following isolation. As the proteins could be expressed at high levels and isolated, refolding strategies would be the logical next step to obtaining functional recombinant proteins.

In conclusion, this thesis has described treatments of intact cells with inhibitors of signalling pathways, quantitation of proteins in whole cells and subcellular fractions and a reductionist approach using an entirely non-cell based assay, with the unifying aim of dissecting the events and interactions that lead from insulin signalling to glucose uptake by means of fusion of GLUT4 vesicles with the plasma membrane. The results described here add to the evidence linking the PI 3-kinase signalling pathway to the regulation of GLUT4 vesicle fusion. Results of quantitation experiments indicate that Munc18c is unlikely to play a major role in intracellular syntaxin4 trafficking, and that SNAP23 availability for SNARE complex formation in the plasma membrane is likely to be highly regulated. SNAP23

availability is therefore a potential point of regulation of GLUT4 vesicle fusion by the insulin signalling pathway.

References

1. Alessi, D. R. (2001). Discovery of PDK1, one of the missing links in insulin signal transduction. Colworth Medal Lecture. Biochem. Soc. Trans. 29, 1-14.

2. Alessi, D. R., Andjelkovic, M., Caudwell, B., Cron, P., Morrice, N., Cohen, P., and Hemmings, B. A. (1996). Mechanism of activation of protein kinase B by insulin and IGF-1. EMBO J. 15, 6541-6551.

3. Alessi, D. R., James, S. R., Downes, C. P., Holmes, A. B., Gaffney, P. R., Reese, C. B., and Cohen, P. (1997). Characterization of a 3-phosphoinositide-dependent protein kinase which phosphorylates and activates protein kinase Balpha. Curr. Biol. 7, 261-269.

4. Anderson, K. E., Coadwell, J., Stephens, L. R., and Hawkins, P. T. (1998). Translocation of PDK-1 to the plasma membrane is important in allowing PDK-1 to activate protein kinase B. Curr. Biol. 8, 684-691.

5. Araki, E., Lipes, M. A., Patti, M. E., Bruning, J. C., Haag, B., III, Johnson, R. S., and Kahn, C. R. (1994). Alternative pathway of insulin signalling in mice with targeted disruption of the IRS-1 gene. Nature 372, 186-190.

6. Araki, S., Tamori, Y., Kawanishi, M., Shinoda, H., Masugi, J., Mori, H., Niki, T., Okazawa, H., Kubota, T., and Kasuga, M. (1997). Inhibition of the binding of SNAP-23 to syntaxin 4 by Munc18c. Biochem. Biophys. Res. Commun. 234, 257-262.

7. Arbuckle, M. I., Kane, S., Porter, L. M., Seatter, M. J., and Gould, G. W. (1996). Structure-function analysis of liver-type (GLUT2) and brain-type (GLUT3) glucose transporters: expression of chimeric transporters in Xenopus oocytes suggests an important role for putative transmembrane helix 7 in determining substrate selectivity. Biochemistry 35, 16519-16527.

8. Avery, J., Ellis, D. J., Lang, T., Holroyd, P., Riedel, D., Henderson, R. M., Edwardson, J. M., and Jahn, R. (2000). A cell-free system for regulated exocytosis in PC12 cells. J. Cell Biol. 148, 317-324.

9. Baldwin, J. M., Gorga, J. C., and Lienhard, G. E. (1981). The monosaccharide transporter of the human erythrocyte. Transport activity upon reconstitution. J. Biol. Chem. 256, 3685-3689.

10. Bandyopadhyay, G., Standaert, M. L., Kikkawa, U., Ono, Y., Moscat, J., and Farese, R. V. (1999a). Effects of transiently expressed atypical (zeta, lambda), conventional (alpha, beta) and novel (delta, epsilon) protein kinase C isoforms on insulin-stimulated translocation of epitope-tagged GLUT4 glucose transporters in rat adipocytes: specific interchangeable effects of protein kinases C-zeta and C-lambda. Biochem. J. 337, 461-470.

11. Bandyopadhyay, G., Standaert, M. L., Sajan, M. P., Karnitz, L. M., Cong, L., Quon, M. J., and Farese, R. V. (1999b). Dependence of insulin-stimulated glucose transporter 4 translocation on 3-phosphoinositide-dependent protein

kinase-1 and its target Threonine-410 in the activation loop of protein kinase C-{zeta}. Mol. Endocrinol. 13, 1766-1772.

12. Bandyopadhyay, G., Standaert, M. L., Zhao, L., Yu, B., Avignon, A., Galloway, L., Karnam, P., Moscat, J., and Farese, R. V. (1997). Activation of protein kinase C (alpha, beta, and zeta) by insulin in 3T3/L1 cells. Transfection studies suggest a role for PKC-zeta in glucose transport. J. Biol. Chem. 272, 2551-2558.

13. Banerjee, A., Kowalchyk, J. A., DasGupta, B. R., and Martin, T. F. (1996). SNAP-25 is required for a late postdocking step in Ca2+-dependent exocytosis. J. Biol. Chem. 271, 20227-20230.

14. Barclay, J. W., Craig, T. J., Fisher, R. J., Ciufo, L. F., Evans, G. J., Morgan, A., and Burgoyne, R. D. (2003). Phosphorylation of Munc18 by protein kinase C regulates the kinetics of exocytosis. J. Biol. Chem. 278, 10538-10545.

15. Barnes, K., Ingram, J. C., Porras, O. H., Barros, L. F., Hudson, E. R., Fryer, L. G., Foufelle, F., Carling, D., Hardie, D. G., and Baldwin, S. A. (2002). Activation of GLUT1 by metabolic and osmotic stress: potential involvement of AMP-activated protein kinase (AMPK). J. Cell Sci. 115, 2433-2442.

16. Baumann, C. A., Ribon, V., Kanzaki, M., Thurmond, D. C., Mora, S., Shigematsu, S., Bickel, P. E., Pessin, J. E., and Saltiel, A. R. (2000). CAP defines a second signalling pathway required for insulin-stimulated glucose transport. Nature 407, 202-207.

17. Bazuine, M., Carlotti, F., Rabelink, M. J., Vellinga, J., Hoeben, R. C., and Maassen, J. A. (2005). The p38 mitogen-activated protein kinase inhibitor SB203580 reduces glucose turnover by the glucose transporter-4 of 3T3-L1 adipocytes in the insulin-stimulated state. Endocrinology 146, 1818-1824.

18. Berfield, A. K., Raugi, G. J., and Abrass, C. K. (1996). Insulin induces rapid and specific rearrangement of the cytoskeleton of rat mesangial cells in vitro. J. Histochem. Cytochem. 44, 91-101.

19. Bock, J. B., Matern, H. T., Peden, A. A., and Scheller, R. H. (2001). A genomic perspective on membrane compartment organization. Nature 409, 839-841.

20. Bose, A., Guilherme, A., Robida, S. I., Nicoloro, S. M., Zhou, Q. L., Jiang, Z. Y., Pomerleau, D. P., and Czech, M. P. (2002). Glucose transporter recycling in response to insulin is facilitated by myosin Myo1c. Nature 420, 821-824.

21. Bose, A., Robida, S., Furcinitti, P. S., Chawla, A., Fogarty, K., Corvera, S., and Czech, M. P. (2004). Unconventional myosin Myo1c promotes membrane fusion in a regulated exocytic pathway. Mol. Cell Biol. 24, 5447-5458.

22. Boulton, T. G., Yancopoulos, G. D., Gregory, J. S., Slaughter, C., Moomaw, C., Hsu, J., and Cobb, M. H. (1990). An insulin-stimulated protein kinase similar to yeast kinases involved in cell cycle control. Science 249, 64-67.

23. Bowen, M. E., Weninger, K., Brunger, A., and Chu, S. (2004). Single Molecule Observation of Liposome - Bilayer Fusion Thermally Induced by SNAREs. Biophys. J. 87, 3569-3584.

24. Brooks, C. C., Scherer, P. E., Cleveland, K., Whittemore, J. L., Lodish, H. F., and Cheatham, B. (2000). Pantophysin is a phosphoprotein component of adipocyte transport vesicles and associates with GLUT4-containing vesicles. J. Biol. Chem. 275, 2029-2036.

25. Bryant, N. J., Govers, R., and James, D. E. (2002). Regulated transport of the glucose transporter GLUT4. Nat. Rev. Mol. Cell Biol. 3, 267-277.

26. Burant, C. F., Takeda, J., Brot-Laroche, E., Bell, G. I., and Davidson, N. O. (1992). Fructose transporter in human spermatozoa and small intestine is GLUT5. J Biol. Chem. 267, 14523-14526.

27. Cain, C. C., Trimble, W. S., and Lienhard, G. E. (1992). Members of the VAMP family of synaptic vesicle proteins are components of glucose transporter-containing vesicles from rat adipocytes. J. Biol. Chem. 267, 11681-11684.

28. Carayannopoulos, M. O., Chi, M. M., Cui, Y., Pingsterhaus, J. M., McKnight, R. A., Mueckler, M., Devaskar, S. U., and Moley, K. H. (2000). GLUT8 is a glucose transporter responsible for insulin-stimulated glucose uptake in the blastocyst. Proc. Natl. Acad. Sci. U. S. A. %20;97, 7313-7318.

29. Carayannopoulos, M. O., Schlein, A., Wyman, A., Chi, M., Keembiyehetty, C., and Moley, K. H. (2004). GLUT9 is differentially expressed and targeted in the preimplantation embryo. Endocrinology 145, 1435-1443.

30. Carlson, C. J., Koterski, S., Sciotti, R. J., Poccard, G. B., and Rondinone, C. M. (2003). Enhanced basal activation of mitogen-activated protein kinases in adipocytes from type 2 diabetes: potential role of p38 in the downregulation of GLUT4 expression. Diabetes 52, 634-641.

31. Carr, C. M., Grote, E., Munson, M., Hughson, F. M., and Novick, P. J. (1999). Sec1p binds to SNARE complexes and concentrates at sites of secretion. J. Cell Biol. 146, 333-344.

32. Carvalho, E, Schellhorn, S. E., Zabolotny, J. M., Martin, S., Tozzo, E., Peroni, O. D., Houseknecht, K. L., Mundt, A., James, D. E., and Kahn, B. B. (2004). GLUT4 overexpression or deficiency in adipocytes of transgenic mice alters the composition of GLUT4 vesicles and the subcellular localization of GLUT4 and insulin-responsive aminopeptidase. J. Biol. Chem. 279, 21598-21605.

33. Chamberlain, L. H., Graham, M. E., Kane, S., Jackson, J. L., Maier, V. H., Burgoyne, R. D., and Gould, G. W. (2001). The synaptic vesicle protein, cysteine-string protein, is associated with the plasma membrane in 3T3-L1 adipocytes and interacts with syntaxin 4. J. Cell Sci. 114, 445-455.

34. Chapman, C. F., Liu, Y., Sonek, G. J., and Tromberg, B. J. (1995). The use of exogenous fluorescent probes for temperature measurements in single living cells. Photochem. Photobiol. 62, 416-425.

35. Cheatham, B., Vlahos, C. J., Cheatham, L., Wang, L., Blenis, J., and Kahn, C. R. (1994). Phosphatidylinositol 3-kinase activation is required for insulin stimulation of pp70 S6 kinase, DNA synthesis, and glucose transporter translocation. Mol. Cell Biol. 14, 4902-4911.

36. Cheatham, B., Volchuk, A., Kahn, C. R., Wang, L., Rhodes, C. J., and Klip, A. (1996). Insulin-stimulated translocation of GLUT4 glucose transporters requires SNARE-complex proteins. Proc. Natl. Acad. Sci. U. S. A. 93, 15169-15173.

37. Cheeseman, C. I. (1993). GLUT2 is the transporter for fructose across the rat intestinal basolateral membrane. Gastroenterology 105, 1050-1056.

38. Chen, F., Foran, P., Shone, C. C., Foster, K. A., Melling, J., and Dolly, J. O. (1997). Botulinum neurotoxin B inhibits insulin-stimulated glucose uptake into 3T3-L1 adipocytes and cleaves cellubrevin unlike type A toxin which failed to proteolyze the SNAP-23 present. Biochemistry 36, 5719-5728.

39. Chen, X., Al Hasani, H., Olausson, T., Wenthzel, A. M., Smith, U., and Cushman, S. W. (2003). Activity, phosphorylation state and subcellular distribution of GLUT4-targeted Akt2 in rat adipose cells. J. Cell Sci. 116, 3511-3518.

40. Chen, Y. A., Scales, S. J., Patel, S. M., Doung, Y. C., and Scheller, R. H. (1999). SNARE complex formation is triggered by Ca2+ and drives membrane fusion. Cell 97, 165-174.

41. Chiang, S. H., Baumann, C. A., Kanzaki, M., Thurmond, D. C., Watson, R. T., Neudauer, C. L., Macara, I. G., Pessin, J. E., and Saltiel, A. R. (2001). Insulin-stimulated GLUT4 translocation requires the CAP-dependent activation of TC10. Nature 410, 944-948.

42. Chieregatti, E., Chicka, M. C., Chapman, E. R., and Baldini, G. (2004). SNAP-23 functions in docking/fusion of granules at low Ca2+. Mol. Biol. Cell 15, 1918-1930.

43. Cho, H., Mu, J., Kim, J. K., Thorvaldsen, J. L., Chu, Q., Crenshaw, E. B., III, Kaestner, K. H., Bartolomei, M. S., Shulman, G. I., and Birnbaum, M. J. (2001a). Insulin resistance and a diabetes mellitus-like syndrome in mice lacking the protein kinase Akt2 (PKB beta). Science 292, 1728-1731.

44. Cho, H., Thorvaldsen, J. L., Chu, Q., Feng, F., and Birnbaum, M. J. (2001b). Akt1/PKBalpha is required for normal growth but dispensable for maintenance of glucose homeostasis in mice. J. Biol. Chem. 276, 38349-38352.

45. Chou, M. M., Hou, W., Johnson, J., Graham, L. K., Lee, M. H., Chen, C. S., Newton, A. C., Schaffhausen, B. S., and Toker, A. (1998). Regulation of protein kinase C zeta by PI 3-kinase and PDK-1. Curr. Biol. 8, 1069-1077.

46. Clarke, J. F., Young, P. W., Yonezawa, K., Kasuga, M., and Holman, G. D. (1994). Inhibition of the translocation of GLUT1 and GLUT4 in 3T3-L1 cells by the phosphatidylinositol 3-kinase inhibitor, wortmannin. Biochem. J. 300, 631-635.

47. Cong, L. N., Chen, H., Li, Y., Zhou, L., McGibbon, M. A., Taylor, S. I., and Quon, M. J. (1997). Physiological role of Akt in insulin-stimulated translocation of GLUT4 in transfected rat adipose cells. Mol. Endocrinol. 11, 1881-1890.

48. Coorssen, J. R., Blank, P. S., Albertorio, F., Bezrukov, L., Kolosova, I., Chen, X., Backlund, P. S., Jr., and Zimmerberg, J. (2003). Regulated secretion: SNARE density, vesicle fusion and calcium dependence. J. Cell Sci. 116, 2087-2097.

49. Coorssen, J. R., Blank, P. S., Tahara, M., and Zimmerberg, J. (1998). Biochemical and functional studies of cortical vesicle fusion: the SNARE complex and Ca2+ sensitivity. J. Cell Biol. 143, 1845-1857.

50. Cross, D. A., Alessi, D. R., Cohen, P., Andjelkovich, M., and Hemmings, B. A. (1995). Inhibition of glycogen synthase kinase-3 by insulin mediated by protein kinase B. Nature 378, 785-789.

51. Czech, M. P. and Buxton, J. M. (1993). Insulin action on the internalization of the GLUT4 glucose transporter in isolated rat adipocytes. J. Biol. Chem. 268, 9187-9190.

52. Davies, S. P., Reddy, H., Caivano, M., and Cohen, P. (2000). Specificity and mechanism of action of some commonly used protein kinase inhibitors. Biochem. J. 351, 95-105.

53. Derijard, B., Hibi, M., Wu, I. H., Barrett, T., Su, B., Deng, T., Karin, M., and Davis, R. J. (1994). JNK1: a protein kinase stimulated by UV light and Ha-Ras that binds and phosphorylates the c-Jun activation domain. Cell 76, 1025-1037.

54. Diamond, J. (2003). The double puzzle of diabetes. Nature 423, 599-602.

55. Diefenbach, R. J., Diefenbach, E., Douglas, M. W., and Cunningham, A. L. (2002). The heavy chain of conventional kinesin interacts with the SNARE proteins SNAP25 and SNAP23. Biochemistry 41, 14906-14915.

56. Doege, H., Bocianski, A., Joost, H. G., and Schurmann, A. (2000a). Activity and genomic organization of human glucose transporter 9 (GLUT9), a novel member of the family of sugar-transport facilitators predominantly expressed in brain and leucocytes. Biochem. J 350, 771-776.

57. Doege, H., Bocianski, A., Scheepers, A., Axer, H., Eckel, J., Joost, H. G., and Schurmann, A. (2001). Characterization of human glucose transporter (GLUT) 11 (encoded by SLC2A11), a novel sugar-transport facilitator specifically expressed in heart and skeletal muscle. Biochem. J 359, 443-449.

58. Doege, H., Schurmann, A., Bahrenberg, G., Brauers, A., and Joost, H. G. (2000b). GLUT8, a novel member of the sugar transport facilitator family with glucose transport activity. J Biol. Chem. 275, 16275-16280.

59. Ducluzeau, P. H., Fletcher, L. M., Welsh, G. I., and Tavare, J. M. (2002). Functional consequence of targeting protein kinase B/Akt to GLUT4 vesicles. J. Cell Sci. 115, 2857-2866.

60. Dulubova, I., Sugita, S., Hill, S., Hosaka, M., Fernandez, I., Sudhof, T. C., and Rizo, J. (1999). A conformational switch in syntaxin during exocytosis: role of munc18. EMBO J. 18, 4372-4382.

61. Dulubova, I., Yamaguchi, T., Gao, Y., Min, S. W., Huryeva, I., Sudhof, T. C., and Rizo, J. (2002). How Tlg2p/syntaxin 16 'snares' Vps45. EMBO J. 21, 3620-3631.

62. Edelmann, L., Hanson, P. I., Chapman, E. R., and Jahn, R. (1995). Synaptobrevin binding to synaptophysin: a potential mechanism for controlling the exocytotic fusion machine. EMBO J. 14, 224-231.

63. Elmendorf, J. S., Boeglin, D. J., and Pessin, J. E. (1999). Temporal separation of insulin-stimulated GLUT4/IRAP vesicle plasma membrane docking and fusion in 3T3L1 adipocytes. J. Biol. Chem. 274, 37357-37361.

64. Emoto, M., Langille, S. E., and Czech, M. P. (2001). A role for kinesin in insulin-stimulated GLUT4 glucose transporter translocation in 3T3-L1 adipocytes. J. Biol. Chem. 276, 10677-10682.

65. Epps-Fung, M., Gupta, K., Hardy, R. W., and Wells, A. (1997). A role for phospholipase C activity in GLUT4-mediated glucose transport. Endocrinology 138, 5170-5175.

66. Evans, G. J., Morgan, A., and Burgoyne, R. D. (2003). Tying everything together: the multiple roles of cysteine string protein (CSP) in regulated exocytosis. Traffic. 4, 653-659.

67. Fasshauer, D., Antonin, W., Margittai, M., Pabst, S., and Jahn, R. (1999). Mixed and non-cognate SNARE complexes. Characterization of assembly and biophysical properties. J. Biol. Chem. 274, 15440-15446.

68. Fasshauer, D., Antonin, W., Subramaniam, V., and Jahn, R. (2002). SNARE assembly and disassembly exhibit a pronounced hysteresis. Nat. Struct. Biol. 9, 144-151.

69. Fath, K. R., Trimbur, G. M., and Burgess, D. R. (1994). Molecular motors are differentially distributed on Golgi membranes from polarized epithelial cells. J. Cell Biol. 126, 661-675.

70. Ferrara, C. M. and Cushman, S. W. (1999). GLUT4 trafficking in insulin-stimulated rat adipose cells: evidence that heterotrimeric GTP-binding proteins regulate the fusion of docked GLUT4-containing vesicles. Biochem. J. 343, 571-577.

71. Fix, M., Melia, T. J., Jaiswal, J. K., Rappoport, J. Z., You, D., Sollner, T. H., Rothman, J. E., and Simon, S. M. (2004). Imaging single membrane fusion events mediated by SNARE proteins. Proc. Natl. Acad. Sci. U. S. A. 101, 7311-7316.

72. Fletcher, L. M., Welsh, G. I., Oatey, P. B., and Tavare, J. M. (2000). Role for the microtubule cytoskeleton in GLUT4 vesicle trafficking and in the regulation of insulin-stimulated glucose uptake. Biochem. J. 352, 267-276.

73. Foster, L. J., Weir, M. L., Lim, D. Y., Liu, Z., Trimble, W. S., and Klip, A. (2000). A functional role for VAP-33 in insulin-stimulated GLUT4 traffic. Traffic 1, 512-521.

74. Foster, L. J., Yaworsky, K., Trimble, W. S., and Klip, A. (1999). SNAP23 promotes insulin-dependent glucose uptake in 3T3-L1 adipocytes: possible interaction with cytoskeleton. Am. J. Physiol. 276, C1108-C1114.

75. Foster, L. J., Yeung, B., Mohtashami, M., Ross, K., Trimble, W. S., and Klip, A. (1998). Binary interactions of the SNARE proteins syntaxin-4, SNAP23, and VAMP-2 and their regulation by phosphorylation. Biochemistry 37, 11089-11096.

76. Fruman, D. A., Meyers, R. E., and Cantley, L. C. (1998). Phosphoinositide kinases. Annu. Rev. Biochem. 67, 481-507.

77. Fujishiro, M., Gotoh, Y., Katagiri, H., Sakoda, H., Ogihara, T., Anai, M., Onishi, Y., Ono, H., Funaki, M., Inukai, K., Fukushima, Y., Kikuchi, M., Oka, Y., and Asano, T. (2001). MKK6/3 and p38 MAPK pathway activation is not necessary for insulin-induced glucose uptake but regulates glucose transporter expression. J. Biol. Chem. 276, 19800-19806.

78. Fukumoto, H., Kayano, T., Buse, J. B., Edwards, Y., Pilch, P. F., Bell, G. I., and Seino, S. (1989). Cloning and characterization of the major insulin-responsive glucose transporter expressed in human skeletal muscle and other insulin-responsive tissues. J Biol. Chem. 264, 7776-7779.

79. Fukumoto, H., Seino, S., Imura, H., Seino, Y., Eddy, R. L., Fukushima, Y., Byers, M. G., Shows, T. B., and Bell, G. I. (1988). Sequence, tissue distribution, and chromosomal localization of mRNA encoding a human glucose transporter-like protein. Proc. Natl. Acad. Sci. U. S. A. 85, 5434-5438.

80. Garvey, W. T., Maianu, L., Zhu, J. H., Brechtel-Hook, G., Wallace, P., and Baron, A. D. (1998). Evidence for defects in the trafficking and translocation of GLUT4 glucose transporters in skeletal muscle as a cause of human insulin resistance. J. Clin. Invest 101, 2377-2386.

81. Gill, S. C. and von Hippel, P. H. (1989). Calculation of protein extinction coefficients from amino acid sequence data. Anal. Biochem. 182, 319-326.

82. Giovannone, B., Scaldaferri, M. L., Federici, M., Porzio, O., Lauro, D., Fusco, A., Sbraccia, P., Borboni, P., Lauro, R., and Sesti, G. (2000). Insulin receptor substrate (IRS) transduction system: distinct and overlapping signaling potential. Diabetes Metab Res. Rev. 16, 434-441.

83. Goldstein, L. S. and Philp, A. V. (1999). The road less traveled: emerging principles of kinesin motor utilization. Annu. Rev. Cell Dev. Biol. 15:141-83., 141-183.

84. Guilherme, A. and Czech, M. P. (1998). Stimulation of IRS-1-associated phosphatidylinositol 3-kinase and Akt/protein kinase B but not glucose transport by beta1-integrin signaling in rat adipocytes. J. Biol. Chem. 273, 33119-33122.

85. Guilherme, A., Emoto, M., Buxton, J. M., Bose, S., Sabini, R., Theurkauf, W. E., Leszyk, J., and Czech, M. P. (2000). Perinuclear Localization and Insulin Responsiveness of GLUT4 Requires Cytoskeletal Integrity in 3T3-L1 Adipocytes. J. Biol. Chem. 275, 38151-38159.

86. Hanson, P. I., Roth, R., Morisaki, H., Jahn, R., and Heuser, J. E. (1997). Structure and conformational changes in NSF and its membrane receptor complexes visualized by quick-freeze/deep-etch electron microscopy. Cell 90, 523-535.

87. Haruta, T., Morris, A. J., Rose, D. W., Nelson, J. G., Mueckler, M., and Olefsky, J. M. (1995). Insulin-stimulated GLUT4 translocation is mediated by a divergent intracellular signaling pathway. J. Biol. Chem. 270, 27991-27994.

88. Hashiramoto, M. and James, D. E. (2000). Characterization of insulin-responsive GLUT4 storage vesicles isolated from 3T3-L1 adipocytes. Mol. Cell Biol. 20, 416-427.

89. Hausdorff, S. F., Fingar, D. C., Morioka, K., Garza, L. A., Whiteman, E. L., Summers, S. A., and Birnbaum, M. J. (1999). Identification of wortmannin-sensitive targets in 3T3-L1 adipocytes. Dissociation of insulin-stimulated glucose uptake and GLUT4 translocation. J. Biol. Chem. 274, 24677-24684.

90. Hayashi, T., McMahon, H., Yamasaki, S., Binz, T., Hata, Y., Sudhof, T. C., and Niemann, H. (1994). Synaptic vesicle membrane fusion complex: action of clostridial neurotoxins on assembly. EMBO J. 13, 5051-5061.

91. Herbst, J. J., Ross, S. A., Scott, H. M., Bobin, S. A., Morris, N. J., Lienhard, G. E., and Keller, S. R. (1997). Insulin stimulates cell surface aminopeptidase activity toward vasopressin in adipocytes. Am. J. Physiol 272, E600-E606.

92. Hickson, G. R., Chamberlain, L. H., Maier, V. H., and Gould, G. W. (2000). Quantification of SNARE protein levels in 3T3-L1 adipocytes: implications for insulin-stimulated glucose transport. Biochem. Biophys. Res. Commun. 270, 841-845.

93. Higaki, Y., Wojtaszewski, J. F., Hirshman, M. F., Withers, D. J., Towery, H., White, M. F., and Goodyear, L. J. (1999). Insulin receptor substrate-2 is not necessary for insulin- and exercise-stimulated glucose transport in skeletal muscle. J. Biol. Chem. 274, 20791-20795.

94. Hill, M. M., Clark, S. F., Tucker, D. F., Birnbaum, M. J., James, D. E., and Macaulay, S. L. (1999). A role for protein kinase Bbeta/Akt2 in insulin-stimulated GLUT4 translocation in adipocytes. Mol. Cell Biol. 19, 7771-7781.

95. Holman, G. D., Kozka, I. J., Clark, A. E., Flower, C. J., Saltis, J., Habberfield, A. D., Simpson, I. A., and Cushman, S. W. (1990). Cell surface labeling of glucose transporter isoform GLUT4 by bis-mannose photolabel. Correlation with stimulation of glucose transport in rat adipose cells by insulin and phorbol ester. J. Biol. Chem. 265, 18172-18179.

96. Holman, G. D. and Sandoval, I. V. (2001). Moving the insulin-regulated glucose transporter GLUT4 into and out of storage. Trends Cell Biol. 11, 173-179.

97. Holroyd, P., Lang, T., Wenzel, D., De Camilli, P., and Jahn, R. (2002). Imaging direct, dynamin-dependent recapture of fusing secretory granules on plasma membrane lawns from PC12 cells. Proc. Natl. Acad. Sci. U. S. A 99, 16806-16811.

98. Hresko, R. C., Murata, H., and Mueckler, M. (2003). Phosphoinositide-dependent kinase-2 is a distinct protein kinase enriched in a novel cytoskeletal fraction associated with adipocyte plasma membranes. J. Biol. Chem. 278, 21615-21622.

99. Hu, C., Ahmed, M., Melia, T. J., Sollner, T. H., Mayer, T., and Rothman, J. E. (2003). Fusion of cells by flipped SNAREs. Science 300, 1745-1749.

100. Hu, K., Carroll, J., Fedorovich, S., Rickman, C., Sukhodub, A., and Davletov, B. (2002). Vesicular restriction of synaptobrevin suggests a role for calcium in membrane fusion. Nature 415, 646-650.

101. Hudson, A. W., Fingar, D. C., Seidner, G. A., Griffiths, G., Burke, B., and Birnbaum, M. J. (1993). Targeting of the "insulin-responsive" glucose transporter (GLUT4) to the regulated secretory pathway in PC12 cells. J. Cell Biol. 122, 579-588.

102. Hunt, J. M., Bommert, K., Charlton, M. P., Kistner, A., Habermann, E., Augustine, G. J., and Betz, H. (1994). A post-docking role for synaptobrevin in synaptic vesicle fusion. Neuron 12, 1269-1279.

103. Ibberson, M., Uldry, M., and Thorens, B. (2000). GLUTX1, a novel mammalian glucose transporter expressed in the central nervous system and insulin-sensitive tissues. J Biol. Chem. 275, 4607-4612.

104. Imamura, T., Huang, J., Usui, I., Satoh, H., Bever, J., and Olefsky, J. M. (2003). Insulin-induced GLUT4 translocation involves protein kinase C-

lambda-mediated functional coupling between Rab4 and the motor protein kinesin. Mol. Cell Biol. 23, 4892-4900.

105. Inoue, G., Cheatham, B., and Kahn, C. R. (1999). Development of an in vitro reconstitution assay for glucose transporter 4 translocation. Proc. Natl. Acad. Sci. U. S. A. 96, 14919-14924.

106. Inoue, M., Chang, L., Hwang, J., Chiang, S. H., and Saltiel, A. R. (2003). The exocyst complex is required for targeting of Glut4 to the plasma membrane by insulin. Nature 422, 629-633.

107. Isakoff, S. J., Taha, C., Rose, E., Marcusohn, J., Klip, A., and Skolnik, E. Y. (1995). The inability of phosphatidylinositol 3-kinase activation to stimulate GLUT4 translocation indicates additional signaling pathways are required for insulin-stimulated glucose uptake. Proc. Natl. Acad. Sci. U. S. A. 92, 10247-10251.

108. Jagadish, M. N., Tellam, J. T., Macaulay, S. L., Gough, K. H., James, D. E., and Ward, C. W. (1997). Novel isoform of syntaxin 1 is expressed in mammalian cells. Biochem. J. 321, 151-156.

109. James, D. E. and Piper, R. C. (1994). Insulin resistance, diabetes, and the insulin-regulated trafficking of GLUT-4. J. Cell Biol. 126, 1123-1126.

110. James, D. E., Piper, R. C., and Slot, J. W. (1994). Insulin stimulation of GLUT-4 translocation: a model for regulated recycling. Trends Cell Biol. 4, 120-126.

111. Jarvis, S. E., Barr, W., Feng, Z. P., Hamid, J., and Zamponi, G. W. (2002). Molecular determinants of syntaxin 1 modulation of N-type calcium channels. J. Biol. Chem. 277, 44399-44407.

112. JeBailey, L., Rudich, A., Huang, X., Ciano-Oliveira, C., Kapus, A., and Klip, A. (2004). Skeletal muscle cells and adipocytes differ in their reliance on TC10 and Rac for insulin-induced actin remodeling. Mol. Endocrinol. 18, 359-372.

113. Jenkins, A. B. and Campbell, L. V. (2004). The genetics and pathophysiology of diabetes mellitus type II. J. Inherit. Metab Dis. 27, 331-347.

114. Jeremic, A., Kelly, M., Cho, J. A., Cho, S. J., Horber, J. K., and Jena, B. P. (2004). Calcium drives fusion of SNARE-apposed bilayers. Cell Biol. Int. 28, 19-31.

115. Jhun, B. H., Rampal, A. L., Liu, H., Lachaal, M., and Jung, C. Y. (1992). Effects of insulin on steady state kinetics of GLUT4 subcellular distribution in rat adipocytes. Evidence of constitutive GLUT4 recycling. J. Biol. Chem. 267, 17710-17715.

116. Ji, J., Muinuddin, A., Kang, Y., Diamant, N. E., and Gaisano, H. Y. (2003). SNAP-25 inhibits L-type Ca2+ channels in feline esophagus smooth muscle cells. Biochem. Biophys. Res. Commun. 306, 298-302.

117. Jiang, T., Sweeney, G., Rudolf, M. T., Klip, A., Traynor-Kaplan, A., and Tsien, R. Y. (1998). Membrane-permeant esters of phosphatidylinositol 3,4,5-trisphosphate. J. Biol. Chem. 273, 11017-11024.

118. Jiang, Z. Y., Chawla, A., Bose, A., Way, M., and Czech, M. P. (2002). A phosphatidylinositol 3-kinase-independent insulin signaling pathway to N-WASP/Arp2/3/F-actin required for GLUT4 glucose transporter recycling. J. Biol. Chem. 277, 509-515.

119. Jiang, Z. Y., Zhou, Q. L., Coleman, K. A., Chouinard, M., Boese, Q., and Czech, M. P. (2003). Insulin signaling through Akt/protein kinase B analyzed by small interfering RNA-mediated gene silencing. Proc. Natl. Acad. Sci. U. S. A. 100, 7569-7574.

120. Johnson, A. O., Lampson, M. A., and McGraw, T. E. (2001). A di-leucine sequence and a cluster of acidic amino acids are required for dynamic retention in the endosomal recycling compartment of fibroblasts. Mol Biol. Cell 12, 367-381.

121. Joost, H. G. and Thorens, B. (2001). The extended GLUT-family of sugar/polyol transport facilitators: nomenclature, sequence characteristics, and potential function of its novel members. Mol. Membr. Biol 18, 247-256.

122. Kanai, F., Nishioka, Y., Hayashi, H., Kamohara, S., Todaka, M., and Ebina, Y. (1993). Direct demonstration of insulin-induced GLUT4 translocation to the surface of intact cells by insertion of a c-myc epitope into an exofacial GLUT4 domain. J. Biol. Chem. 268, 14523-14526.

123. Kanda, H., Tamori, Y., Shinoda, H., Yoshikawa, M., Sakaue, M., Udagawa, J., Otani, H., Tashiro, F., Miyazaki, J., and Kasuga, M. (2005). Adipocytes from Munc18c-null mice show increased sensitivity to insulin-stimulated GLUT4 externalization. J. Clin. Invest 115, 291-301.

124. Karnieli, E., Zarnowski, M. J., Hissin, P. J., Simpson, I. A., Salans, L. B., and Cushman, S. W. (1981). Insulin-stimulated translocation of glucose transport systems in the isolated rat adipose cell. Time course, reversal, insulin concentration dependency, and relationship to glucose transport activity. J. Biol. Chem. 256, 4772-4777.

125. Kato, Y., Nakamura, K., and Hashimoto, T. (1983). New ion exchanger for the separation of proteins and nucleic acids. J. Chromatogr. 266:385-94., 385-394.

126. Katso, R., Okkenhaug, K., Ahmadi, K., White, S., Timms, J., and Waterfield, M. D. (2001). Cellular function of phosphoinositide 3-kinases: implications for development, homeostasis, and cancer. Annu. Rev. Cell Dev. Biol. 17:615-75., 615-675.

127. Kayali, A. G., Austin, D. A., and Webster, N. J. (2000). Stimulation of MAPK cascades by insulin and osmotic shock: lack of an involvement of p38 mitogen-activated protein kinase in glucose transport in 3T3-L1 adipocytes. Diabetes 49, 1783-1793.

128. Kayali, A. G., Eichhorn, J., Haruta, T., Morris, A. J., Nelson, J. G., Vollenweider, P., Olefsky, J. M., and Webster, N. J. (1998). Association of the insulin receptor with phospholipase C-gamma (PLCgamma) in 3T3-L1 adipocytes suggests a role for PLCgamma in metabolic signaling by insulin. J. Biol. Chem. 273, 13808-13818.

129. Kayano, T., Burant, C. F., Fukumoto, H., Gould, G. W., Fan, Y. S., Eddy, R. L., Byers, M. G., Shows, T. B., Seino, S., and Bell, G. I. (1990). Human facilitative glucose transporters. Isolation, functional characterization, and gene localization of cDNAs encoding an isoform (GLUT5) expressed in small intestine, kidney, muscle, and adipose tissue and an unusual glucose transporter pseudogene-like sequence (GLUT6). J Biol. Chem. 265, 13276-13282.

130. Kayano, T., Fukumoto, H., Eddy, R. L., Fan, Y. S., Byers, M. G., Shows, T. B., and Bell, G. I. (1988). Evidence for a family of human glucose transporter-like proteins. Sequence and gene localization of a protein expressed in fetal skeletal muscle and other tissues. J Biol. Chem. 263, 15245-15248.

131. Keller, S. R., Scott, H. M., Mastick, C. C., Aebersold, R., and Lienhard, G. E. (1995). Cloning and characterization of a novel insulin-regulated membrane aminopeptidase from Glut4 vesicles. J. Biol. Chem. 270, 23612-23618.

132. Kessler, A., Tomas, E., Immler, D., Meyer, H. E., Zorzano, A., and Eckel, J. (2000). Rab11 is associated with GLUT4-containing vesicles and redistributes in response to insulin. Diabetologia 43, 1518-1527.

133. Kessler, A., Uphues, I., Ouwens, D. M., Till, M., and Eckel, J. (2001). Diversification of cardiac insulin signaling involves the p85 alpha/beta subunits of phosphatidylinositol 3-kinase. Am. J. Physiol Endocrinol. Metab 280, E65-E74.

134. King, C. C. and Newton, A. C. (2004). The adaptor protein Grb14 regulates the localization of 3-phosphoinositide-dependent kinase-1. J. Biol. Chem. 279, 37518-37527.

135. Kitamura, T., Ogawa, W., Sakaue, H., Hino, Y., Kuroda, S., Takata, M., Matsumoto, M., Maeda, T., Konishi, H., Kikkawa, U., and Kasuga, M. (1998). Requirement for activation of the serine-threonine kinase Akt (protein kinase B) in insulin stimulation of protein synthesis but not of glucose transport. Mol. Cell Biol. 18, 3708-3717.

136. Kohn, A. D., Summers, S. A., Birnbaum, M. J., and Roth, R. A. (1996). Expression of a constitutively active Akt Ser/Thr kinase in 3T3-L1 adipocytes stimulates glucose uptake and glucose transporter 4 translocation. J. Biol. Chem. 271, 31372-31378.

137. Konrad, D., Somwar, R., Sweeney, G., Yaworsky, K., Hayashi, M., Ramlal, T., and Klip, A. (2001). The antihyperglycemic drug alpha-lipoic acid stimulates glucose uptake via both GLUT4 translocation and GLUT4

activation: potential role of p38 mitogen-activated protein kinase in GLUT4 activation. Diabetes 50, 1464-1471.

138. Kotani, K., Carozzi, A. J., Sakaue, H., Hara, K., Robinson, L. J., Clark, S. F., Yonezawa, K., James, D. E., and Kasuga, M. (1995). Requirement for phosphoinositide 3-kinase in insulin-stimulated GLUT4 translocation in 3T3-L1 adipocytes. Biochem. Biophys. Res. Commun. 209, 343-348.

139. Kupriyanova, T. A. and Kandror, K. V. (2000). Cellugyrin is a marker for a distinct population of intracellular Glut4-containing vesicles. J. Biol. Chem. 275, 36263-36268.

140. Kweon, D. H., Kim, C. S., and Shin, Y. K. (2002). The membrane-dipped neuronal SNARE complex: a site-directed spin labeling electron paramagnetic resonance study. Biochemistry 41, 9264-9268.

141. Laage, R. and Langosch, D. (1997). Dimerization of the synaptic vesicle protein synaptobrevin (vesicle-associated membrane protein) II depends on specific residues within the transmembrane segment. Eur. J. Biochem. 249, 540-546.

142. Laage, R. and Langosch, D. (2001). Strategies for prokaryotic expression of eukaryotic membrane proteins. Traffic. 2, 99-104.

143. Laemmli, U. K. (1970). Cleavage of structural proteins during the assembly of the head of bacteriophage T4. Nature 227, 680-685.

144. Lali, F. V., Hunt, A. E., Turner, S. J., and Foxwell, B. M. (2000). The pyridinyl imidazole inhibitor SB203580 blocks phosphoinositide-dependent protein kinase activity, protein kinase B phosphorylation, and retinoblastoma hyperphosphorylation in interleukin-2-stimulated T cells independently of p38 mitogen-activated protein kinase. J. Biol. Chem. 275, 7395-7402.

145. Lang, T., Bruns, D., Wenzel, D., Riedel, D., Holroyd, P., Thiele, C., and Jahn, R. (2001). SNAREs are concentrated in cholesterol-dependent clusters that define docking and fusion sites for exocytosis. EMBO J. 20, 2202-2213.

146. Lang, T., Margittai, M., Holzler, H., and Jahn, R. (2002). SNAREs in native plasma membranes are active and readily form core complexes with endogenous and exogenous SNAREs. J. Cell Biol. 158, 751-760.

147. Laurie, S. M., Cain, C. C., Lienhard, G. E., and Castle, J. D. (1993). The glucose transporter GluT4 and secretory carrier membrane proteins (SCAMPs) colocalize in rat adipocytes and partially segregate during insulin stimulation. J. Biol. Chem. 268, 19110-19117.

148. Lavan, B. E., Lane, W. S., and Lienhard, G. E. (1997). The 60-kDa phosphotyrosine protein in insulin-treated adipocytes is a new member of the insulin receptor substrate family. J. Biol. Chem. 272, 11439-11443.

149. Lawrence, G. W. and Dolly, J. O. (2002). Multiple forms of SNARE complexes in exocytosis from chromaffin cells: effects of Ca(2+), MgATP and botulinum toxin type A. J Cell Sci. 115, 667-673.

150. Le Good, J. A., Ziegler, W. H., Parekh, D. B., Alessi, D. R., Cohen, P., and Parker, P. J. (1998). Protein kinase C isotypes controlled by phosphoinositide 3-kinase through the protein kinase PDK1. Science 281, 2042-2045.

151. Lee, C., Levin, A., and Branton, D. (1987). Copper staining: a five-minute protein stain for sodium dodecyl sulfate-polyacrylamide gels. Anal. Biochem. 166, 308-312.

152. Leveque, C., Boudier, J. A., Takahashi, M., and Seagar, M. (2000). Calcium-dependent dissociation of synaptotagmin from synaptic SNARE complexes. J. Neurochem. 74, 367-374.

153. Li, L., Omata, W., Kojima, I., and Shibata, H. (2000). Direct Interaction of Rab4 with Syntaxin 4. J. Biol. Chem. 276, 5265-5273.

154. Li, Q., Manolescu, A., Ritzel, M., Yao, S., Slugoski, M., Young, J. D., Chen, X. Z., and Cheeseman, C. I. (2004). Cloning and functional characterization of the human GLUT7 isoform SLC2A7 from the small intestine. Am. J Physiol Gastrointest. Liver Physiol 287, G236-G242.

155. Lin, R. C. and Scheller, R. H. (1997). Structural organization of the synaptic exocytosis core complex. Neuron 19, 1087-1094.

156. Livingstone, C., James, D. E., Rice, J. E., Hanpeter, D., and Gould, G. W. (1996). Compartment ablation analysis of the insulin-responsive glucose transporter (GLUT4) in 3T3-L1 adipocytes. Biochem. J. 315, 487-495.

157. Lorenzo, M., Teruel, T., Hernandez, R., Kayali, A. G., and Webster, N. J. (2002). PLCgamma participates in insulin stimulation of glucose uptake through activation of PKCzeta in brown adipocytes. Exp. Cell Res. 278, 146-157.

158. Macaulay, S. L., Grusovin, J., Stoichevska, V., Ryan, J. M., Castelli, L. A., and Ward, C. W. (2002). Cellular munc18c levels can modulate glucose transport rate and GLUT4 translocation in 3T3L1 cells. FEBS Lett. 528, 154-160.

159. Macaulay, S. L., Hewish, D. R., Gough, K. H., Stoichevska, V., MacPherson, S. F., Jagadish, M., and Ward, C. W. (1997). Functional studies in 3T3L1 cells support a role for SNARE proteins in insulin stimulation of GLUT4 translocation. Biochem. J. 324, 217-224.

160. Macheda, M. L., Kelly, D. J., Best, J. D., and Rogers, S. (2002). Expression during rat fetal development of GLUT12 - a member of the class III hexose transporter family. Anat. Embryol. (Berl) 205, 441-452.

161. Maffucci, T., Brancaccio, A., Piccolo, E., Stein, R. C., and Falasca, M. (2003). Insulin induces phosphatidylinositol-3-phosphate formation through TC10 activation. EMBO J. 22, 4178-4189.

162. Mahal, L. K., Sequeira, S. M., Gureasko, J. M., and Sollner, T. H. (2002). Calcium-independent stimulation of membrane fusion and SNAREpin formation by synaptotagmin I. J. Cell Biol. 158, 273-282.

163. Malikova, M., Shi, J., and Kandror, K. V. (2004). V-type ATPase is involved in biogenesis of GLUT4 vesicles. Am. J. Physiol. Endocrinol. Metab. 287, E547-E552.

164. Marsh, B. J., Martin, S., Melvin, D. R., Martin, L. B., Alm, R. A., Gould, G. W., and James, D. E. (1998). Mutational analysis of the carboxy-terminal phosphorylation site of GLUT-4 in 3T3-L1 adipocytes. Am. J. Physiol 275, E412-E422.

165. Martin, S., Tellam, J., Livingstone, C., Slot, J. W., Gould, G. W., and James, D. E. (1996). The glucose transporter (GLUT-4) and vesicle-associated membrane protein-2 (VAMP-2) are segregated from recycling endosomes in insulin-sensitive cells. J. Cell Biol. 134, 625-635.

166. Matsumoto, H., Nagasaka, T., Hattori, A., Rogi, T., Tsuruoka, N., Mizutani, S., and Tsujimoto, M. (2001). Expression of placental leucine aminopeptidase/oxytocinase in neuronal cells and its action on neuronal peptides. Eur. J. Biochem. 268, 3259-3266.

167. Mayer, A. (2002). Membrane fusion in eukaryotic cells. Annu. Rev. Cell Dev. Biol. 18, 289-314.

168. McNew, J. A., Parlati, F., Fukuda, R., Johnston, R. J., Paz, K., Paumet, F., Sollner, T. H., and Rothman, J. E. (2000a). Compartmental specificity of cellular membrane fusion encoded in SNARE proteins. Nature 407, 153-159.

169. McNew, J. A., Weber, T., Parlati, F., Johnston, R. J., Melia, T. J., Sollner, T. H., and Rothman, J. E. (2000b). Close is not enough: SNARE-dependent membrane fusion requires an active mechanism that transduces force to membrane anchors. J. Cell Biol. 150, 105-117.

170. McVie-Wylie, A. J., Lamson, D. R., and Chen, Y. T. (2001). Molecular cloning of a novel member of the GLUT family of transporters, SLC2a10 (GLUT10), localized on chromosome 20q13.1: a candidate gene for NIDDM susceptibility. Genomics 72, 113-117.

171. Mehta, P. P., Battenberg, E., and Wilson, M. C. (1996). SNAP-25 and synaptotagmin involvement in the final Ca(2+)-dependent triggering of neurotransmitter exocytosis. Proc. Natl. Acad. Sci. U. S. A. 93, 10471-10476.

172. Melia, T. J., Weber, T., McNew, J. A., Fisher, L. E., Johnston, R. J., Parlati, F., Mahal, L. K., Sollner, T. H., and Rothman, J. E. (2002). Regulation of membrane fusion by the membrane-proximal coil of the t-SNARE during zippering of SNAREpins. J. Cell Biol. 158, 929-940.

173. Merz, A. J. and Wickner, W. T. (2004). Trans-SNARE interactions elicit Ca2+ efflux from the yeast vacuole lumen. J. Cell Biol. 164, 195-206.

174. Millar, C. A., Meerloo, T., Martin, S., Hickson, G. R. X., Shimwell, N. J., Wakelam, M. J. O., James, D. E., and Gould, G. W. (2000). Adipsin and the glucose transporter GLUT4 traffic to the cell surface via independent pathways in adipocytes. Traffic 1, 141-151.

175. Millar, C. A., Shewan, A., Hickson, G. R., James, D. E., and Gould, G. W. (1999). Differential regulation of secretory compartments containing the insulin-responsive glucose transporter 4 in 3T3-L1 adipocytes. Mol. Biol. Cell 10, 3675-3688.

176. Min, J., Okada, S., Kanzaki, M., Elmendorf, J. S., Coker, K. J., Ceresa, B. P., Syu, L. J., Noda, Y., Saltiel, A. R., and Pessin, J. E. (1999). Synip: a novel insulin-regulated syntaxin 4-binding protein mediating GLUT4 translocation in adipocytes. Mol. Cell 3, 751-760.

177. Mitra, P., Zheng, X., and Czech, M. P. (2004). RNAi-based analysis of CAP, Cbl, and CrkII function in the regulation of GLUT4 by insulin. J. Biol. Chem. 279, 37431-37435.

178. Molero, J. C., Whitehead, J. P., Meerloo, T., and James, D. E. (2001). Nocodazole inhibits insulin-stimulated glucose transport in 3T3-L1 adipocytes via a microtubule-independent mechanism. J. Biol. Chem. 276, 43829-43835.

179. Montessuit, C., Rosenblatt-Velin, N., Papageorgiou, I., Campos, L., Pellieux, C., Palma, T., and Lerch, R. (2004). Regulation of glucose transporter expression in cardiac myocytes: p38 MAPK is a strong inducer of GLUT4. Cardiovasc. Res. 64, 94-104.

180. Mueckler, M., Caruso, C., Baldwin, S. A., Panico, M., Blench, I., Morris, H. R., Allard, W. J., Lienhard, G. E., and Lodish, H. F. (1985). Sequence and structure of a human glucose transporter. Science 229, 941-945.

181. Nakae, J., Park, B. C., and Accili, D. (1999). Insulin stimulates phosphorylation of the forkhead transcription factor FKHR on serine 253 through a Wortmannin-sensitive pathway. J. Biol. Chem. 274, 15982-15985.

182. Nave, B. T., Ouwens, M., Withers, D. J., Alessi, D. R., and Shepherd, P. R. (1999). Mammalian target of rapamycin is a direct target for protein kinase B: identification of a convergence point for opposing effects of insulin and amino-acid deficiency on protein translation. Biochem. J. 344, 427-431.

183. Neel, J. V. (1962). Diabetes mellitus: a "thrifty" genotype rendered detrimental by "progress"? Am. J. Hum. Genet. 14, 353-362.

184. Nelson, B. A., Robinson, K. A., and Buse, M. G. (2002). Insulin acutely regulates Munc18-c subcellular trafficking: altered response in insulin-resistant 3T3-L1 adipocytes. J. Biol. Chem. 277, 3809-3812.

185. Nickel, W., Weber, T., McNew, J. A., Parlati, F., Sollner, T. H., and Rothman, J. E. (1999). Content mixing and membrane integrity during membrane fusion driven by pairing of isolated v-SNAREs and t-SNAREs. Proc. Natl. Acad. Sci. U. S. A. 96, 12571-12576.

186. Nobes, C. D., Hawkins, P., Stephens, L., and Hall, A. (1995). Activation of the small GTP-binding proteins rho and rac by growth factor receptors. J. Cell Sci. 108, 225-233.

187. Okada, T., Kawano, Y., Sakakibara, T., Hazeki, O., and Ui, M. (1994). Essential role of phosphatidylinositol 3-kinase in insulin-induced glucose transport and antilipolysis in rat adipocytes. Studies with a selective inhibitor wortmannin. J. Biol. Chem. 269, 3568-3573.

188. Olson, A. L., Knight, J. B., and Pessin, J. E. (1997). Syntaxin 4, VAMP2, and/or VAMP3/cellubrevin are functional target membrane and vesicle SNAP receptors for insulin-stimulated GLUT4 translocation in adipocytes. Mol. Cell Biol. 17, 2425-2435.

189. Omata, W., Shibata, H., Li, L., Takata, K., and Kojima, I. (2000). Actin filaments play a critical role in insulin-induced exocytotic recruitment but not in endocytosis of GLUT4 in isolated rat adipocytes. Biochem. J. 346, 321-328.

190. Otto, H., Hanson, P. I., and Jahn, R. (1997). Assembly and disassembly of a ternary complex of synaptobrevin, syntaxin, and SNAP-25 in the membrane of synaptic vesicles. Proc. Natl. Acad. Sci. U. S. A. 94, 6197-6201.

191. Palacios, S., Lalioti, V., Martinez-Arca, S., Chattopadhyay, S., and Sandoval, I. V. (2001). Recycling of the insulin-sensitive glucose transporter GLUT4. Access of surface internalized GLUT4 molecules to the perinuclear storage compartment is mediated by the Phe5-Gln6-Gln7-Ile8 motif. J. Biol. Chem. 276, 3371-3383.

192. Parlati, F., McNew, J. A., Fukuda, R., Miller, R., Sollner, T. H., and Rothman, J. E. (2000). Topological restriction of SNARE-dependent membrane fusion. Nature 407, 194-198.

193. Parlati, F., Varlamov, O., Paz, K., McNew, J. A., Hurtado, D., Sollner, T. H., and Rothman, J. E. (2002). Distinct SNARE complexes mediating membrane fusion in Golgi transport based on combinatorial specificity. Proc. Natl. Acad. Sci. U. S. A. 99, 5424-5429.

194. Parlati, F., Weber, T., McNew, J. A., Westermann, B., Sollner, T. H., and Rothman, J. E. (1999). Rapid and efficient fusion of phospholipid vesicles by the alpha-helical core of a SNARE complex in the absence of an N-terminal regulatory domain. Proc. Natl. Acad. Sci. U. S. A. 96, 12565-12570.

195. Patti, M. E. and Kahn, C. R. (1998). The insulin receptor--a critical link in glucose homeostasis and insulin action. J. Basic Clin. Physiol Pharmacol. 9, 89-109.

196. Pellizzari, R., Rossetto, O., Schiavo, G., and Montecucco, C. (1999). Tetanus and botulinum neurotoxins: mechanism of action and therapeutic uses. Philos. Trans. R. Soc. Lond B Biol. Sci. 354, 259-268.

197. Peters, C., Bayer, M. J., Buhler, S., Andersen, J. S., Mann, M., and Mayer, A. (2001). Trans-complex formation by proteolipid channels in the terminal phase of membrane fusion. Nature 409, 581-588.

198. Pevsner, J., Hsu, S. C., Braun, J. E., Calakos, N., Ting, A. E., Bennett, M. K., and Scheller, R. H. (1994). Specificity and regulation of a synaptic vesicle docking complex. Neuron 13, 353-361.

199. Phay, J. E., Hussain, H. B., and Moley, J. F. (2000). Strategy for identification of novel glucose transporter family members by using internet-based genomic databases. Surgery 128, 946-951.

200. Raingeaud, J., Gupta, S., Dickens, M., and Han, J. (1995). Pro-inflammatory cytokines and environmental stress cause p38 mitogen-activated protein kinase activation by dual phosphorylation on tyrosine and threonine. J. Biol. Chem. 270, 7420-7426.

201. Randhawa, V. K., Thong, F. S., Lim, D. Y., Li, D., Garg, R. R., Rudge, R., Galli, T., Rudich, A., and Klip, A. (2004). Insulin and hypertonicity recruit GLUT4 to the plasma membrane of muscle cells by using N-ethylmaleimide-sensitive factor-dependent SNARE mechanisms but different v-SNAREs: role of TI-VAMP. Mol Biol. Cell 15, 5565-5573.

202. Rane, M. J., Coxon, P. Y., Powell, D. W., Webster, R., Klein, J. B., Pierce, W., Ping, P., and McLeish, K. R. (2001). p38 Kinase-dependent MAPKAPK-2 activation functions as 3-phosphoinositide-dependent kinase-2 for Akt in human neutrophils. J. Biol. Chem. 276, 3517-3523.

203. Rea, S., Martin, L. B., McIntosh, S., Macaulay, S. L., Ramsdale, T., Baldini, G., and James, D. E. (1998). Syndet, an adipocyte target SNARE involved in the insulin-induced translocation of GLUT4 to the cell surface. J. Biol. Chem. 273, 18784-18792.

204. Ribe, D., Yang, J., Patel, S., Koumanov, F., Cushman, S. W., and Holman, G. D. (2005). Endofacial competitive inhibition of glucose transporter-4 intrinsic activity by the mitogen-activated protein kinase inhibitor SB203580. Endocrinology 146, 1713-1717.

205. Ribon, V., Printen, J. A., Hoffman, N. G., Kay, B. K., and Saltiel, A. R. (1998). A novel, multifuntional c-Cbl binding protein in insulin receptor signaling in 3T3-L1 adipocytes. Mol. Cell Biol. 18, 872-879.

206. Ridley, A. J. and Hall, A. (1992). The small GTP-binding protein rho regulates the assembly of focal adhesions and actin stress fibers in response to growth factors. Cell 70, 389-399.

207. Robinson, L. J., Pang, S., Harris, D. S., Heuser, J., and James, D. E. (1992). Translocation of the glucose transporter (GLUT4) to the cell surface in

permeabilized 3T3-L1 adipocytes: effects of ATP insulin, and GTP gamma S and localization of GLUT4 to clathrin lattices. J. Cell Biol. 117, 1181-1196.

208. Rogers, S., Chandler, J. D., Clarke, A. L., Petrou, S., and Best, J. D. (2003). Glucose transporter GLUT12 - functional characterization in Xenopus laevis oocytes. Biochem. Biophys. Res. Commun. 308, 422-426.

209. Ross, S. A., Keller, S. R., and Lienhard, G. E. (1998). Increased intracellular sequestration of the insulin-regulated aminopeptidase upon differentiation of 3T3-L1 cells. Biochem. J. 330, 1003-1008.

210. Ross, S. A., Scott, H. M., Morris, N. J., Leung, W. Y., Mao, F., Lienhard, G. E., and Keller, S. R. (1996). Characterization of the insulin-regulated membrane aminopeptidase in 3T3-L1 adipocytes. J. Biol. Chem. 271, 3328-3332.

211. Rossetti, L. (1989). Normalization of insulin sensitivity with lithium in diabetic rats. Diabetes 38, 648-652.

212. Rowe, J., Calegari, F., Taverna, E., Longhi, R., and Rosa, P. (2001). Syntaxin 1A is delivered to the apical and basolateral domains of epithelial cells: the role of munc-18 proteins. J. Cell Sci. 114, 3323-3332.

213. Rowe, J., Corradi, N., Malosio, M. L., Taverna, E., Halban, P., Meldolesi, J., and Rosa, P. (1999). Blockade of membrane transport and disassembly of the Golgi complex by expression of syntaxin 1A in neurosecretion-incompetent cells: prevention by rbSEC1. J. Cell Sci. 112, 1865-1877.

214. Ruan, H., Zarnowski, M. J., Cushman, S. W., and Lodish, H. F. (2003). Standard isolation of primary adipose cells from mouse epididymal fat pads induces inflammatory mediators and down-regulates adipocyte genes. J. Biol. Chem. 278, 47585-47593.

215. Ryder, J. W., Yang, J., Galuska, D., Rincon, J., Bjornholm, M., Krook, A., Lund, S., Pedersen, O., Wallberg-Henriksson, H., Zierath, J. R., and Holman, G. D. (2000). Use of a novel impermeable biotinylated photolabeling reagent to assess insulin- and hypoxia-stimulated cell surface GLUT4 content in skeletal muscle from type 2 diabetic patients. Diabetes 49, 647-654.

216. Ryu, J., Hah, J. S., Park, J. S., Lee, W., Rampal, A. L., and Jung, C. Y. (2002). Protein kinase C-zeta phosphorylates insulin-responsive aminopeptidase in vitro at Ser-80 and Ser-91. Arch. Biochem. Biophys. 403, 71-82.

217. Sanchez-Margalet, V., Goldfine, I. D., Vlahos, C. J., and Sung, C. K. (1994). Role of phosphatidylinositol-3-kinase in insulin receptor signaling: studies with inhibitor, LY294002. Biochem. Biophys. Res. Commun. 204, 446-452.

218. Sandoval, I. V., Martinez-Arca, S., Valdueza, J., Palacios, S., and Holman, G. D. (2000). Distinct reading of different structural determinants modulates the dileucine-mediated transport steps of the lysosomal membrane protein LIMPII and the insulin-sensitive glucose transporter GLUT4. J. Biol. Chem. 275, 39874-39885.

219. Sano, H., Kane, S., Sano, E., Miinea, C. P., Asara, J. M., Lane, W. S., Garner, C. W., and Lienhard, G. E. (2003). Insulin-stimulated phosphorylation of a Rab GTPase-activating protein regulates GLUT4 translocation. J. Biol. Chem. 278, 14599-14602.

220. Sato, T. K., Rehling, P., Peterson, M. R., and Emr, S. D. (2000). Class C Vps protein complex regulates vacuolar SNARE pairing and is required for vesicle docking/fusion. Mol. Cell. 6, 661-671.

221. Satoh, S., Nishimura, H., Clark, A. E., Kozka, I. J., Vannucci, S. J., Simpson, I. A., Quon, M. J., Cushman, S. W., and Holman, G. D. (1993). Use of bismannose photolabel to elucidate insulin-regulated GLUT4 subcellular trafficking kinetics in rat adipose cells. Evidence that exocytosis is a critical site of hormone action. J. Biol. Chem. 268, 17820-17829.

222. Schoch, S., Deak, F., Konigstorfer, A., Mozhayeva, M., Sara, Y., Sudhof, T. C., and Kavalali, E. T. (2001). SNARE function analyzed in synaptobrevin/VAMP knockout mice. Science 294, 1117-1122.

223. Schraw, T. D., Lemons, P. P., Dean, W. L., and Whiteheart, S. W. (2003). A role for Sec1/Munc18 proteins in platelet exocytosis. Biochem. J. 374, 207-217.

224. Scott, B. L., Van Komen, J. S., Irshad, H., Liu, S., Wilson, K. A., and McNew, J. A. (2004). Sec1p directly stimulates SNARE-mediated membrane fusion in vitro. J. Cell Biol. 167, 75-85.

225. Sevilla, L., Tomas, E., Munoz, P., Guma, A., Fischer, Y., Thomas, J., Ruiz-Montasell, B., Testar, X., Palacin, M., Blasi, J., and Zorzano, A. (1997). Characterization of two distinct intracellular GLUT4 membrane populations in muscle fiber. Differential protein composition and sensitivity to insulin. Endocrinology 138, 3006-3015.

226. Shah, J. H., DeLeon-Jones, F. A., Schickler, R., Nasr, S., Mayer, M., and Hurks, C. (1986). Symptomatic reactive hypoglycemia during glucose tolerance test in lithium-treated patients. Metabolism 35, 634-639.

227. Sharma, P. M., Egawa, K., Huang, Y., Martin, J. L., Huvar, I., Boss, G. R., and Olefsky, J. M. (1998). Inhibition of phosphatidylinositol 3-kinase activity by adenovirus-mediated gene transfer and its effect on insulin action. J. Biol. Chem. 273, 18528-18537.

228. Shigematsu, S., Khan, A. H., Kanzaki, M., and Pessin, J. E. (2002). Intracellular insulin-responsive glucose transporter (GLUT4) distribution but not insulin-stimulated GLUT4 exocytosis and recycling are microtubule dependent. Mol. Endocrinol. 16, 1060-1068.

229. Skehel, J. J. and Wiley, D. C. (1998). Coiled coils in both intracellular vesicle and viral membrane fusion. Cell 95, 871-874.

230. Smith, D. B. and Johnson, K. S. (1988). Single-step purification of polypeptides expressed in Escherichia coli as fusions with glutathione S-transferase. Gene 67, 31-40.

231. Smith-Hall, J., Pons, S., Patti, M. E., Burks, D. J., Yenush, L., Sun, X. J., Kahn, C. R., and White, M. F. (1997). The 60 kDa insulin receptor substrate functions like an IRS protein (pp60IRS3) in adipose cells. Biochemistry 36, 8304-8310.

232. Sollner, T., Whiteheart, S. W., Brunner, M., Erdjument-Bromage, H., Geromanos, S., Tempst, P., and Rothman, J. E. (1993). SNAP receptors implicated in vesicle targeting and fusion. Nature 362, 318-324.

233. Somwar, R., Kim, D. Y., Sweeney, G., Huang, C., Niu, W., Lador, C., Ramlal, T., and Klip, A. (2001a). GLUT4 translocation precedes the stimulation of glucose uptake by insulin in muscle cells: potential activation of GLUT4 via p38 mitogen-activated protein kinase. Biochem. J. 359, 639-649.

234. Somwar, R., Koterski, S., Sweeney, G., Sciotti, R., Djuric, S., Berg, C., Trevillyan, J., Scherer, P. E., Rondinone, C. M., and Klip, A. (2002). A dominant-negative p38 MAPK mutant and novel selective inhibitors of p38 MAPK reduce insulin-stimulated glucose uptake in 3T3-L1 adipocytes without affecting GLUT4 translocation. J. Biol. Chem. 277, 50386-50395.

235. Somwar, R., Niu, W., Kim, D. Y., Sweeney, G., Randhawa, V. K., Huang, C., Ramlal, T., and Klip, A. (2001b). Differential effects of phosphatidylinositol 3-kinase inhibition on intracellular signals regulating GLUT4 translocation and glucose transport. J. Biol. Chem. 276, 46079-46087.

236. Somwar, R., Perreault, M., Kapur, S., Taha, C., Sweeney, G., Ramlal, T., Kim, D. Y., Keen, J., Cote, C. H., Klip, A., and Marette, A. (2000). Activation of p38 mitogen-activated protein kinase alpha and beta by insulin and contraction in rat skeletal muscle: potential role in the stimulation of glucose transport. Diabetes 49, 1794-1800.

237. St Denis, J. F., Cabaniols, J. P., Cushman, S. W., and Roche, P. A. (1999). SNAP-23 participates in SNARE complex assembly in rat adipose cells. Biochem. J. 338, 709-715.

238. Standaert, M. L., Bandyopadhyay, G., Kanoh, Y., Sajan, M. P., and Farese, R. V. (2001). Insulin and PIP3 activate PKC-zeta by mechanisms that are both dependent and independent of phosphorylation of activation loop (T410) and autophosphorylation (T560) sites. Biochemistry 40, 249-255.

239. Standaert, M. L., Galloway, L., Karnam, P., Bandyopadhyay, G., Moscat, J., and Farese, R. V. (1997). Protein kinase C-zeta as a downstream effector of phosphatidylinositol 3-kinase during insulin stimulation in rat adipocytes. Potential role in glucose transport. J. Biol. Chem. 272, 30075-30082.

240. Stewart, B. A., Mohtashami, M., Trimble, W. S., and Boulianne, G. L. (2000). SNARE proteins contribute to calcium cooperativity of synaptic transmission. Proc. Natl. Acad. Sci. U. S. A. 97, 13955-13960.

241. Subtil, A., Lampson, M. A., Keller, S. R., and McGraw, T. E. (2000). Characterization of the insulin-regulated endocytic recycling mechanism in 3T3-L1 adipocytes using a novel reporter molecule. J. Biol. Chem. 275, 4787-4795.

242. Sun, X. J., Rothenberg, P., Kahn, C. R., Backer, J. M., Araki, E., Wilden, P. A., Cahill, D. A., Goldstein, B. J., and White, M. F. (1991). Structure of the insulin receptor substrate IRS-1 defines a unique signal transduction protein. Nature 352, 73-77.

243. Sun, X. J., Wang, L. M., Zhang, Y., Yenush, L., Myers, M. G., Jr., Glasheen, E., Lane, W. S., Pierce, J. H., and White, M. F. (1995). Role of IRS-2 in insulin and cytokine signalling. Nature 377, 173-177.

244. Sweeney, G., Garg, R. R., Ceddia, R. B., Li, D., Ishiki, M., Somwar, R., Foster, L. J., Neilsen, P. O., Prestwich, G. D., Rudich, A., and Klip, A. (2004). Intracellular delivery of phosphatidylinositol (3,4,5)-trisphosphate causes incorporation of glucose transporter 4 into the plasma membrane of muscle and fat cells without increasing glucose uptake. J. Biol. Chem. 279, 32233-32242.

245. Sweeney, G., Somwar, R., Ramlal, T., Volchuk, A., Ueyama, A., and Klip, A. (1999). An inhibitor of p38 mitogen-activated protein kinase prevents insulin-stimulated glucose transport but not glucose transporter translocation in 3T3-L1 adipocytes and L6 myotubes. J. Biol. Chem. 274, 10071-10078.

246. Szule, J. A. and Coorssen, J. R. (2003). Revisiting the role of SNAREs in exocytosis and membrane fusion. Biochim. Biophys. Acta 1641, 121-135.

247. Tahara, M., Coorssen, J. R., Timmers, K., Blank, P. S., Whalley, T., Scheller, R., and Zimmerberg, J. (1998). Calcium can disrupt the SNARE protein complex on sea urchin egg secretory vesicles without irreversibly blocking fusion. J. Biol. Chem. 273, 33667-33673.

248. Takuma, T., Arakawa, T., Okayama, M., Mizoguchi, I., Tanimura, A., and Tajima, Y. (2002). Trafficking of green fluorescent protein-tagged SNARE proteins in HSY cells. J. Biochem. (Tokyo) 132, 729-735.

249. Tamemoto, H., Kadowaki, T., Tobe, K., Yagi, T., Sakura, H., Hayakawa, T., Terauchi, Y., Ueki, K., Kaburagi, Y., Satoh, S., and . (1994). Insulin resistance and growth retardation in mice lacking insulin receptor substrate-1. Nature 372, 182-186.

250. Tamori, Y., Hashiramoto, M., Araki, S., Kamata, Y., Takahashi, M., Kozaki, S., and Kasuga, M. (1996). Cleavage of vesicle-associated membrane protein (VAMP)-2 and cellubrevin on GLUT4-containing vesicles inhibits the

translocation of GLUT4 in 3T3-L1 adipocytes. Biochem. Biophys. Res. Commun. 220, 740-745.

251. Tamori, Y., Kawanishi, M., Niki, T., Shinoda, H., Araki, S., Okazawa, H., and Kasuga, M. (1998). Inhibition of insulin-induced GLUT4 translocation by Munc18c through interaction with syntaxin4 in 3T3-L1 adipocytes. J. Biol. Chem. 273, 19740-19746.

252. Tanti, Jean Francois, Grillo, Sophie, Gremeaux, Thierry, Coffer, Paul J., Van Obberghen, Emmanuel, and Marchand-Brustel, Yannick. (1997). Potential Role of Protein Kinase B in Glucose Transporter 4 Translocation in Adipocytes. Endocrinology 138, 2005-2010.

253. Taylor, L. P. and Holman, G. D. (1981). Symmetrical kinetic parameters for 3-O-methyl-D-glucose transport in adipocytes in the presence and in the absence of insulin. Biochim. Biophys. Acta 642, 325-335.

254. Tellam, J. T., Macaulay, S. L., McIntosh, S., Hewish, D. R., Ward, C. W., and James, D. E. (1997). Characterization of Munc-18c and syntaxin-4 in 3T3-L1 adipocytes. Putative role in insulin-dependent movement of GLUT-4. J. Biol. Chem. 272, 6179-6186.

255. Thirone, A. C., Carvalheira, J. B., Hirata, A. E., Velloso, L. A., and Saad, M. J. (2004). Regulation of Cbl-associated protein/Cbl pathway in muscle and adipose tissues of two animal models of insulin resistance. Endocrinology 145, 281-293.

256. Thorens, B. (2001). GLUT2 in pancreatic and extra-pancreatic gluco-detection. Mol. Membr. Biol 18, 265-273.

257. Thorens, B. (2003). A gene knockout approach in mice to identify glucose sensors controlling glucose homeostasis. Pflugers Arch. 445, 482-490.

258. Thurmond, D. C., Ceresa, B. P., Okada, S., Elmendorf, J. S., Coker, K., and Pessin, J. E. (1998). Regulation of insulin-stimulated GLUT4 translocation by Munc18c in 3T3L1 adipocytes. J. Biol. Chem. 273, 33876-33883.

259. Thurmond, D. C., Kanzaki, M., Khan, A. H., and Pessin, J. E. (2000). Munc18c function is required for insulin-stimulated plasma membrane fusion of GLUT4 and insulin-responsive amino peptidase storage vesicles. Mol. Cell Biol. 20, 379-388.

260. Thurmond, D. C. and Pessin, J. E. (2000). Discrimination of GLUT4 vesicle trafficking from fusion using a temperature-sensitive Munc18c mutant. EMBO J 19, 3565-3575.

261. Thurmond, D. C. and Pessin, J. E. (2001). Molecular machinery involved in the insulin-regulated fusion of GLUT4-containing vesicles with the plasma membrane (review). Mol Membr. Biol 18, 237-245.

262. Timmers, K. I., Clark, A. E., Omatsu-Kanbe, M., Whiteheart, S. W., Bennett, M. K., Holman, G. D., and Cushman, S. W. (1996). Identification of SNAP

receptors in rat adipose cell membrane fractions and in SNARE complexes co-immunoprecipitated with epitope-tagged N-ethylmaleimide-sensitive fusion protein. Biochem. J. 320, 429-436.

263. Tokumaru, H., Umayahara, K., Pellegrini, L. L., Ishizuka, T., Saisu, H., Betz, H., Augustine, G. J., and Abe, T. (2001). SNARE complex oligomerization by synaphin/complexin is essential for synaptic vesicle exocytosis. Cell 104, 421-432.

264. Towbin, H., Staehelin, T., and Gordon, J. (1979). Electrophoretic transfer of proteins from polyacrylamide gels to nitrocellulose sheets: procedure and some applications. Proc. Natl. Acad. Sci. U. S. A. 76, 4350-4354.

265. Tsakiridis, T., Vranic, M., and Klip, A. (1994). Disassembly of the actin network inhibits insulin-dependent stimulation of glucose transport and prevents recruitment of glucose transporters to the plasma membrane. J. Biol. Chem. 269, 29934-29942.

266. Tsujimoto, M., Mizutani, S., Adachi, H., Kimura, M., Nakazato, H., and Tomoda, Y. (1992). Identification of human placental leucine aminopeptidase as oxytocinase. Arch. Biochem. Biophys. 292, 388-392.

267. Tucker, W. C., Weber, T., and Chapman, E. R. (2004). Reconstitution of Ca2+-regulated membrane fusion by synaptotagmin and SNAREs. Science 304, 435-438.

268. Uchida, Tohru, Myers, Martin G., Jr., and White, Morris F. (2000). IRS-4 Mediates Protein Kinase B Signaling during Insulin Stimulation without Promoting Antiapoptosis. Mol. Cell. Biol. 20, 126-138.

269. Uldry, M., Ibberson, M., Horisberger, J. D., Chatton, J. Y., Riederer, B. M., and Thorens, B. (2001). Identification of a mammalian H(+)-myo-inositol symporter expressed predominantly in the brain. EMBO J. 20, 4467-4477.

270. Uldry, M., Ibberson, M., Hosokawa, M., and Thorens, B. (2002). GLUT2 is a high affinity glucosamine transporter. FEBS Lett. 524, 199-203.

271. Ungermann, C., Sato, K., and Wickner, W. (1998). Defining the functions of trans-SNARE pairs. Nature 396, 543-548.

272. van Dam, E. M., Govers, R., and James, D. E. (2005). Akt activation is required at a late stage of insulin-induced GLUT4 translocation to the plasma membrane. Mol. Endocrinol. 19, 1067-1077.

273. Vanhaesebroeck, B., Leevers, S. J., Panayotou, G., and Waterfield, M. D. (1997). Phosphoinositide 3-kinases: a conserved family of signal transducers. Trends Biochem. Sci. 22, 267-272.

274. Verderio, C., Pozzi, D., Pravettoni, E., Inverardi, F., Schenk, U., Coco, S., Proux-Gillardeaux, V., Galli, T., Rossetto, O., Frassoni, C., and Matteoli, M. (2004). SNAP-25 modulation of calcium dynamics underlies differences in

GABAergic and glutamatergic responsiveness to depolarization. Neuron 41, 599-610.

275. Voets, T., Toonen, R. F., Brian, E. C., de Wit, H., Moser, T., Rettig, J., Sudhof, T. C., Neher, E., and Verhage, M. (2001). Munc18-1 promotes large dense-core vesicle docking. Neuron 31, 581-591.

276. Volchuk, A., Wang, Q., Ewart, H. S., Liu, Z., He, L., Bennett, M. K., and Klip, A. (1996). Syntaxin 4 in 3T3-L1 adipocytes: regulation by insulin and participation in insulin-dependent glucose transport. Mol. Biol. Cell 7, 1075-1082.

277. Walch-Solimena, C., Blasi, J., Edelmann, L., Chapman, E. R., von Mollard, G. F., and Jahn, R. (1995b). The t-SNAREs syntaxin 1 and SNAP-25 are present on organelles that participate in synaptic vesicle recycling. J. Cell Biol. 128, 637-645.

278. Walch-Solimena, C., Blasi, J., Edelmann, L., Chapman, E. R., von Mollard, G. F., and Jahn, R. (1995a). The t-SNAREs syntaxin 1 and SNAP-25 are present on organelles that participate in synaptic vesicle recycling. J. Cell Biol. 128, 637-645.

279. Wang, G., Witkin, J. W., Hao, G., Bankaitis, V. A., Scherer, P. E., and Baldini, G. (1997). Syndet is a novel SNAP-25 related protein expressed in many tissues. J. Cell Sci. 110, 505-513.

280. Wang, Q., Bilan, P. J., Tsakiridis, T., Hinek, A., and Klip, A. (1998). Actin filaments participate in the relocalization of phosphatidylinositol3-kinase to glucose transporter-containing compartments and in the stimulation of glucose uptake in 3T3-L1 adipocytes. Biochem. J. 331, 917-928.

281. Washbourne, P., Thompson, P. M., Carta, M., Costa, E. T., Mathews, J. R., Lopez-Bendito, G., Molnar, Z., Becher, M. W., Valenzuela, C. F., Partridge, L. D., and Wilson, M. C. (2002). Genetic ablation of the t-SNARE SNAP-25 distinguishes mechanisms of neuroexocytosis. Nat. Neurosci. 5, 19-26.

282. Watson, R. T., Shigematsu, S., Chiang, S. H., Mora, S., Kanzaki, M., Macara, I. G., Saltiel, A. R., and Pessin, J. E. (2001). Lipid raft microdomain compartmentalization of TC10 is required for insulin signaling and GLUT4 translocation. J. Cell Biol. 154, 829-840.

283. Weber, T., Parlati, F., McNew, J. A., Johnston, R. J., Westermann, B., Sollner, T. H., and Rothman, J. E. (2000). SNAREpins are functionally resistant to disruption by NSF and alphaSNAP. J. Cell Biol. 149, 1063-1072.

284. Weber, T., Zemelman, B. V., McNew, J. A., Westermann, B., Gmachl, M., Parlati, F., Sollner, T. H., and Rothman, J. E. (1998). SNAREpins: minimal machinery for membrane fusion. Cell 92, 759-772.

285. Weber, T. M. H. G. Joost I. A. Simpson and S. W. Cushman. (1988). Methods for assessment of glucose transport activity and the number of glucose

transporters in isolated rat adipose cells and membrane fractions. In: The Insulin Receptor, vol. 2. 171-187. Liss. C.R.Kahn,and L.C.Harrison, Eds.

286. Wei, M. L., Bonzelius, F., Scully, R. M., Kelly, R. B., and Herman, G. A. (1998). GLUT4 and transferrin receptor are differentially sorted along the endocytic pathway in CHO cells. J. Cell Biol. 140, 565-575.

287. Weir, M. L., Klip, A., and Trimble, W. S. (1998). Identification of a human homologue of the vesicle-associated membrane protein (VAMP)-associated protein of 33 kDa (VAP-33): a broadly expressed protein that binds to VAMP. Biochem. J. 333, 247-251.

288. Whitehead, J. P., Molero, J. C., Clark, S., Martin, S., Meneilly, G., and James, D. E. (2001). The role of Ca2+ in insulin-stimulated glucose transport in 3T3-L1 cells. J. Biol. Chem. 276, 27816-27824.

289. Whiteheart, S. W. and Matveeva, E. A. (2004). Multiple binding proteins suggest diverse functions for the N-ethylmaleimide sensitive factor. J. Struct. Biol. 146, 32-43.

290. Whitesell, R. R. and Gliemann, J. (1979). Kinetic parameters of transport of 3-O-methylglucose and glucose in adipocytes. J. Biol. Chem. 254, 5276-5283.

291. Whitley, P., Reaves, B. J., Hashimoto, M., Riley, A. M., Potter, B. V., and Holman, G. D. (2003). Identification of mammalian Vps24p as an effector of phosphatidylinositol 3,5 bisphosphate dependent endosome compartmentalization. J. Biol. Chem. 278, 38786-38795.

292. Widberg, C. H., Bryant, N. J., Girotti, M., Rea, S., and James, D. E. (2003). Tomosyn Interacts with the t-SNAREs Syntaxin4 and SNAP23 and Plays a Role in Insulin-stimulated GLUT4 Translocation. J. Biol. Chem. 278, 35093-35101.

293. Withers, D. J., Gutierrez, J. S., Towery, H., Burks, D. J., Ren, J. M., Previs, S., Zhang, Y., Bernal, D., Pons, S., Shulman, G. I., Bonner-Weir, S., and White, M. F. (1998). Disruption of IRS-2 causes type 2 diabetes in mice. Nature 391, 900-904.

294. Wong, P. P., Daneman, N., Volchuk, A., Lassam, N., Wilson, M. C., Klip, A., and Trimble, W. S. (1997). Tissue distribution of SNAP-23 and its subcellular localization in 3T3-L1 cells. Biochem. Biophys. Res. Commun. 230, 64-68.

295. Woodbury, D. J. and Rognlien, K. (2000). The t-SNARE syntaxin is sufficient for spontaneous fusion of synaptic vesicles to planar membranes. Cell Biol. Int. 24, 809-818.

296. Xi, X., Han, J., and Zhang, J. Z. (2001). Stimulation of glucose transport by AMP-activated protein kinase via activation of p38 mitogen-activated protein kinase. J. Biol. Chem. 276, 41029-41034.

297. Xiao, J., Xia, Z., Pradhan, A., Zhou, Q., and Liu, Y. (2004). An immunohistochemical method that distinguishes free from complexed SNAP-25. J. Neurosci. Res. 75, 143-151.

298. Xu, Z. and Kandror, K. V. (2002). Translocation of small pre-formed vesicles is responsible for the insulin activation of glucose transport in adipose cells. Evidence from the in vitro reconstitution assay. J. Biol. Chem. 277, 47972-47975.

299. Yamada, E., Okada, S., Saito, T., Ohshima, K., Sato, M., Tsuchiya, T., Uehara, Y., Shimizu, H., and Mori, M. (2005). Akt2 phosphorylates Synip to regulate docking and fusion of GLUT4-containing vesicles. J. Cell Biol. 168, 921-928.

300. Yamaguchi, T., Dulubova, I., Min, S. W., Chen, X., Rizo, J., and Sudhof, T. C. (2002). Sly1 binds to Golgi and ER syntaxins via a conserved N-terminal peptide motif. Dev. Cell 2, 295-305.

301. Yang, B., Gonzalez, L., Jr., Prekeris, R., Steegmaier, M., Advani, R. J., and Scheller, R. H. (1999). SNARE interactions are not selective. Implications for membrane fusion specificity. J. Biol. Chem. 274, 5649-5653.

302. Yang, J., Clark, A. E., Harrison, R., Kozka, I. J., and Holman, G. D. (1992). Trafficking of glucose transporters in 3T3-L1 cells. Inhibition of trafficking by phenylarsine oxide implicates a slow dissociation of transporters from trafficking proteins. Biochem. J. 281, 809-817.

303. Yang, J., Hodel, A., and Holman, G. D. (2002). Insulin and isoproterenol have opposing roles in the maintenance of cytosol pH and optimal fusion of GLUT4 vesicles with the plasma membrane. J. Biol Chem. 277, 6559-6566.

304. Yang, J. and Holman, G. D. (1993). Comparison of GLUT4 and GLUT1 subcellular trafficking in basal and insulin-stimulated 3T3-L1 cells. J. Biol. Chem. 268, 4600-4603.

305. Zeigerer, A., McBrayer, M. K., and McGraw, T. E. (2004). Insulin stimulation of GLUT4 exocytosis, but not its inhibition of endocytosis, is dependent on RabGAP AS160. Mol. Biol. Cell 15, 4406-4415.

306. Zerial, M. and McBride, H. (2001). Rab proteins as membrane organizers. Nat. Rev. Mol. Cell Biol. 2, 107-117.

307. Zhou, M., Vallega, G., Kandror, K. V., and Pilch, P. F. (2000). Insulin-mediated translocation of GLUT-4-containing vesicles is preserved in denervated muscles. Am. J. Physiol Endocrinol. Metab 278, E1019-E1026.

308. Zhou, Q. L., Park, J. G., Jiang, Z. Y., Holik, J. J., Mitra, P., Semiz, S., Guilherme, A., Powelka, A. M., Tang, X., Virbasius, J., and Czech, M. P. (2004). Analysis of insulin signalling by RNAi-based gene silencing. Biochem. Soc. Trans. 32, 817-821.